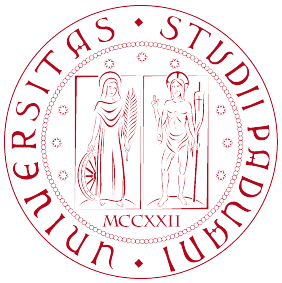

UNIVERSITÀ
DEGLI STUDI
DI PADOVA

PROTEIN KINASE CK2 PHOSPHORYLATES THE NEURONAL CHAPERONE HSJ1: A PARADIGMATIC EXAMPLE OF UBIQUITIN SIGNALING REGULATION

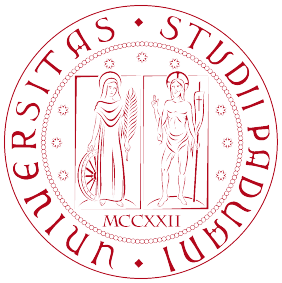

UNIVERSITÀ
DEGLI STUDI
DI PADOVA

Università degli Studi di Padova
Dipartimento di Biologia

CORSO DI DOTTORATO DI RICERCA IN
BIOSCIENZE E BIOTECNOLOGIE

CURRICULUM IN BIOCHIMICA E BIOFISICA
CICLO XXIX

PROTEIN KINASE CK2 PHOSPHORYLATES THE NEURONAL CHAPERONE HSJ1: A PARADIGMATIC EXAMPLE OF UBIQUITIN SIGNALLING REGULATION

COORDINATORE: CH.MO PROF. PAOLO BERNARDI

SUPERVISORE: CH.MA PROF.SSA MARIA RUZZENE

DOTTORANDO: DANIELE OTTAVIANI

A Elena

Contents

Summary

Protein kinase CK2 is an anti-apoptotic, constitutively active and ubiquitous Ser/Thr protein kinase. CK2 phosphorylates hundreds of substrates, characterized by the presence of acidic residues near the Ser/Thr target; its minimal consensus sequence is the motif S/TXXE/D/pS,pY,pT, where X is any amino acid and E/D/pX are acidic residues or previously phosphorylated ones. CK2 stabilizes anti-apoptotic signalling pathways and therefore is regarded as a pro-survival kinase. It is highly expressed in cancer where it sustains abnormal cell growth and survival. Therefore, CK2 represents a promising drug target against which several inhibitory compounds have been developed so far. However, there are now compelling evidences for a critical function of CK2 in neurons and a role in neurodegeneration has been suggested, but never studied in detail. Interestingly, we noticed that the CK2 consensus is superimposable to a sequence inside the ubiquitin interacting motif (UIM) of the neuronal-specific chaperone HSJ1. HSJ1 has a neuroprotective role and controls the folding, misfolding, aggregation and degradation of protein clients, thus maintaining their homeostasis (proteostasis). Consistently, functional mutations in its gene have been associated to neurodegenerative disease (NDs). The project presented in this thesis is based on the working hypothesis that phosphorylation of residues conforming to the CK2 consensus on HSJ1 could affect its functions.

HSJ1 belongs to the DNAJ protein family. It is preferentially expressed in neuronal tissues and contains an N-terminal J domain and two UIM domains near the C-terminus. It is codified by the *DNAJB2* gene and alternatively spliced to produce two isoforms: HSJ1a and HSJ1b. The former is mainly located in the nuclear and cytosolic compartments, the latter is anchored to the cytosolic face of the endoplasmic reticulum. HSJ1b participates in the endoplasmic

reticulum-associated protein degradation (ERAD) system as a folding controller of membrane-associated proteins. HSJ1a cooperates with Hsp70 in binding and delivering ubiquitylated proteins to proteasomal degradation. In particular, it suppresses the deposition of aggregation-prone proteins such as SOD1 (Superoxide Dismutase 1) in amiotrophic lateral sclerosis, polyglutamine expanded huntingtin in Huntington's disease, ataxin-3 in spinocerebellar ataxias, and promotes the refolding of a Parkin mutant in Parkinson's disease. Genetic studies have provided further evidences for a role of HSJ1 in neuronal survival, as mutations in *DNAJB2* cause distal hereditary motor neuropathy and Charcot-Marie-Tooth type 2. Nevertheless, the biochemical mechanisms by which HSJ1 acts in these pathologies are only partially understood.

The results we obtained suggest that CK2 is a prominent HSJ1 phosphorylating kinase. As mentioned above, HSJ1 UIMs display canonical CK2 consensus sites. Therefore, we first performed *in vitro* phosphorylation experiments on HSJ1a. We expressed the protein in HEK-293T cells and confirmed the phosphorylation of HSJ1 by means of cell loading with [^{32}P]phosphate, followed by the immunoprecipitation of the chaperone. In this assay, the HSJ1 phosphorylation was assessed by autoradiography of the immunoprecipitated protein and the CK2-dependendece by demonstrating its sensitivity to the CK2 inhibitor CX-4945. A mass spectrometry analysis revealed that Ser247, Ser250 and Ser264 are phosphorylated and are inside the second UIM. Then, we produced Serine-to-Alanine mutants of each CK2 target-residue, both in prokaryotic and eukaryotic expression vectors. We performed *in vitro* kinase assays on recombinant purified proteins or upon their expression in HEK-293T cells and subsequent immunoprecipitation. Collectively, the data demonstrated that Ser250 is the main phospho-site on HSJ1. The Ser264 only marginally contributes to the overall HSJ1 phosphorylation and Ser247 is a hierarchical site. In fact, Ser247 does not fulfil the CK2 minimal consensus sequence, because it does not have an acidic residue in +3 position. However, once Ser250 is phosphorylated the residue becomes acidic and fits the consensus sequence. This implies that a hierarchical phosphorylation can occur in HSJ1, where the previous phosphorylation of Ser250 primes Ser247 for subsequent phosphorylation.

Then, we successfully designed and developed a strategy for the production of phospho-specific antibodies against the main Ser247/Ser250 phospho-sites. The signal of he purified antibodies strongly reduced in response to cell treatments with different CK2 specific inhibitors. They were also useful to confirm the phosphorylation of both HSJ1 isoforms, a and b, in cells.

We then aimed at investigating the effects of HSJ1a phosphorylation on its functions and in particular on the binding to its ubiquitylated clients. To this purpose, we exploited the transfection of phospho-null and phospho-mimetic mutants into HEK-293T cells. The analysis of the ubiquitylated proteins co-immunoprecipitated with WT or mutated HSJ1a followed. Results showed that HSJ1a is able to bind more ubiquitylated clients when the phosphorylation at its CK2 sites is prevented. Moreover, we also found that these not-phosphorylated forms have enhanced activities in delivering the reporter luciferase protein to proteasomal degradation. We concluded that the phosphorylation of HSJ1a by CK2 impairs its chaperone function.

With this study, we disclosed an unanticipated HSJ1/CK2 connection with important implications for the molecular mechanisms of neurodegeneration and hopefully for the development of associated therapies. The HSJ1 co-chaperone function is critical in preventing neurodegeneration and is enhanced by the dephosphorylation of the sites targeted by CK2; therefore, treatments with CK2 inhibitors could be explored in the future as novel therapeutic compounds in NDs.

Since we observed that UIMs residues are evolutionary conserved in other proteins and superimposable to the CK2 consensus, with this work we suggest that other UIM-containing proteins could be phosphorylated. Indeed, we already showed that the UIM-containing proteasome subunit S5a is phosphorylated by CK2. Therefore, the CK2/HSJ1 connection could be a paradigmatic example of a broader regulation mechanism able to influence the processing of ubiquitylated proteins.

Related Projects

Protein kinase CK2 appeared to be a prominent druggable target after the discovery of its deregulated activity in cancer. Cancer cells were demonstrated to be more sensitive to the inhibition of CK2 than their healthy counterparts. This observation promotes the design and testing of several inhibitory molecules some of which are currently patented and/or in clinical trials. However, the use of inhibitors was also of invaluable support in helping understanding the role of CK2 in other pathologies. From the work described in the main project, is now evident that CK2 inhibitors should be indeed considered in a therapeutic perspective for neurodegeneration.

Despite the wide use and availability of CK2 inhibitory compounds, the characterization of their mechanism of action and tolerability are still under intensive investigations. Most inhibitors have been designed as competitors for the ATP-binding pocket on protein kinases. However, different strategies have been explored in order to increase the therapeutic efficacy. We designed, developed and characterized two alternative inhibition strategies. A first project concerned the analysis of a chimeric molecule named CK2-MCP, designed to specifically target the consensus recognized by CK2 in its substrates. We showed that CK2-MCP is able to double-hit both substrates and the kinase itself. A second project concerned a different kind of 'double-hit' strategy addressed by a compound named TDB. It was designed to multitarget both CK2 and Pim-1, another kinase implied in cancer onset and progression. We compared TDB and CX-4945 in term of their ability to inhibit the CK2 activity and to reduce cancer cells viability. Our results, in different treatments times and protocols, revealed that TDB displays a higher persistence of the inhibitory effect on CK2. This peculiarity produced a more pronounced toxicity for cancer cells, despite the superiority of CX-4945 efficacy *in vitro*. We suggest that the optimization of the cellular persistence of the CK2-inhibitor complex is a crucial aspect that should be considered during the optimization of inhibitory compounds.

Riassunto

La proteinchinasi CK2 è una serina/treonina chinasi espressa ubiquitariamente in tutti i tessuti dove svolge un importante ruolo anti-apoptotico. Questo enzima fosoforila una molteplicità di substrati coinvolti nella proliferazione e sopravvivenza cellulari ed accomunati dalla presenza di un "sito consenso". Questo sito presenta un residuo di serina (S) o treonina (T) inserito in un intorno di amminoacidi acidi che definiscono il motivo minimo S/TXXE/pS/pY/pT: X rappresenta un generico amminoacido mentre E/D/pX sono residui acidi o fosforilati in precedenza. Elevati livelli di espressione di CK2 sono stati riscontrati in neoplasie dove il suo ruolo anti-apoptotico promuove la proliferazione e l'invasione delle cellule cancerose. Di conseguenza, l'enzima è considerato un importante bersaglio, contro cui sono stati sviluppati negli anni diversi inibitori in grado di ridurne l'attività. Tuttavia, vi sono ormai evidenze del coinvolgimento di CK2 nello sviluppo e funzione neuronali; inoltre, è stato suggerito, ma non studiato nel dettaglio, che il ruolo di CK2 nei neuroni possa avere ripercussioni nella progressione e sviluppo di malattie neurodegenerative. Abbiamo notato che uno dei "sito consenso" riconosciti da CK2 nei suoi substrati, coincide con una sequenza all'interno di un motivo in grado di legare l'ubiquitina (UIM) della proteina HSJ1. HSJ1, espressa prevalentemente in cellule neuronali, agisce da "chaperone molecolare": controlla l'assemblaggio (*folding*), disassemblaggio, aggregazione e degradazione delle proteine che riconosce mediante i suoi domini UIM, mantenendo i loro livelli in equilibrio dinamico (proteostasi). Ne consegue che HSJ1 esercita un ruolo neuroprotettore. Infatti, sono state identificate alcune mutazioni a carico del suo gene *DNAJB2*, ed associate all'insorgenza di alcune malattie neurodegenerative. Inoltre, alcune di queste mutazioni sono in grado di compromettere la funzione neuroprotettiva di HSJ1.

Il progetto di questa tesi si pone come obiettivo di dimostrare che la fosforilazione di alcuni residui di HSJ1 da parte di CK2 è in grado di influenzarne la funzione.
HSJ1 è una proteina appartenente alla famiglia detta DNAJ cui membri sono accomunati dalla presenza del dominio proteico detto "dominio J". HSJ1, come detto prima, contiene anche due domini UIM localizzati al C-terminale. Il genoma umano codifica un unico trascritto, poi processato per produrre due isoforme: HSJ1a, espressa nel citosol, ed HSJ1b, ancorata alla faccia esterna del reticolo endoplasmatico. Entrambe le isoforme cooperano con la proteina Hsp70 nel legare e dirigere proteine ubiquitilate al proteasoma per essere degradate. In particolare, HSJ1a promuove la degradazione di proteine prone all'aggregazione. Infatti, il non corretto *folding* proteico può causarne la deposizione come aggregati intracellulari tossici, detti amiloidi, e considerati come un sintomo indicativo nella diagnosi di molte malattie neurodegenerative. Ad esempio, HSJ1a è tra i mediatori della degradazione della proteina SOD1 (superossido dismutasi 1) coinvolta nella sclerosi laterale amiotrofica, di proteine con tratti poliglutamminici espansi ed associati alla malattia di Huntington, ed infine della proteina ataxina-3, considerata agente eziologico nelle atassie spinocerebellari. Inoltre, HSJ1a coadiuva il *folding* della proteina parkina coinvolta nell'insorgenza di alcune forme del morbo di Parkinson. Studi di associazione genetica hanno anche dimostrato che alcune mutazioni nel gene *DNAJB2* causano neuropatie motorie ereditarie e la malattia di Charcot Marie Tooth - tipo 2. Tuttavia i meccanismi molecolari mediante cui HSJ1 agisce sono stati compresi solo parzialmente.
I risultati che abbiamo ottenuto dimostrano che HSJ1 è fosforilata da CK2. Come detto in precedenza, HSJ1 presenta alcuni residui amminoacidici all'interno del suo dominio UIM che sono potenzialmente fosforilabili da CK2. Abbiamo quindi svolto un'analisi in spettrometria di massa della proteina fosforilata che ci ha permesso di identificare i siti riconosciuti da CK2 che sono: i residui di serina alle posizione 247, 250 e 264. Successivamente, abbiamo espresso HSJ1 in cellule mediante vettori di espressioni eucariotici. Questi esperimenti erano atti a dimostrare che HSJ1 è fosforilata anche in cellule da CK2. Infatti, trattamenti in cui l'attività dell'enzima è stata ridotta mediante l'uso dell'inibitore CX-4945, hanno dimostrato che HSJ1 è substrato di CK2. Inoltre, abbiamo operato singole

sostituzioni amminoacidiche a carico dei residui serinici riconosciuti dall'enzima che sono stati mutati in residui alaninici. Ciò ha confermato ulteriormente i siti da noi identificati su HSJ1 come fosforilati da CK2, sia *in vitro* che in cellule. Collettivamente, i dati raccolti confermano che il sito principale di fosforilazione è la serina alla posizione 250. Il residuo alla posizione 264 contribuisce solo marginalmente. La serina 247 invece è definita come un sito gerarchico. Infatti, l'intorno amminoacidico del residuo alla posizione 247 non soddisfa i requisiti minimi per essere definito "sito consenso" per CK2. Ciò può avvenire solo una volta che la serina 250 è fosforilata. Di conseguenza, la serina 247 potrà essere riconosciuta da CK2 grazie al residuo acidico in posizione +3, in questo caso rappresentato dalla serina 250 fosforilata in precedenza.

Abbiamo poi ideato e sviluppato una strategia che ci ha permesso di produrre anticorpi in grado di riconoscere in maniera specifica le serine alla posizione 247 e 250, solo nel caso esse siano fosforilate da CK2. Questo strumento è stato utilizzato per confermare che entrambe le isoforme di HSJ1, a e b, sono fosforilate in cellule. Inoltre, abbiamo potuto verificare che la fosforilazione di HSJ1a è sensibile all'inibizione esercitata da un ampio pannello di inibitori specifici di CK2. Abbiamo poi analizzato se la fosforilazione di HSJ1 possa avere un impatto sulla sua funzione di legare proteine ubiquitinate da convogliare al proteasoma per la degradazione. Abbiamo quindi espresso HSJ1 in cellule, nella sua forma originale o mutata nei siti di fosforilazione. Mediante la co-precipitazione della proteina, a cui permangono legati i partner ubiquitilati, abbiamo potuto dimostrare che la fosforilazione dei siti-chiave da noi identificati causa una minor funzionalità del dominio UIM di HSJ1. Al contrario, la prevenzione della fosforilazione aumenta la capacità del dominio UIM di legare proteine ubiquitilate e di trasportarle al proteasoma, come abbiamo verificato nei riguardi della proteina luciferasi. Abbiamo potuto così concludere che la fosforilazione di HSJ1 da parte di CK2 contrasta la sua funzione di "chaperone molecolare".

Questo studio ci ha consentito di dimostrare una nuova connessione tra HSJ1 e CK2, in grado di aiutarci a comprendere meglio i meccanismi molecolari che sottendono l'insorgenza e lo sviluppo delle malattie neurodegenerative. Vi sono inoltre importanti risvolti terapeutici, dal momento che l'uso di inibitori di CK2

potrebbe essere proposto per aumentare la funzionalità di HSJ1.

Infine, abbiamo notato che alcuni residui amminoacidici all'interno del motivo UIM sono evolutivamente conservati e coincidono con la "sequenza consenso" minima richiesta per la fosforilazione da parte di CK2. Pertanto consideriamo altamente probabile che altre proteine contenenti domini UIM possano essere substrati di CK2, come dimostriamo in questa tesi anche per la proteina S5a, una subunità del proteasoma. Pertanto, HSJ1 vuole porsi come esempio paradigmatico di una possibile più ampia regolazione da parte di CK2 in grado di influenzare questa via di segnale mediata dall'ubiquitina.

Progetti complementari

Dalla scoperta del coinvolgimento della proteinchinasi CK2 nel cancro, le cellule neoplastiche si sono rivelate essere più sensibili all'inibizione della sua attività, rispetto alle cellule sane. Questo ha favorito lo sviluppo di molti inibitori alcuni dei quali sono al momento brevettati e/o in trials clinici. Tuttavia, come suggerito dal lavoro principale di questa tesi, queste molecole si sono rivelate utili strumenti per meglio comprendere il ruolo di CK2 in altre patologie (i.e. nelle malattie neurodegenerative) e potrebbero essere presi in considerazione per il loro trattamento.

Nonostante l'uso diffuso di inibitori di CK2, la comprensione del loro meccanismo d'azione e tollerabilità non sono stati ancora del tutto chiariti. Molti degli inibitori sviluppati fino ad ora sono ATP-competitivi, quindi in grado di legarsi alla tasca per i nucleotidi in CK2. Tuttavia, si stanno prendendo in considerazione strategie differenti per cercare di aumentarne l'efficacia terapeutica. In progetti complementari all'argomento principale di questa tesi, abbiamo analizzato due strategie di inibizione alternative. La prima ha riguardato lo sviluppo di una molecola chimerica chiamata CK2-MCP. Questa è in grado di legare per complementarietà il "sito consenso" di CK2 nei suoi substrati, impedendo all'enzima di accedervi per fosforilarli. Abbiamo però dimostrato che questa classe di composti è in grado di legare sia i substrati di CK2, come atteso, che l'enzima stesso.

Nel secondo progetto complementare, abbiamo invece preso in considerazione un

altro tipo di strategia duale, mediante l'uso di un inibitore sviluppato recentemente, detto TDB. Questo composto è in grado di inibire sia CK2 che Pim-1, un'altra proteinchinasi implicata nello sviluppo tumorale. Abbiamo comparato i composti CX-4945 e TDB per la loro capacità di inibire CK2 e di ridurre la vitalità delle cellule cancerose. Differenti tempi e condizioni di trattamento hanno dimostrato la più alta persistenza dell'inibizione di CK2 esercitata dal TDB in cellule, nonostante la superiorità del CX-4945 *in vitro*. La maggior durata dell'inibizione di CK2, indipendentemente dal fatto che il TDB inibisca anche Pim-1, sembra essere responsabile dei maggiori effetti citotossici indotti dal TDB nelle cellule tumorali. Questo suggerisce che l'ottimizzazione di inibitori di CK2 in cellule debba tenere conto anche di questo parametro.

AMINO ACIDS

Ala	Alanine	A
Arg	Arginine	R
Asn	Asparagine	N
Asp	Aspartic acid	D
Cys	Cysteine	C
Glu	Glutamic acid	E
Gln	Glutamine	Q
Gly	Glycine	G
His	Histidine	H
Ile	Isoleucine	I
Leu	Leucine	L
Lys	Lysine	K
Met	Methionine	M
Phe	Phenylalanine	F
Pro	Proline	P
Ser	Serine	S
Thr	Threonine	T
Trp	Tryptophan	W
Tyr	Tyrosine	Y
Val	Valine	V

ABBREVIATIONS

AD: Alzheimer's disease

ALS: amyotrophic lateral sclerosis

CK1: protein kinase CK1

CK2: protein kinase CK1

CMT2: Charcot-Marie-Tooth type 2

dHMN: distal hereditary motor neuropathy

DUIM: double-sided ubiquitin interacting motif

G-CK: genuine-protein kinase

HD: Huntington's diseases

Htt: huntingtin

IF: immunofluorescence

IP: immunoprecipitation

ND: neurodegenerative disease

PD: Parkinson's disease

PK: protein kinase

Poly-Ub: poly-ubiquitylated

pSer: phospho-serine

pThr: phospho-threonine

pTyr: phospho-tyrosine

SPR: surface plasmon resonance

Ub: ubiquitin

UBD: ubiquitin binding domains

Ub-clients: ubiquitylated-clients

Ub-proteins: ubiquitylated proteins

UIM: ubiquitin interacting motif

UPS: ubiquitin proteasome system

WB: western blot

Part I

Introduction

Chapter 1

Protein phosphorylation

The discovery of protein phosphorylation began with the classic studies on glycogen metabolism (Cohen, 2002). The first observation that the enzyme responsible of glycogen degradation, the so called glycogen phosphorylase, exists in two different states was performed by Carl and Gerty Cori in the late 1930s (*ex-aequo* Nobel Prize for Medicine in 1947). However, only in the '50s Edmond H. Fischer and Edwin G. Krebs (*ex-aequo* Nobel Prize in 1992) clarified that the Cori's observation corresponds to a change in the phosphorylation state of the enzyme catalysed by the later called phosphorylase kinase. The second kinase to be discovered was the cAMP-dependent kinase (PKA) which earned Earl Southerland the Nobel Prize in 1971. In the '80s Paul Nurse (Nobel Prize in 2001) showed that the cell cycle is profoundly regulated by phosphorylation; in the same years T. Hunter discovered the phospho-tyrosine residues (Eckhart et al., 1979). Since then, protein phosphorylation has been established as a mechanism of regulation in cell division, metabolism, movement, survival and apoptosis.

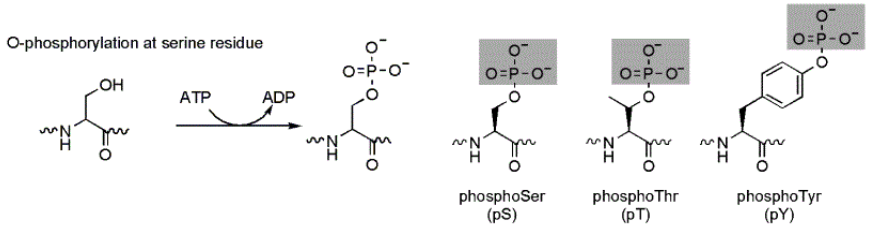

Figure 1.1: **Protein phosphorylation**
Schematic representation of the phosphorylation of a serine residue catalysed by a protein kinase. The figure also reported the structure of phospho-threonine and phospho-tyrosine residues. Adapted from Walsh et al. (2005).

The phosphorylation reaction is catalysed by protein kinases (PKs). Their mechanism of action is exemplified in Figure 1.1: they use ATP (or rarely also GTP) as phospho-donor to transfer the γ-phosphate (γ-PO_3^{2-}) onto phospho-acceptor substrates. The reaction is supported by magnesium or manganese co-factors which chelate the α- and β- phosphate groups on ATP. The reaction is unidirectional and the γ-PO_3^{2-} is bound to serine (Ser), threonine (Thr) or tyrosine (Tyr) residues to make pSer, pThr, pTyr phospho-residues (Figure 1.1). Therefore, proteins achieve a net negative charge that can have a huge impact on their structure and function. The reaction is reversed by protein phosphatases.

1.1 The human kinome

Protein kinases are among the largest protein families in the cell proteome and are collectively known as "the human kinome" (Manning et al., 2002) (Figure 1.2). Members can be either classified by substrate specificity or by evolutionary basis. The first divides PKs in tyrosine kinases (TKs) or serine/threonine kinase (S/TKs). The latter classification distinguishes among 518 PKs: 478 canonical protein kinases, 40 atypical protein kinases and 106 pseudokinases. Atypical PKs share kinase activity but have dissimilar catalytic domains.

The main branches in the eukaryotic PKs tree are: tyrosine kinases (TKs), cyclic nucleotide- and calcium-phospholipid-dependent kinases (AGC, which comprises PKA, PKG and PKC subfamilies), Ca2+/calmodulin kinases (CAMK), the CMGC group (including cyclin-dependent kinases (CDKs), mitogen activated protein kinases (MAPKs), glycogen synthase kinase (GSK), homeodomain-interacting protein kinases (HIPKs) and protein kinase CK2, homologous of yeast sterile 7, sterile 11, sterile 20 kinases (STE), tyrosine kinase-like (TKL) and casein kinase 1 family (CK1).

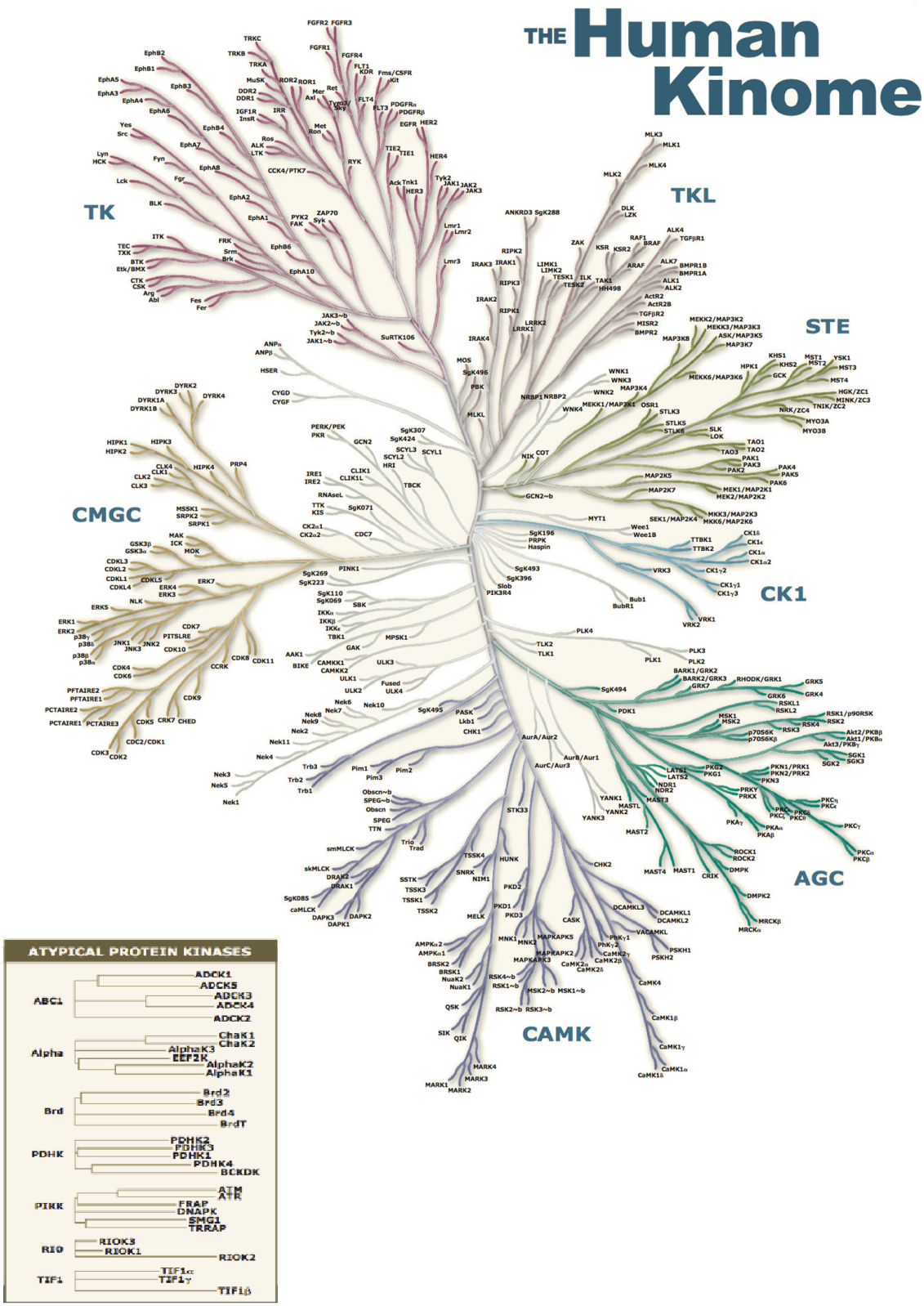

Figure 1.2: **The human kinome**

Dendrogram showing the evolutionary relationships between human protein kinases (Manning et al., 2002) (Adapted from Cell Signaling Technology).

1.2 Common structural features

The first protein kinase structure was determined for PKA (Taylor et al., 1993). Since then, many crystals have been solved unveiling common features between PKs.

The catalytic domain contains the pocket for ATP and the sites for Mg^{2+}/Mn^{2+} (co-factors) interaction. It cooperates in orienting the substrate in order to have the γ-$PO_3{}^{2-}$ transferred from ATP. The catalytic core is embedded between two distinct PK lobes:

- The N-terminal lobe is made by five β-sheets coupled to one α-helix known as αC-helix (see Figure 2.1 as an example). It has a glycine-rich loop containing the motif G-x-G-x-x-G. The N-term lobe also contains:
  - the ATP binding pocket;
  - the catalytic loop that contains a conserved Asp and Lys amino acids, essential for the catalysis;
  - the Mg^{2+}/Mn^{2+} binding loop which contains the conserved motif D-F-G. The D residue switches between two available conformation: 'in' when PK is active and therefore able to bind co-factors, 'out' when is inactive;
  - the T-loop or activation loop which gates the accessibility to the catalytic core. Many PKs reach full activity when the T-loop is phosphorylated by upstream PKs and is consequently displaced;
  - the substrate binding site.
- The C-terminal lobe is rich in α-helices and is essential in accommodating substrates.

Despite these general characteristics, many differences are known in individual PKs. For example, constitutively active PKs do not require the phosphorylation of their T-loop to be activated. Among them, an outstanding example is protein kinase CK2 (since constitutively active, ubiquitously expressed and a critical hub between numerous cell-survival pathways).

Chapter 2

Protein kinase CK2

The characterization of protein kinase CK2 started in 1883 with the pioneering studies of Olaf Hammarsten who reported small traces of phosphorus bound to the protein casein (Hammarsten, 1883). Phosphorous was bound to Ser residues on casein with a marginal contribution of Thr but not Tyr residues. In 1954, Burnett and Kennedy were able to isolate a liver proteinaceous fraction. It contained the enzyme responsible for transferring phosphate from ATP to casein *in vitro* (Burnett and Kennedy, 1954). Whilst this activity was found in all mammalian tissues and conserved throughout organisms, the isolated fraction contained two distinct enzymes, none of which were able to phosphorylate casein *in vivo*. These enzymes were later named protein kinase CK1 and protein kinase CK2 although they are still known with the misleading names of Casein Kinase 1 and Casein Kinase 2 (Venerando et al., 2014). The minimal consensus sequences required by substrates in order to be phosphorylated by CK1 or CK2 were not fully superimposable with casein phosphoresidues. It is now clear that the kinase responsible for the phosphorylation of casein *in vivo* is the genuine casein kinase (G-CK). Interestingly, whilst the G-CK activity was already discovered, the positioning of the enzyme in the human kinome remained unknown till the 21th century when Tagliabracci and collaborators showed that it is placed outside the PKs evolutionary tree (Tagliabracci et al., 2012). The analysis of CK1 and G-CK goes beyond the purposes of this thesis but it is worth to mention that CK1 is involved in diverse neurodegenerative diseases (NDs) such as Alzheimer's disease (AD) and Parkinson's disease (PD), infectious disease, hepatitis C and cancer.

G-CK instead, has been recently associated with syndromes characterized by ectopic calcification deposits (Tagliabracci et al., 2012; Venerando et al., 2014).
CK2 is present in all tissues and phosphorylates hundreds of proteins involved in practically all cellular processes: CK2 alone accounts for up to 20% of the entire cellular phosphorylations, compared with more than 500 PKs. CK2 is constitutively active, since it does not require any phosphorylation event or signal to be activated, and is essential for cellular life and survival. The enzyme is implicated in cell cycle regulation, cell proliferation, and gene expression. It has a global anti-apoptotic role, meaning that it counteracts the so called "programmed cell death" (or apoptosis), whose occurrence is essential for healthy conditions. It is not surprising that CK2 has a pivotal role in tumours, where it can sustain abnormal cell proliferation and survival. Indeed, CK2 has been found overexpressed in all tumours where a direct comparison with their healthy counterpart has been performed (Ruzzene and Pinna, 2010). This immediately suggested that CK2 could be a putative target for anti-cancer drugs. Moreover, there are now compelling evidences that CK2 could exert a prominent role also in neuronal function, possibly neurodegeneration, where CK2 inhibitors can be explored as novel therapeutics tools.

2.1 Protein kinase CK2 structure

CK2 is a tetrameric enzyme composed of two catalytic and two regulatory subunits. The gene *CSNK2A1* codifies for α catalytic subunits of 45 kDa while the gene *CSNK2B* for 28 kDa regulatory β subunits. Another gene named *CSNK2A2* codifies for an isoform of the catalytic subunit α' (41 kDa) which shares 75% identity with α. Both α and α' can be interchangeable in the tetramer assembly without affecting the enzyme activity. Recently, another *CSNK2A3* gene was characterized and categorized as pseudogene since it does not lead to the production of an active protein. Its physiological relevance is not demonstrated yet (Wirkner and Pyerin, 1999). CK2 is an atypical kinase since its catalytic subunits are constitutively active both as free monomers or when complexed with the

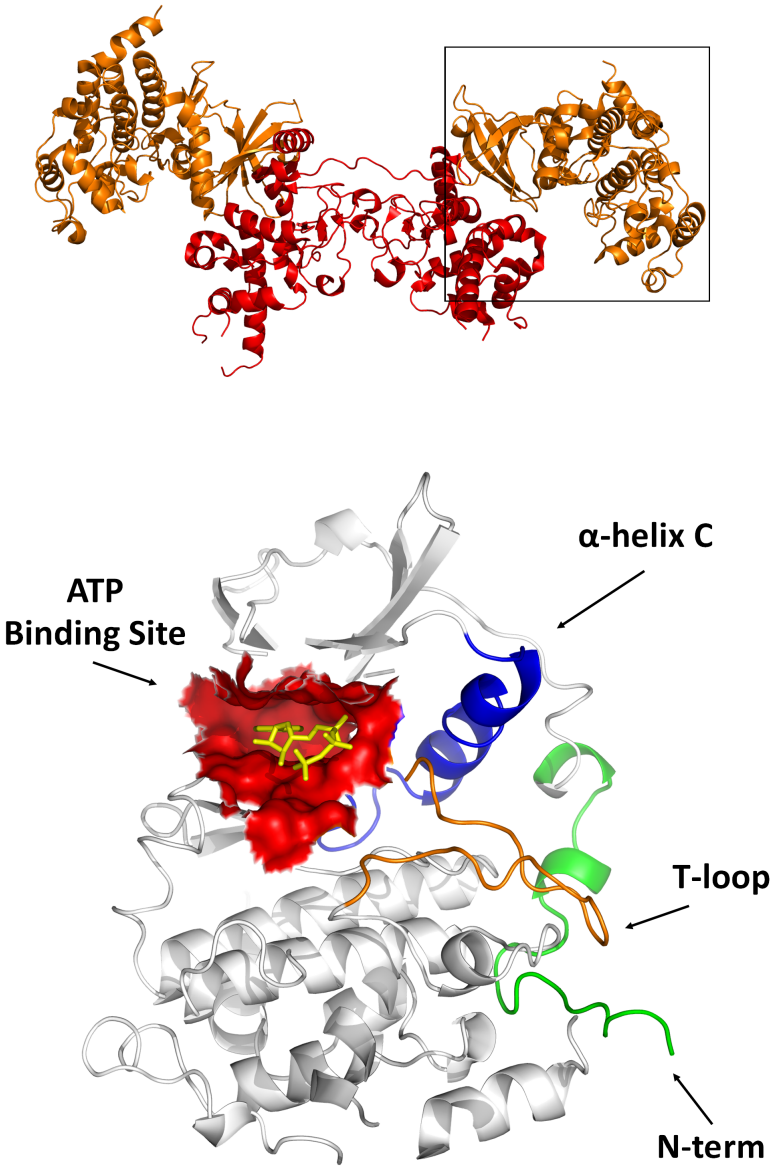

Figure 2.1: **Protein kinase CK2 structural features**
Above panel. CK2 tetrameric structure made by two β regulatory subunits (red) and two α catalytic subunits (gold). **Below panel.** Magnification of an α catalytic subunit showing the nucleotide binding site (red) with the ATP-analog ANP inside the pocket (yellow). The α-helix C (blue), the T-loop (orange) and the N-term (green) are also highlighted. The figures are generated by the PDB entry 4MD8 with PyMOL software.

regulatory β. Unlike other PKs, CK2 does not require any phosphorylation event or displacement of inhibitory proteins to reach its full activity. β subunits are not real regulators of the enzymatic activity. Instead, they are important in stabilizing and protecting α subunits from proteolysis, and are regarded as docking stations for specific substrates.

CK2 substrates are categorized in three classes on the basis of their requirement of β subunits (Pinna, 2002). Class I substrates can be phosphorylated by either monomeric or tetrameric CK2. Class II substrates are recognized by free α/α' CK2, while the tetramer heavily impairs their phosphorylation. Finally, class III substrates strictly depend on the tetrameric enzyme. However, the physiological relevance of this classification is not known yet, since the occurrence of free catalytic subunits in cells is still a matter of debate.

The resolution of the CK2 tetrameric structure contributed to decode the reasons of its peculiarities. The enzyme structure was solved in 2001 (Niefind et al., 2001): the CK2 tetramer has a butterfly shape with a central β-dimer and two α-subunits, one on each side and not in contact between them (Figure 2.1). The catalytic subunits belong to the CMGC subfamily and display the structural motifs conserved throughout the human kinome: a small lobe rich in β-strands, a large lobe rich in α-helices separated by a short loop called 'hinge region'. However, CK2 has some exceptional features:

- usually, the access of ATP, co-factors and substrates to the respective binding sites on PKs are gated by the T-loop. The full activation of the enzymes requires the displacement of the activation loop, usually mediated by single/multiple phosphorylation(s) of key residues. In CK2, the N-terminal region (residues from 1 to 30) plays a fundamental role in maintaining the T-loop always in the 'active state' in the absence of any phosphorylation event. Therefore, it accounts for the constitutive activity of CK2;

- the third Gly residue in the common G-x-G-x-x-G motif is replaced by Ser that plays a crucial role in the substrate recognition at the n-2 position. Furthermore, the presence of the α-helixC favours the binding to substrates at the positions n+1 and n+3. This is due to unique stretches of basic residues located in and nearby the α-helixC;

- the cofactor-binding site motif D-F-G is substituted by the sequence D-V-G that blocks the D residue always in the 'in' active position;

- the nucleotide-binding cleft can either bind ATP or GTP as phospho-donors. CK2 displays bulky residues (Val66 and Met163) at positions where most PKs present Ala and Leu, respectively. This accounts for the reduced size and higher hydrophobicity of the CK2 phosphonucleotide cavity. These features make CK2 sensitive to the inhibition by relatively small and hydrophobic compounds (i.e. CX-4945);

- the regulatory β subunits are conserved and unique in the eukaryotic kingdom. They host sites (Ser2 and Ser3) that are auto-phosphorylated by CK2; their phosphorylation has no effect on the kinase activity, but are regarded to stabilisers of the enzyme structure (Zhang et al., 2002). Indeed, these auto-phosphorylation sites have been recently proposed to lead to supramolecular complexes made by CK2 tetramers, and for which a functional explanation is still pending (Pagano et al., 2005).

2.2 Protein kinase CK2 physiopathology

CK2 is a ubiquitous kinase and its constitutive activity has represented a fascinating enigma for scientists and a big burden for the discovery of its function. Moreover, the CK2 deregulated expression has been showed to contribute to the onset of several pathologies, mainly cancer. Therefore, unveiling the function of CK2 is still a priority in searching for treatments for human diseases.

CK2 is ubiquitously expressed and localizes in all cellular compartments, where it phosphorylates hundreds of substrates (Meggio and Pinna, 2003). While the enzyme has been shown to control many cellular processes, its extraordinary pleiotropicity delayed the discovery of a general physiological function.

2.2.1 Protein kinase CK2 is a pro-survival kinase

The main role of CK2 is to counteract apoptosis (Ahmad et al., 2008; Duncan et al., 2010; Ruzzene and Pinna, 2010) and nowadays it is considered a global anti apoptotic kinase.

CK2 is a constitutively active enzyme and cooperates with several pathways that are activated by external signals; therefore, it represents a lateral player: it works from the side in order to potentiate 'vertical', descending pro-survival pathways such as the PI3K/Akt (PKB), NF-kB, Wnt and DNA repair signalling. They are briefly described below (Figure 2.2):

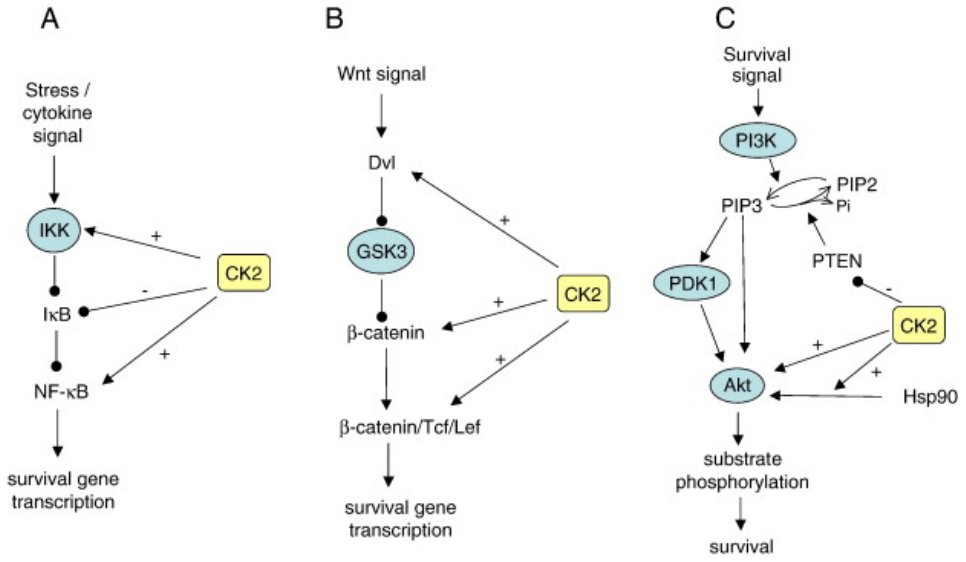

Figure 2.2: **Main descending pro-survival pathways influenced by the 'lateral player' CK2.** Lateral CK2-dependent regulation (yellow) of descending (blue) NF-κB **(A)**, β-catenin **(B)** and Akt **(C)** signalling pathways. A negative effect is indicated by the minus symbol (–) while a positive effect by the plus symbol (+). Adapted from Ruzzene and Pinna (2010).

- NF-kB is a transcription factor for anti-apoptotic and pro-proliferation genes and is essential for cell development. NF-kB is retained in the cytosol when complexed to IkB. Upon upstream stimuli, IKK phosphorylates IkB causing its degradation. In turn, NF-kB is free to move in the nucleus where it promotes gene transcription. The deregulated activity of the NF-kB pathway promotes oncogenesis (Garg and Aggarwal, 2002) and the intervention of CK2 occurs at multiple levels. Indeed, CK2 was demonstrated to phosphorylate IkB favouring its degradation. (McElhinny et al., 1996). Furthermore, CK2 regulates IKK expression (Eddy et al., 2005) and prevents

IkB association to NF-kB by phosphorylating β-arrestin (Luan et al., 2005). Finally, CK2 phosphorylates the p65 subunit of NF-kB enhancing its functionality (Wang et al., 2000).

- Wnt/β-catenin is a proliferation signal essential for the embryonic development and often found deregulated in cancer. CK2 phosphorylates β-catenin thus stabilizing the protein (Song et al., 2003), whereas GSK3 activity promotes its degradation. Moreover, CK2 phosphorylates the upstream protein dishevelled (Dvl) and primes it as CK1 substrate. This, in turn, promotes Dvl synthesis (Bernatik et al., 2011).

- PI3K/Akt is a pro-survival signalling pathway. Particularly, the lipid phosphatase activity of the tumour suppressor phosphate and tensin homologue deleted on chromosome 10 (PTEN) has a net inhibitory effect on this pathway. It dephosphorylates PIP3 thus maintaining the pro-survival signalling down. CK2 stabilises PTEN while decreasing its phosphatase activity (Torres and Pulido, 2001). Whilst many cancer cells have been shown to loose PTEN expression, it is easily conceivable that also PTEN-expressing cells could display an hyperactive PI3K/Akt partway whenever CK2 activity is increased. CK2 is also able to phosphorylate neprilysin preventing its inhibitory effect on PTEN (Siepmann et al., 2010). Furthermore, CK2 directly phosphorylates Akt at Ser129. This is an additional phospho-site in respect to the canonical Thr308, Ser473, and contributes to the full-activation of Akt (Di Maira et al., 2005). Currently, phospho-Ser129 Akt is regarded as one of the most reliable probe for CK2 activity. In fact, the high turnover at this Akt site allows to easily monitor the CK2 activity in response to inhibitors. The up-regulation of the Ser192 Akt phospho-signal supports the aberrant activity of the PI3K pathway, as demonstrated in several cancer cells. Moreover, the inhibition of CK2 is detrimental for the survival of these neoplastic cells. This has been reported in various blood malignancies such as leukemia (Piazza et al., 2012), in prostate, breast, lung cancers, glioblastoma, skin squamous carcinomas and thyroid cancer (Guerra and Issinger, 2008).

  Beside the direct phosphorylation of Akt by CK2 (Di Maira et al., 2005),

there are other connections between these two enzymes such as their direct association (Guerra, 2006). Moreover, CK2 promotes the binding of Akt to the chaperone Hsp90 which protects the Thr308 phospho-residue from the activity of protein phosphatases thus maintaining the pathway active (Di Maira et al., 2009). All together, these findings demonstrate that the CK2 and Akt functions are intimately related.

Many other substrates have been identified for CK2 that are related to its pro-survival anti apoptotic function. In the nucleus, CK2 binds and phosphorylates the transcription factor IIIB mediating the activation of the DNA repairing system by the RNA-polymerase III. RNA-polymerase I and II activity is also influenced by the CK2-mediated phosphorylation of other transcription factors and proto-oncogenes (i.e. c-Fos, c-Jun, c-Myb and c-Myc).

2.2.2 CK2 and cancer

The CK2 activity is strictly connected to pro-survival and pro-proliferation conditions. CK2 is a pro-survival kinase fundamental for cell growth and viability. It supports, among others, the Wnt and NF-kB signalling pathways and its activity is essential during embryogenesis. Consistently, CK2 knock-out in test animals was lethal during embryogenesis (Dominguez et al., 2009). Therefore, CK2 inhibition is detrimental during development; however it is a powerful strategy in treating cancer.

The involvement of CK2 in cancer has been demonstrated in several models. Acute and chronic myelogenous leukemia was the first blood cancer in which abnormal levels of CK2 were reported. In this pathology CK2 is now considered as an unfavourable prognostic marker (Wang et al., 1995; Kelliher et al., 1996). Since then, CK2 was shown to lead to proliferation of lymphoid cells in several haematological malignancies (Piazza et al., 2012). Abnormally high levels of CK2 have been reported in several solid tumours (Guerra and Issinger, 2008) such as squamous cells carcinoma of the head and neck and in colon, rectum, kidney and prostate cancers. In breast cancer CK2 promotes the aberrant activation of the Wnt signalling (Dominguez et al., 2009; Filhol et al., 2015). In any case, cells with higher levels of CK2 are positively selected since they owe survival advantages

toward apoptotic signals (Figure 2.3). The mechanism by which CK2 elevates in cancer remains to be understood. It might involves the stabilization of the CK2 mRNA or the inhibition of the enzyme degradation.

CK2 is also involved in the mechanism of drug resistance to apoptosis, and in a MDR (multidrug-resistant) leukemia cell line was reported an unbalanced expression of the α/α' and β subunits (Di Maira et al., 2007). Moreover, the inhibition of CK2 can promote an increased sensitivity to pro-apoptotic drugs in different resistant cells. To date, no gain-of function mutations have been found in the CK2 genes and it cannot be considered a proper oncogene. Therefore, cancer cells are presently regarded as 'addicted' to CK2 (Ruzzene and Pinna, 2010) and the enzyme represents an example of 'non oncogene addiction' of tumours (Solimini et al., 2007). This refers to the observation that cancer cells rely on CK2 more then normal ones for their survival. This is probably due to the fact that, in tumours, several pro-survival pathways crucially require CK2 to be fully active and promote tumourigenesis. Addiction also explains why cancer cells are more sensitive than normal ones to CK2 inhibition (Cozza et al., 2013) or to its genetic ablation (Borgo C, Salvi M, personal communication). The encouraging results obtained with CK2 inhibitors in test animals (reviewed in Venerando et al. 2014) and in clinical trials, fully confirm that tumour cells are more sensitive then healthy cells to the CK2 reduction.

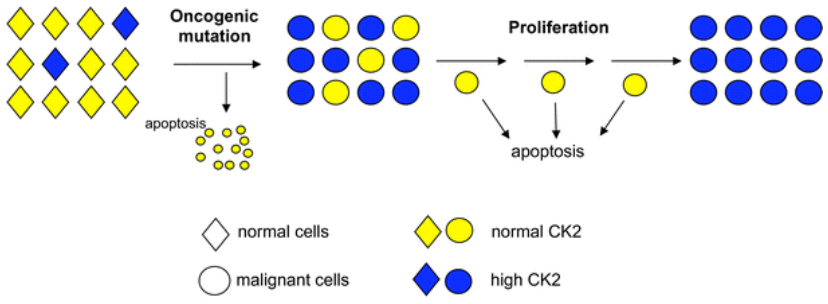

Figure 2.3: **Selection of cancer cells.**
Selection by malignancy of cancer cells expressing higher levels of CK2. Adapted from Ruzzene et al. (2011).

2.2.3 CK2 and other diseases

The multi-faceted profile of CK2 suggests a broader involvement in other human diseases. Without the pretension to be exhaustive, it is worth to mention the enzyme role in inflammatory processes where a deregulated expression of CK2 was found (Guerra and Issinger, 2008). Moreover, CK2 was shown to be a stress-induced PK in response to UV irradiation through a mechanism mediated by p38 MAP kinase (Kato et al., 2003). The enzyme was also demonstrated to enhance the production of prostacyclin and prostaglandin E2 by phosphorylating the angiotensin-converting enzyme (Kohlstedt et al., 2002). CK2 was reported to be a key regulator of angiogenesis and angiogenesis-related diseases further suggesting its importance in tumour growth. CK2 promotes the formation of newly synthesized vessels in cultured retinal endothelial cells (Ljubimov et al., 2004). Moreover, it was shown to mediate disease severity in a mouse model of oxygen-induced retinopathy where the CK2 inhibition by CX-4945 ameliorates the pathology (Kramerov et al., 2006). Results suggested that CK2 inhibitors can counteract vessels formation and they can be useful for the treatment in angiogenesis-related pathologies. To be mentioned, the CK2 deregulated activity was reported in cardiovascular diseases such as cardiomyocyte hypertrophy, in autoimmune disease (Crunkhorn, 2016) and in viral infections, where CK2 promotes the HIV-1 reverse transcriptase activity (Harada et al., 1999).

Among the several diseases where the enzyme is involved, we can mention the CK2/cystic-fibrosis associated channel (CFTR) interconnection. Recently, CFTR was shown as phosphorylated by CK2 and this leads to its degradation. Moreover, CK2 inhibition by CX-4945 was shown to increase CFTR half-life with important therapeutic implication in the treatment of cystic fibrosis (Venerando et al., 2013).

2.2.4 CK2 and neurodegeneration

CK2 has a pleiotropic distribution throughout the brain (with a preferential expression in neurons than in the glia) where it phosphorylates substrates related to synaptic transmission, neuritogenesis, long-term potentiation and plasticity (Guerra and Issinger, 2008).

A prominent role of CK2 in neurodegeneration has been suggested (Meggio and

Pinna, 2003; Pagano et al., 2006) and related to several neurodegenerative disorders. A strong enzyme staining was found in neurofibrillary tangles, the hallmarks of Alzheimer's disease (Iimoto et al., 1990), and appeared to correlate to disease severity. CK2 phosphorylates the protein tau *in vitro*, but its relevance for the disease is not clear yet. In Parkinson's disease CK2 was found to phosphorylate α-synuclein at Ser129, a hallmark of Parkinson's disease proteinaceous inclusions termed Lewy bodies (Okochi et al., 2000). Interestingly, immunohistochemical studies showed a marked presence of the CK2 β, but not α, subunits suggesting a specific role in alpha-synucleinopathies of the CK2 regulatory particles. Among others, a role for CK2 was suggested in Guam-Parkinson dementia, supranuclear palsy and Pick's disease (Guerra and Issinger, 2008).

Presently, the importance of CK2 is also emerging in memory where it appears to sustain the synaptic and cognitive functions (Bulat et al., 2014). Moreover, mutations in the CK2 gene *CSNK2A1* were recently reported as causative of neurodevelopmental disorders associated with developmental delay, intellectual disability, behavioural problems, hypotonia, speech problems, microcephaly, and dysmorphic features (Okur et al., 2016).

In summary, there are compelling evidences for a physiopathological role of CK2 in the brain, possibly neurodegeneration, that are still challenging and to be examined in details.

2.3 CK2 inhibitors

Protein kinase CK2 is a prominent druggable target. Indeed, cells relying on its increased amount (referred to as addicted to CK2, see Chapter 2.2.2) have been characterized as more sensitive to the inhibition of the enzyme (Ruzzene and Pinna, 2010). This promoted the designing and testing of several inhibitory compounds (Cozza et al., 2012). The use of inhibitors is of invaluable support in a therapeutic prospective and in helping understanding the physiopathological role of CK2. Most of the inhibitors developed so far are targeting the ATP-binding site on CK2. Whilst the structure of the ATP pocket is shared by most of PKs, CK2 has distinguished structural features initially reported by Niefind and collaborators in *zea mays* (Niefind et al., 1998). Briefly, the CK2 ATP-binding site is smaller, due to the presence of bulky and more hydrophobic residues (namely Val66, Ile66 in *zea mays*, and Ile174) in respect to others PKs (see Chapter 2.1 for more detailed information). Therefore, CK2 is sensitive to relatively small inhibitors (Cozza et al., 2013). On the contrary, the enzyme has low responsiveness to compounds with bigger molecular masses, particularly staurosporine, which instead targets the majority of PKs (Meggio et al., 1995).

The design of inhibitors targeting the ATP-binding pocket has been deeply exploited producing a variety of compounds. They share an hydrophobic core and hydrophilic portions that take advantage of a peculiar charge distribution of the ATP pocket in CK2. Inhibitors aiming at hitting CK2 should particularly target the Val66 and Ile174 residues with their hydrophobic portion. Moreover, contacts should be also established both with the hinge and the phosphate-binding regions (particularly the Lys68 residue, essential for catalysis). Therefore, they will acquire competitiveness against ATP and water molecules in order to access the CK2 nucleotide-binding pocket. The prototype of inhibitors with such characteristic is CX-4945 that reached clinical trials (Siddiqui-Jain et al., 2010). CX-4945 displays an IC_{50} of 2 nM *in vitro*. When inhibitors are tested in cells, their DC_{50} (the concentration able to induce 50% of cell death) displays discrepancies in respect to the IC_{50} value. This phenomenon is usually observed with PKs inhibitors. It is partly due to the high concentration of intracellular ATP, beside the dilution factors that contribute to reduce the real inhibitor concentration

in the cellular compartments. Another aspect that should be considered is the residence time of inhibitors inside the ATP pocket. As we suggested in a recent paper (Girardi et al., 2015) this could differ between inhibitors thus affecting the therapeutic doses that could be potentially used in clinic. The compounds used in this work are hereafter briefly described.

TBB (or 4,5,6,7-tetrabrombobenzotriazole) is a benzimidazole molecule derived from DRB, or 5,6-dichloro-1-(β-D-ribofuranosyl)benzomidazole, the first ATP-mimetic CK2 inhibitor described (Zandomeni et al., 1986). Benzimidazole compounds present an hydrophobic region made by a benzene ring with four bromine atoms. They establish interactions with the Val66 and Ile174 inside the CK2 ATP binding pocket and with the hinge region. TBB has been largely employed as CK2 inhibitor and displays a good selectively and an IC_{50} of 0.16 μM (Sarno et al., 2001).

CX-4945, or 5-3-(Chlorophenyl)amino]benzo[c][2,6]naphthyridine-8-carboxylic acid, is a carboxyl acid derivative from indoloquinazoline (the first compound belonging to this class and developed by Novartis). CX-4945 establishes contacts with the nucleotide-binding pocket of CK2 and has the strongest potency with a significant selectively for CK2. CX-4945 was firstly patented by Cylene Pharmaceuticals. It is also called Silmitasertib and is presently in clinical trials. We also exploited a molecule modified from CX-4945: CX-5011. This compound substitutes the pyridine core of CX-4945 with a pyrimidine that confer specificity for CK2, when compared to a wide panel of PKs (Battistutta et al., 2011).

Many other CK2 inhibitors, also derived from natural compounds (i.e. emodin, ellagic acid), have been developed so far. They usually display IC_{50} in the low μM range and lower selectivity in respect to CX-4945. A detailed descriptions of them goes beyond the focus of this thesis and an exhaustive review was recently published (Cozza et al., 2013). Beside ATP-competitive inhibitors, we also investigated novel strategies to inhibit CK2 (see Part V - related projects).

2.4 Protein kinase CK2 specificity

The CK2 consensus sequence has been extensively investigated (Meggio et al., 1994; Salvi et al., 2009) and is one of the most specific and well-defined among PKs. Figure 2.4 reports the minimal sequence displayed by CK2 substrates compared to the one of CK1 and of G-CK. CK2 is an acidophilic kinase that prefers Ser/Thr sites surrounded by acidic residues. The minimal requirement is represented by an acidic determinant (E/D/pS/pT) at position +3 downstream to the target site (Figure 2.4A). A bioinformatic analysis of more than 500 *bona fide* CK2 substrates generated a graphical analysis of its preferences around the phospho-acceptor site (Figure 2.4B) (Cesaro et al., 2015). Beside the residues at position +3, CK2 displays a preference for acidic residues spanning the sequence -7/+7 in respect to the phospho-site. Basic residues are negatively selected while a proline residue at position +1 is absolutely detrimental. CK2 is also a priming kinase for its own sites since pSer or pThr residues can substitute for glutamic (E) or aspartic (D) acids as determinants for CK2 recognition. Indeed, the phosphorylation of amino acidic residues is often a hierarchical event, where the activity of PKs primes the sequence for the recognition by other enzymes. Moreover, a recent phosphoproteomic analysis suggests that stretches of pSer/pThr residues are highly phosphorylated in the human proteome (Sharma et al., 2014). A physiopathological example of such phenomenon is the GSK3β/CK1 hierarchical phosphorylation of the protein Tau which enhances its aggregation propensity in AD (Hanger et al., 2007).

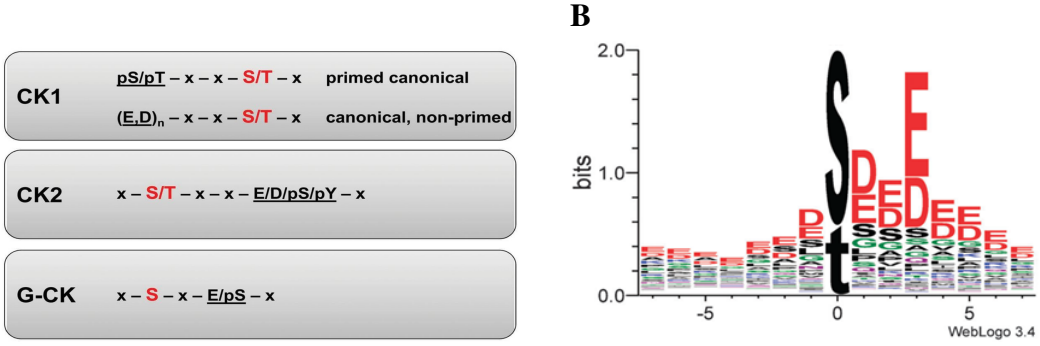

Figure 2.4: **Protein kinases consensuses.**
A. CK1, CK2, G-CK phospho-consensuses (Venerando et al., 2014). **B.** The most representative amino acidic residues found, among CK2 substrates, in the neighbourhood of phospho-Ser/Thr. (Cesaro et al., 2015).

Chapter 3

Protein Ubiquitylation

Ubiquitylation is the dynamic and reversible post-translational modification of proteins by linking the small protein ubiquitin (Ub). The high complexity of the pathways involved has emerged as pivotal in diverse cellular functions and proteostasis.

3.1 The ubiquitylation machinery

Ub is a small protein of 76 amino acids, ubiquitously expressed and conserved among eukaryotes. It folds in a compact β-sheet with an hydrophobic patch constituted by Leu8, Ile44, and Val70 amino acids. Ub can be covalently bound to substrates by a 3-step catalysis (Figure 3.1). First, Ub is activated by 'activating enzymes E1'. Two ATP-dependent E1 are expressed in humans and catalyse the formation of a thioesteric bond between the Ub C-terminus and a Cys residue on the enzyme. Ub is then transferred to a Cys residue on conjugating enzymes E2 (around 40 are expressed in the human proteome). In the final step, E2 links E3 enzymes thus leading to the binding of Ub to Lys residues on target proteins. Less frequently, Ub can be also attached to Cys, Ser, Thr residues or to the substrates N-terminus. More than 600 E3 enzymes have been identified and account for substrate specificity. The reaction is reversed by deubiquitinating enzymes (more then 100 are known) (Husnjak and Dikic, 2012).

Protein ubiquitylation comes in different flavours: Ub can be linked to substrates either as a single (mono-ubiquitylation), multiple (multiple mono-ubiquitylation)

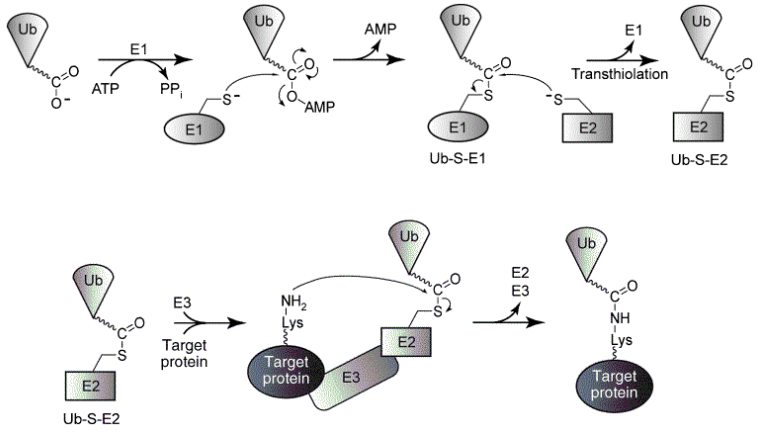

Figure 3.1: **Protein ubiquitylation**
The picture depicts a typical ubiquitylation reaction which started with the activation of the C-terminus of ubiquitin by E1 enzymes. Following, ubiquitin is transferred to a Cys residue in the active site of E2 enzymes. Finally, E3 enzymes recruit specific proteins for ubiquitylation at Lys side chains (Walsh et al., 2005).

or chained molecule (poly-ubiquitylation). In the latter case, several Ub moieties are linked via isopeptide bonds: iterative ubiquitylation cycles lead to the formation of branched Ub chains by utilizing any of the seven available Lys residues on the Ub molecule (Lys 6, 11, 27, 29, 33, 48 or 63) as well as the N-terminus (linear poly–Ub). Strong evidences showed that poly-ubiquitylated (poly-Ub) chains of different typologies channel proteins to specific cellular pathways (Figure 3.2). There are growing evidences that Lys-48 poly-Ub chains convey proteins to proteasomal degradation. Lys-63 linked chains have been implied in lysosomal-endosomal protein trafficking and non-proteolytic functions. However, several findings support a wide interplay between different type of poly-Ub chains and their respective significance in cell signalling. Moreover, the role(s) of other poly-Ub is not fully elucidated yet (Sokratous et al., 2014).

3.2 Ubiquitin binding domains

Different protein classes mediate the ubiquitylation, deubiquitylation and transport of ubiquitylated cargoes. They contain one or more ubiquitin binding domains (UBDs) able to non-covalently interact with Ub in its β-sheet hydrophobic region. More than 20 UBD have been described so far. In addition to the topology of Ub-chains, UBDs account for the specificity of the signalling. Hereafter some

examples are reported (Figure 3.3 and Figure 3.4).

Ubiquitin-associated domain (UBA)

The UBA domain was the first described by comparing sequences of proteins involved in Ub binding and trafficking (Hofmann and Bucher, 1996). They are made by three bundled helices that preferentially bind poly-Ub chains. Class 1 members selectively bind Lys-48 branched moieties while class 2 Lys-63 linked poly-Ub. Class 3 UBAs do not bind Ub and their function is still missing. Finally, proteins containing class 4 UBA bind Ub and poly-Ub without any linkage specificity (Hurley et al., 2006).

Zinc-finger ubiquitin-binding protein domain (ZnF UBP)

The ZnF UBP domain is the second major class of UBD, discovered after a deeper analysis of Ub-binding proteins (Reyes-Turcu et al., 2006). They are divided in subclasses: NZF is a 30-residues domain that binds Ub with very low affinity (K_d of 100 μM or lower); the UBZ domain which occurs in Y-family DNA polymerases; the UBP that is a module found in diverse deubiquitinating enzymes. They are built around a single zinc-binding site fused to an α/β structure. UBPs has an exceptionally high affinity for Ub (3 μM) (Hurley et al., 2006).

Coupling of ubiquitin to ER degradation (CUE)

CUE domains were discovered by aligning sequences of proteins implied in various degradation pathways. The domain is closely related to UBAs and is made by three packed α-helices. CUE binding affinity for Ub can vary as much as 20 - 150 μM in relation to the number of bonds established with Ub (Hurley et al., 2006).

A further class of UBD is represented by the ubiquitin interacting motif (UIM). Given the high relevance of this motif for the purposes of this thesis, UIM features will be described in the following paragraph.

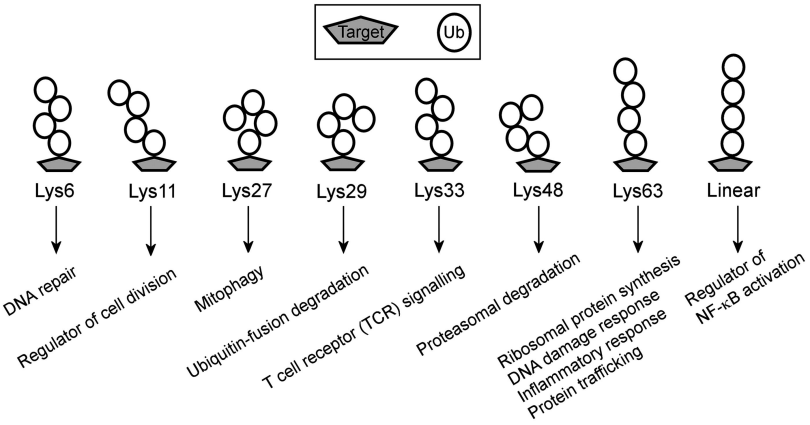

Figure 3.2: **Ubiquitin chains comes in different flavours**
Cellular pathways associated with poly-Ub chains of different typologies. Adapted from Sokratous et al. (2014).

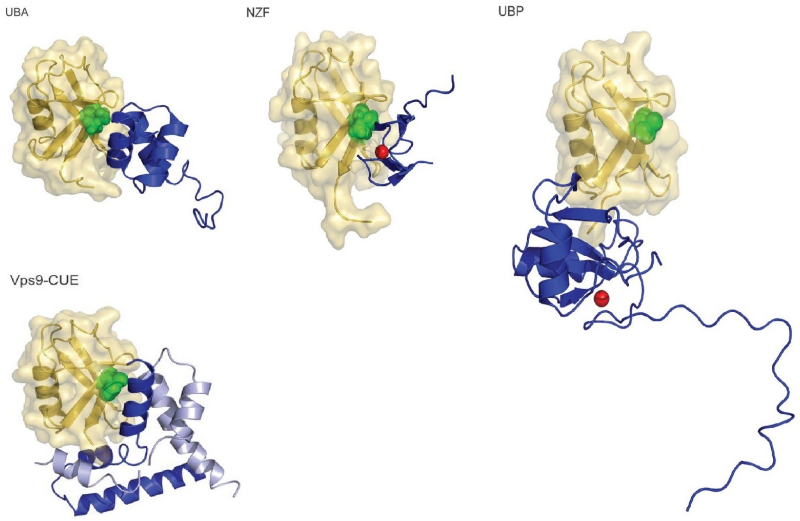

Figure 3.3: **Ubiquitin-binding domain structures**
The ubiquitin molecule (yellow) is shown with the corresponding helical domain (blue). The hydrophobic binding site on ubiquitin is shown as green spheres whereas zinc ions are drawn as red spheres. Protein data bank authentication codes are: UBA, 1WR1; NZF, 1Q5W; UBP, 2G45; Vps9 CUE, 1P3Q. Adapted from Hurley et al. (2006).

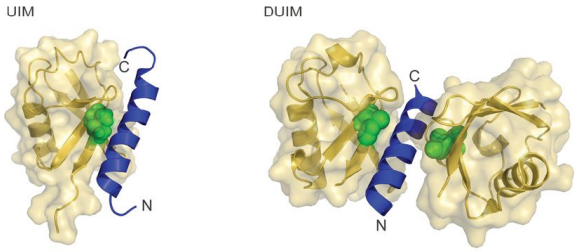

Figure 3.4: **UIM and DUIM domain structures**
The ubiquitin molecule (yellow) is shown with corresponding helical domain (blue). The hydrophobic binding site on ubiquitin is shown as green spheres. Protein data bank identification codes are: UIM, 1Q0W; DUIM, 2D3G. Adapted from Hurley et al. (2006).

3.2.1 The ubiquitin interacting motif (UIM)

The ubiquitin interacting motif (UIM) was firstly described by Hofmann and Falquet in 2001 (Hofmann and Falquet, 2001). It is a short α-helix present in different protein structures thus accounting for differences in its affinity for Ub (Figure 3.4). Indeed, because the UIM is a relatively small cluster, its biological role often depends on the domains in cooperation with it acts (Miller et al., 2004).
UIM has conserved amino acidic determinants that confer affinity for Ub (Figure 3.5), as demonstrated by Hofmann and Falquet. They performed an *in silico* analysis, starting from the protein S5a (or Rpn10), a component of the 19S regulatory subunits of the proteasome. In 1998, the S5a region that interacts with poly-Ub was mapped into two short motifs, present in all S5a homologous (Young et al., 1998). Then, authors searched for other proteins sharing the same domain using the S5a motif as input for a bioinformatic analysis. They characterized a set of proteins containing a conserved sequence of 20 amino acids in length (Figure 3.5): x-E-D-E-x-L-x-x-A-x-x-x-S-x-x-E-x-x-x-x. Uppercase residues were demonstrated to be indispensable for the UIM function. Moreover, Hirano and collaborators identified sub-consensuses inside UIMs that account for their ability to bind Ub moieties at one side (single-sided motif, UIM) or both halves of the α-helix (double-sides motif, DUIM) as exemplified by the crystal structures in Figure 3.4. In the case of the DUIM, residues shape the α-helix with a mirrored arrangement that is likely responsible for its ability to bind ubiquitylated-clients (Ub-clients) on both sides (Hirano et al., 2006).
UIMs have been identified in deubiquitinating enzymes and in one family of HECT E3 Ub-ligases. By contrast, nor E1 or E2 enzymes have been shown to contain UIMs. Interestingly, this domain mainly occurs in proteins involved in endocytic and proteasomal pathways. For example, the protein Eps15 binds to epsin thus inducing the endocytosis of the epidermal grow factor (EGF). Eps15 contains two UIMs separated by a spacer containing the Tyr850 residue that undergoes phosphorylation. Also Vps27, a protein involved in sorting clients to the vacuole, can be Tyr-phosphorylated near its UIM. These examples suggested a possible interplay between phosphorylation signalling and UIM function.

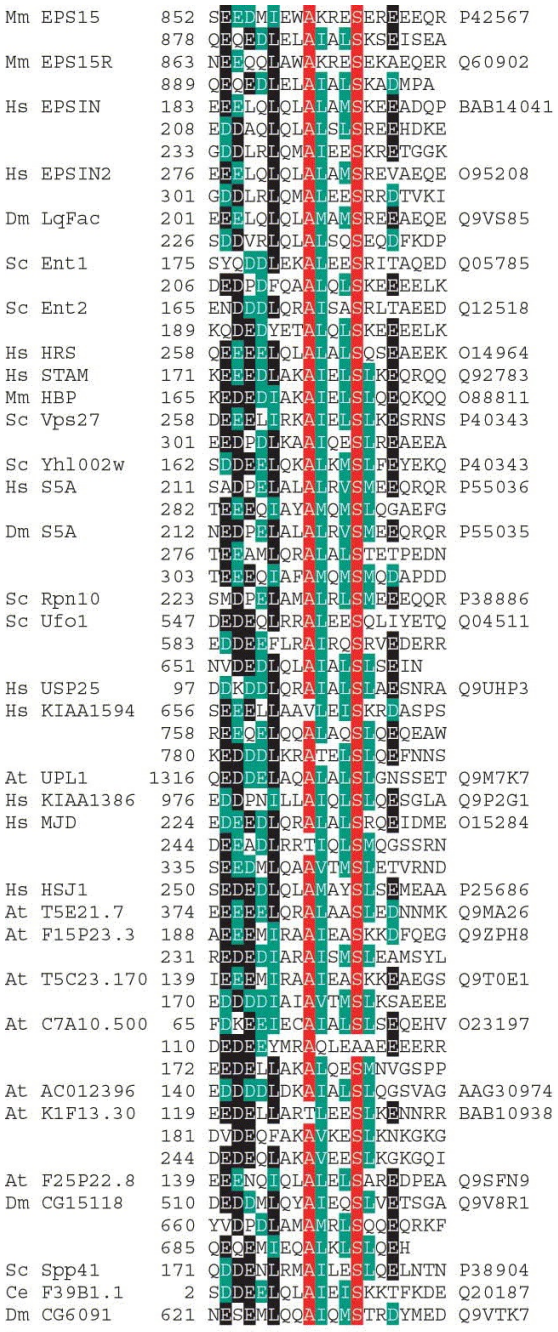

Figure 3.5: **Characterization of the UIM consensus motif**

Alignment of representative proteins containing UIM domains. Residues that are conserved or substituted with amino acids with similar properties in $\geq$50% of the sequences are reported in black and green, respectively. The conserved Ala and Ser positions are in red. The species are given on the left and are followed by the protein name whereas accession numbers to the SwissProt database are given on the right. The bottom line indicates the consensus motif detected: uppercase letters represent positions conserved in $\geq$50% of the sequences and lowercase letters those present in <50%. Abbreviations of organisms are: Hs, *Homo sapiens*; Mm,*Mus musculus*; Dm, *Drosophila melanogaster*; At,*Arabidopsis thaliana*; Ce, *Caenorhabditis elegans*; Sc, *Saccharomyces cerevisiae.* Adapted from Hofmann and Falquet (2001).

Chapter 4

Cellular Proteostasis

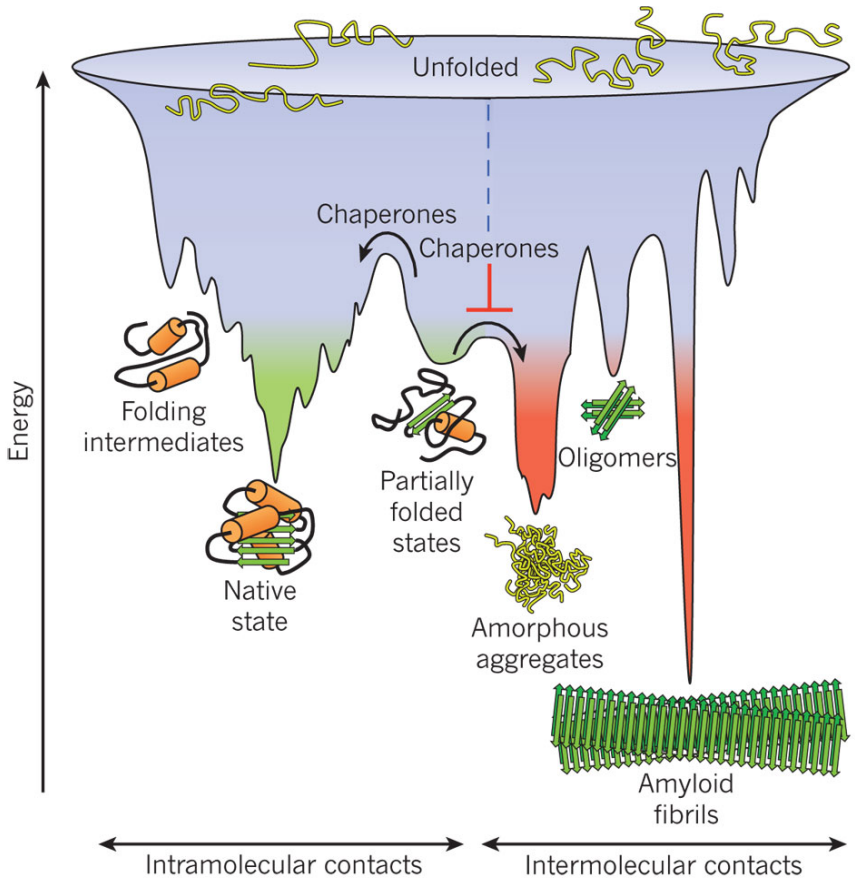

Figure 4.1: **Energy funnel during protein folding**
Schematic representation of the funnel-shaped free-energy that proteins have to explore to reach their native conformation (green). The randomized search results in the accumulation of trapped conformations. *In vivo*, molecular chaperones help proteins to escape the unfolded conformations in order to reach their native state. The crowded environment where protein folding take place may lead to intermolecular aggregation and formation of amorphous aggregates on-pathways to toxic oligomers and amyloid fibrils (red). This is normally prevented by molecular chaperones. Adapted from Hartl et al. (2011).

Cell life evolves in constant need of protein turnover in order to maintain viability. Indeed, proteins are cyclically degraded synthesized and folded to reach functionality. During folding, proteins seek the most thermodynamic favourable conformation. The process can be plotted as a funnel-shaped energy landscape with many high-energy unfolded structures and only a few low-energy folded conformations (Figure 4.1). While proteins are synthesized, hydrophobic interactions drive the spontaneous collapse of the amino acidic sequence in a compact state referred to as 'molten globule'. Then, the funnel further narrows as well as the number of available conformations searched by proteins aiming at reaching their native state. However, the crowded cellular environment can lead to protein misfolding and aggregation, also in association with stress conditions such as heat, oxidative stress and inflammations. Therefore, cells developed several checkpoints to control protein folding, misfolding, aggregation and degradation thus maintaining their homeostasis (proteostasis) (Hartl et al., 2011). The first line of defence are molecular chaperones.

4.1 Molecular chaperones

Molecular chaperones are able to assist other client proteins without being part of their final structure. Chaperones can assist or stabilize the *de novo* folding of nascent proteins, can regulate their trafficking and assembly, possibly delivering them to degradation. Indeed, they cooperate with the Ubiquitin Proteasome System (UPS) and autophagic pathways (Husnjak and Dikic, 2012).

The core of the UPS system is the proteasome machinery. It receives proteins labelled by Ub moieties carrying the signal for their degradation. The 26S proteasome is a 2.5 MDa complex made by a 20S core and two 19S capping particles. The core of the proteasome structure is a ring made by β subunits displaying caspase-like, trypsin-like and chimotrypsin-like peptidase activities. The access to the proteolytic sites is gated by outer α rings and 19S regulatory particles. These latter carry Ub-binding domains (i.e. UIM), ATPase and/or deubiquitinase activities. Some subunits (i.e. S5a and Rpn11) are able to unload and recycle Ub from substrates and to unfold clients, allowing them to enter the

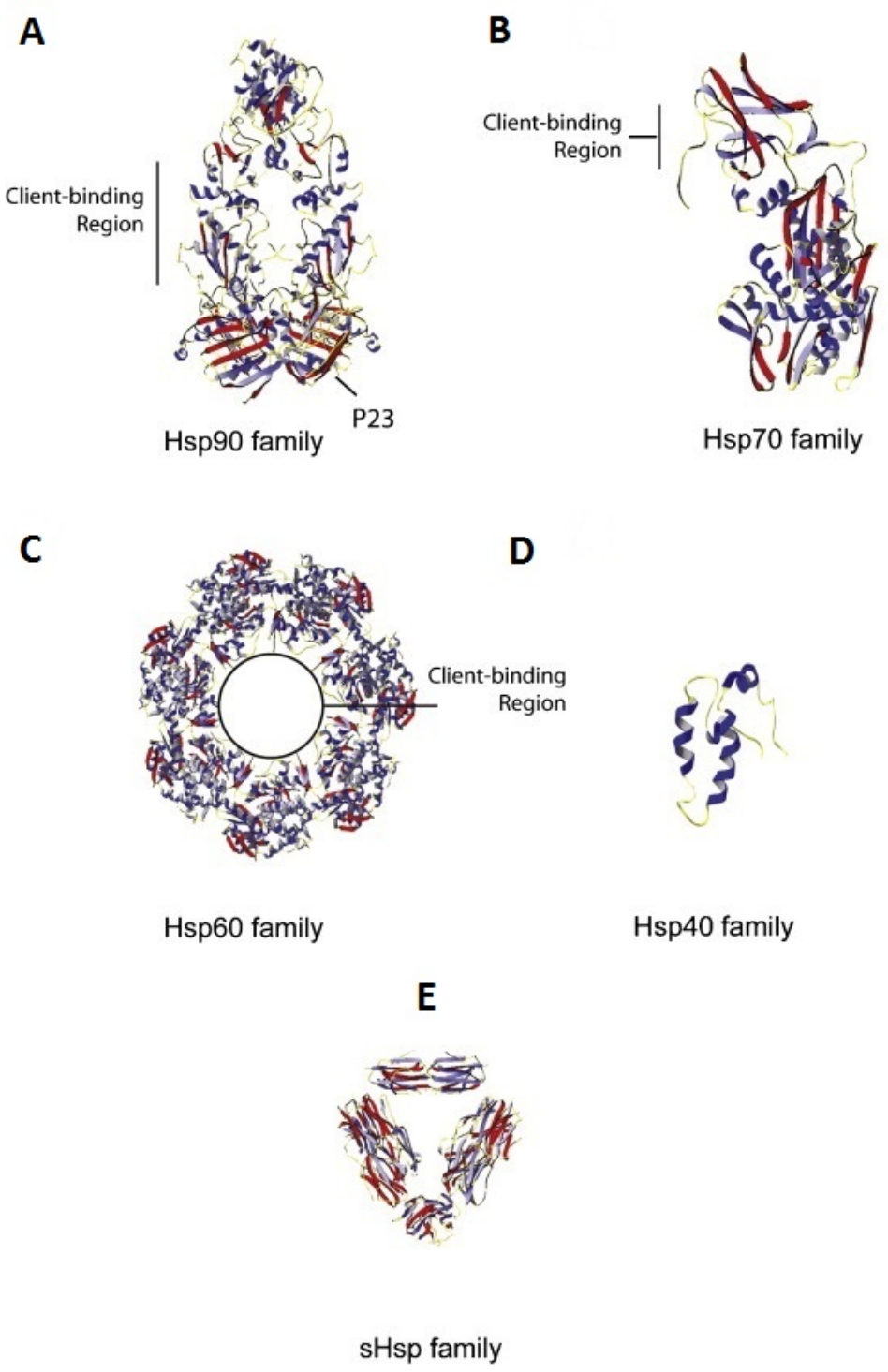

Figure 4.2: **Different structural features of molecular chaperones**
Representations of the structures and protein clients binding sites in diverse chaperones. **A.** The yeast Hsp90 in complex with the co-chaperone p23/Sba1 and an ATP analogue (PDB 2CG9). **B.** The bovine Hsc70 (PDB 1YUW). **(C)** The Hsp60 GroEL (PDB 1GR1). **D.** The J-domain of human Hsp40 HDJ-1 (PDB 1HDJ). **E.** The structure of Hsp16.3 from *Mycobacterium tuberculosis* (PDB 2BYU). Adapted from Kosmaoglou et al. (2008).

core of the proteasome. The small peptides emerging from the proteasome are finally digested by cytosolic peptidases.

While UPS cleaves short-living proteins, autophagy instead recycles larger structures such as complexes, organelles and proteins with slow turnover. Different types of autophagy have been described. In microautophagy lysosomes engulfs cytosolic molecules by direct invaginations of their membranes. In macroautophagy, substrates are included in vesicles by endosomes that mature in lysosomes whose acidification allows the degradation of their content. Finally, the chaperone-mediated autophagy occurs for proteins containing the consensus eptapeptide KFERQ, recognised by Hsp70 which releases them to lysosomes via the integral lysosomal membrane protein LAMP2A.

Many molecular chaperones are referred to as heat-shock proteins (Hsp) since they are up-regulated under stress-conditions such as high temperatures. They are usually classified as Hsp90, Hsp70, Hsp60, Hsp40 (or DNAJ) and small Hsp families, according to their molecular weight (Smith et al., 2015) (Figure 4.2).

4.1.1 Hsp90

Hsp90s (or HSPC) are ATP-dependent, homodimeric chaperones with key regulator functions in proteostasis (Figure 4.2A). They have an N-terminal ATP-binding domain, a substrate-binding domain and a C-terminal domain which allows dimerisation (N-, M- and C- domain respectively). In the ATP-free state, Hsp90s adopt an open conformation that gives access to substrates. Upon binding to ATP, the N-domain closes as a “lid” over the substrate-binding pocket. The subsequent ATP hydrolysis by the N-term induces Hsp90s to return to the open conformation and to release the substrate.

The Hsp90 activity is often supported by co-chaperones that shuttle substrates to the active site or between diverse chaperon systems.

4.1.2 Hsp70

The Hsp70 (or HSPA) system is a main controller of protein stability (Figure 4.2B). Similarly to Hsp90, also Hsp70 contains an ATP-binding pocket (NBD) at the N-terminus and a hydrophobic substrate-binding site (SBD) at the C-terminus. The

hydrolysis of ATP on increases the affinity of the SBD for substrates and induces conformational changes and the closure of a "lid". The cycling of ADP and ATP is catalysed by nucleotide exchanging factors (NEFs) and triggers Hsp70 to return to the open conformation and to release the substrate.

Hsp70s help the *de novo* folding of synthesized proteins and are key actors in the refolding of misfolded, aggregation-prone clients. These functions often require iterative cycles of binding and release of substrates that are supported by co-chaperones, frequently represented by DNAJ proteins. Furthermore, members of the DNAJ family cooperate through their conserved J domains in enhancing the ATP-ase activity of the NBD.

4.1.3 Hsp60

Hsp60s, also referred to as chaperonins, are ring complexes (Figure 4.2C). They have a central core able to sequester unfolded intermediates thereby shielding hydrophobic residues that could trigger aggregation. They can be divided in two groups:

- Group I chaperonins (HSPD) present in bacteria (GroEL) and in the mitochondrial matrix (Hsp60);
- Group II chaperonins (HSPE) found in *archea* and in the eukaryotic cytosol (TRiC or CCT).

Hsp60s differ in the number of subunits but share a common mechanism of action: they bind ATP at each subunit thus triggering the recruitment of a GroES protein that functions as a "lid" and closes the accessibility to the substrate binding site. Then, conformational changes form a shielded chamber where protein folding can occur. ATP hydrolysis to ADP induces the dissociation of the lid and the release of the substrate.

4.1.4 Hsp40 (DNAJ)

Hsp40s (Figure 4.2D) are characterized by an highly conserved sequence of 70 amino acid called J domain which is made by four α-helices with an antiparallel arrangement. They can be divided in three classes:

- Class I DNAJs have a conserved J domain resembling that of *E. coli* Hsp40, a

region rich in glycine and phenylalanine aminoacids, and a zinc-binding domain;
- Class II proteins share with class I the J and the Gly/Phe domains but not the zinc-finger domain;
- Class III Hsp40s conserve the J domain only.

As mentioned above, DNAJs support Hsp70s activity and are therefore considered co-chaperones. They are committed to different pathways depending on other functional domains. As a relevant example for this thesis, the DNAJ protein HSJ1 contains J and UIM domains that enable the direct transfer of clients to Hsp70 and stimulate its ATPase activity (see below).

4.1.5 Small Hsp

Small heat shock proteins are ATP independent chaperones that range in size from 12 to 42 kDa. They bind misfolded clients thus avoiding their aggregation and delivering them to the Hsp 90/70/40 systems.

4.2 Molecular chaperones in neurodegenerative diseases

Neurodegenerative diseases (NDs) are collectively characterized by progressive loss of neurons in the brain and spinal cord. Whilst the affected neuronal populations differ between NDs, common mechanisms underlying these pathologies has been suggested (Leliveld and Korth, 2007). PD, AD, Amyotrophic Lateral Sclerosis (ALS) and Huntington's (HD) diseases are the most widely studied NDs. They are mostly sporadic, and hereditary forms represents the 5-10% of cases only. Great efforts have tried to dissect the mechanisms underlying the onset and progression NDs, such as for the role of α-synuclein in PD (Spillantini et al., 1998), amyloid-β in AD (Hardy and Higgins, 1992), SOD1 in ALS (Rosen et al., 1993) and huntingtin in HD (DiFiglia et al., 1997) (Table 4.1). Clinical symptoms differ between NDs, but they are all related to the presence of proteinaceous deposits,which are presently regarded as hallmarks in both sporadic and familiar cases.

Chaperones that combat neurodegeneration related protein misfolding.

Chaperone family	Chaperone	Disease/protein(s)	Comments
HSP110	HSP110 (HSPH2)	ALS/SOD1	Improved vesicle transport deficit in SOD1^{G85R} squid axoplasm [67]; with DNAJB1 suppressed polyQ toxicity in flies [68]
		HD/Htt	
	HSP105 (HSPH1)	AD/tau	HSP105 knock out mouse had increased p-tau and Aβ [69]; suppressed aggregation of SOD1^{G93A} in cells [70]
		ALS/SOD1	
HSP90	HSP86 (HSPC1)	AD/Aβ	Reduced Aβ aggregation in vitro[22]; with Hsp60 and Hsp70 reduced Aβ mitochondrial dysfunction in cells [71]
HSP70	BiP (HSPA5)	AD/Aβ	Bound APP and reduced Aβ secretion [72]; reduced polyQ aggregation and toxicity in cells [73]; reduced α-synuclein toxicity in rat [74]; reduced P23H rhodopsin aggregation and photoreceptor cell death [75] and [76]
		HD/Htt	
		PD/α-syn	
		RP/Rho	
	Hsc70 (HSPA8)	AD/tau	Binds tau and facilitates microtubule polymerization reducing insoluble tau [25], [77] and [78]; QBP1 fusion reduced polyQ aggregation and toxicity in cells and mice [79], ATPase mutant reduced large polyQ aggregates but no effect on toxicity [80], reduced axonal transport defect in polyQ fly [81]; binds α-synuclein and reduced toxicity of fibrils [82] and [83]; binding to mutant SOD1 [84]
		HD/Htt	
		PD/α-syn	
		ALS/SOD1	
	Hsp70 (HSPA1A*)	AD/Aβ	Reduced Aβ aggregation in vitro[22] and in transgenic mice [85]; modest effect on R6/2 Htt mice [31] but increased aggregation on knock-down in HD flies [86]; suppression of α-synuclein toxicity in flies [17] cells and mice [16], but another report found no effect in mice [87]; reduced mutant SOD1 aggregation in cells [88] but had no effect in mice [89]; suppressed TDP-43 toxicity in fly [90]
		AD/tau	
		HD/Htt	
		PD/α-syn	
		ALS/SOD1	
		ALS/TDP43	
HSP60	HSP60 (HSPD1)	AD/Aβ	Reduced Aβ aggregation in vitro[22] and improved mitochondria function in a cell model [71]
HSP40/DNAJ	DNAJA1	AD/tau	Antagonized protective effect of Hsp70 on tau [91]; increased polyQ aggregation in some cell models [92]; increase binding of Hsp70 to α-synuclein [83]
		HD/Htt	
		PD/α-syn	
	DNAJB1 (Hsp40 or Hdj1)	AD/Aβ	Reduced Aβ aggregation in vitro with Hsp70 [22]; suppressed Htt inclusion formation but did not affect toxicity in cells [93] but protective with Hsp110 in flies [68]; increase binding of Hsp70 to α-synuclein [83]
		HD/Htt	
		PD/α-syn	
	DNAJB2a (HSJ1a)	HD/Htt	Reduce polyQ aggregation in vitro, in cells, in mice [37] and [39] and rats [94]; reduced mutant SOD1 aggregation in cells [48] and [45] and mice [45]; suppress mutant parkin aggregation and promote functional refolding in cells [95]
		ALS/SOD1	
		PD/parkin	
	DNAJB6	AD/Aβ	Efficient block of Aβ aggregation in vitro[21]; block polyQ aggregation and toxicity in cells and frogs [35] and [96]
		HD/Htt	
	DNAJB8	HD/Htt	Block polyQ aggregation and toxicity in cells and frogs [35] and [96]
	DNAJC10	RP/Rho	Reduced P23H rhodopsin aggregation in cells [97]
Small HSP	HSP27 (HSPB1)	AD/Aβ	Reduced Aβ aggregation in vitro and toxicity on cells [98] and in mice [99]; alters tau dynamics in mice [100]; reduced polyQ aggregation and toxicity in cells [101] and by viral delivery in rats [102] but not transgenic mice [103]; reduced α-synuclein fibril formation in vitro [104] and toxicity in cells [105]; reduced SOD1 aggregation in vitro[41] but small effects in mice [44] and [106]
		AD/tau	
		HD/Htt	
		PD/α-syn	
		ALS/SOD1	
	HSP22 (HSPB8)	AD/Aβ	Reduced Aβ aggregation in vitro and toxicity on cells [98]; reduced polyQ aggregation [32]; most effective small Hsp at reducing α-synuclein fibril formation in vitro[104]; enhanced autophagic clearance of SOD1 and TDP-43 [107]
		HD/Htt	
		PD/α-syn	
		ALS/SOD1	
		ALS/TDP43	
	αB-crystallin (HSPB5)	AD/Aβ	Reduced Aβ aggregation in vitro and toxicity on cells [98] and [108]; reduced toxicity of α-synuclein in cells [105]; reduced α-synuclein fibril formation in vitro [104]; SOD1 aggregation in vitro [41] but does not protect in mice [109]
		PD/α-syn	
		ALS/SOD1	
	HSP20 (HSPB6)	AD/Aβ	Reduced Aβ aggregation in vitro and toxicity on cells [98] and [110] and in worms [111]; reduced α-synuclein fibril formation in vitro [104]
		PD/α-syn	
	cvHSP (HSPB7)	HD/Htt	Most potent small Hsp against polyQ in cell model [32]
Co-chaperone	CHIP	AD/tau	Reduced tau aggregation in cell [26] and in mice [112]; reduced polyQ (ataxin-1) aggregation and toxicity in cells [113]; enhanced ubiquitylation of α-synuclein [114]; degradation of mutant SOD1 [84]
		PD/α-syn	
		ALS/SOD1	
	Cdc37	AD/tau	Regulates tau stability with Bag5 [115]; with Hsp90 in enhanced authophagic clearance of TDP-43 [116]
		ALS/TDP43	
	Bag-1	AD/tau	With Hsc70 to target degradation of tau [117]; protects against α-synuclein in cells and MPTP in mice [118]
		PD/α-syn	
	Bag-3	ALS/SOD1	Reduction in polyQ (SCA3) with Hspb8 in cells and flies [119]; With HspB8 to stimulate autophagy of SOD1 in cells [34] and [107]
	Bag-5	PD/α-syn	Enhanced ubiquitylation of α-synuclein [114]

Table 4.1: **Molecular chaperones are neuroprotective**
Chaperones that combat neurodegeneration related protein misfolding. Adapted from Smith et al. (2015).

Proteins deposition begins with the formation of small ring-shape soluble oligomers, able to disrupt cellular homeostasis and to trigger the formation of higher ordered protofibrils and fibrils. Then, they deposit as inclusions characterized by common β-sheet structures referred to as amyloids. They are likely to be toxic too since able to sequester functional proteins and to impede intracellular trafficking. Amyloids have been demonstrated to be ubiquitylated and the impairment of proteostasis has been suggested as a common mechanism underlying NDs (Soto and Estrada, 2008; Ebrahimi-Fakhari et al., 2012). The accumulation of misfolded proteins can overwhelm chaperones leading to the collapse of quality control machineries. Proof-of-principle studies suggested that the manipulation of chaperones could be a potential therapeutic strategy. Indeed, their overexpression successfully delayed the onset of NDs (Table 4.1) (Smith et al., 2015).

The study of hereditary forms could help increase our understanding of NDs and mutations in molecular chaperones were demonstrated to cause inherited NDs (Table 4.2) (Smith et al., 2015). As an example, autosomal dominant mutations in Hsp27 and Hsp22 have been reported in distal hereditary motor neuropathy (dHMN) and Charcot-Marie-Tooth type 2 (CMT2) (Evgrafov et al., 2004; Irobi et al., 2004; Engert et al., 2000). Hsp27 mutants cause an impairment of the axonal transport while Hsp22 mutations collapse the autophagic pathway. The 520 kDa DNAJ protein scasin (DNAJC29) was shown to cause autosomal recessive spastic ataxia of Charlevoix-Saguenay (ARSACS) (Engert et al., 2000) and over 170 mutations have been identify to deregulate its Hsp90-like chaperone activity and its association to the proteasome machinery. Interestingly, mutations in the *DNAJB2* gene, which codifies for the HSJ1 protein were demonstrated to cause autosomal recessive neuropathies such as dHMN, CMT2, PD.

HSJ1 was the focus of my main PhD project. The relevance of HSJ1 in proteostasis is widely documented: when overexpressed, it contributes to prevent protein misfolding and aggregation. HSJ1 binds ubiquitylated clients through its UIMs and facilitates their delivery to the proteasome degradation system (Westhoff et al., 2005). However, the physiological role of this chaperone is still poorly understood and a detailed investigation of its regulation is still lacking.

Chaperones mutations identified in neurodegenerative diseases.

Chaperone family	Chaperone	Inheritance	Disease
Hsp70	HSPA9 (Mortalin)	Dominant	Parkinson's disease
Hsp60	HSP60 (HSPD)	Dominant	Spastic paraplegia
		Recessive	Hypomyelinating leukodystrophy
	CCT4	Recessive	Hereditary sensory neuropathy
	CCT5	Recessive	Sensory neuropathy with spastic paraplegia
Hsp40 (DnaJ)	DNAJB2 (HSJ1)	Recessive	Distal hereditary motor neuropathy, Charcot Marie Tooth disease
	DNAJB6 (Mrj)	Dominant	Limb-girdle muscular dystrophy
	DNAJC3 (ERdj6)	Recessive	Diabetes and multisystemic neurodegeneration
	DNAJC5 (CSPα)	Dominant	Neuronal ceroid lipofusinosis
	DNAJC6 (Auxilin)	Recessive	Juvenile Parkinsonism
	DNAJC13 (RME-8)	Dominant	Parkinson's disease
	DNAJC19 (TIM14)	Recessive	Dilated cardiomyopathy and cerebellar ataxia
	DNAJC29 (Sacsin)	Recessive	Spastic ataxia of Charlevoix-Saguenay
Small Hsp	HSPB1 (Hsp27)	Dominant and recessive	Distal hereditary motor neuropathy, Charcot Marie Tooth type 2
	HSPB3 (HspL27)	Dominant	Hereditary motor neuropathy
	HSPB5 (αβ-crystallin)	Recessive	Infantile muscular dystrophy
	HSPB8 (Hsp22)	Dominant	Distal hereditary motor neuropathy, Charcot Marie Tooth disease
Chaperone co-factors	SIL1	Recessive	Cerebellar ataxia
	VCP	Dominant	Amyotrophic lateral sclerosis
	BAG3	Dominant	Muscular dystrophy
			Giant axonal neuropathy

Table 4.2: **Chaperones mutation can cause neurodegenerative diseases**
Partial list of chaperones mutations identified in neurodegenerative diseases. Adapted from Smith et al. (2015).

4.3 HSJ1 (*DNAJB2*)

HSJ1, which gene is referred to as *DNAJB2*, is a key component in neuronal protein quality control. It is a molecular chaperone preferentially expressed in neurons and acts as a shuttling factor to sort chaperone clients to the proteasome (Westhoff et al., 2005).

Two isoforms are expressed in humans, HSJ1a and HSJ1b, as a result of alternative splicing (Cheetham et al., 1992) (Figure 4.3A). They share the same domain structure, but their intracellular localization differs: HSJ1a is cytosolic and nuclear, while HSJ1b has a longer C-terminus and is anchored to cytoplasmic face of ER due to C-terminal geranylgeranylation through the CAAX box (Chapple and Cheetham, 2003). At the N-terminus, HSJ1 presents the typical J domain of DnaJ (Hsp40) heat shock protein family members (Cyr and Ramos, 2015), that stimulates substrate loading onto the Hsp70 chaperone (Cheetham et al., 1994; Westhoff et al., 2005). Near the C-terminus HSJ1 has two UIMs, that function to bind ubiquitin chains and help prevent client protein aggregation. Therefore, by the coordinate actions of its functional domains, HSJ1 functions to regulate the

proteasome targeting of misfolded proteins, and protects neurons against cytotoxic protein aggregation (Figure 4.4).

The neuroprotective role of HSJ1 has been shown in different disease models (Smith et al., 2015): it suppresses the aggregation of polyglutamine expanded proteins, significantly enhancing mutant huntingtin solubility in Huntington disease in cells and in mice (Westhoff et al., 2005; Labbadia et al., 2012), and promoting misfolded protein targeting to the ubiquitin-proteasome system (Howarth et al., 2007); HSJ1a cooperates with Hsp70 to promote proteasome-degradation of ataxin-3, a protein responsible for spinocerebellar ataxia type 3 (SCA3) (Gao et al., 2011); HSJ1a prevents the aggregation of the misfolded C289G Parkin, a Parkinson disease-associated ubiquitin-protein ligase mutant and restore its function in mitophagy (Rose et al., 2011). Interestingly, a protective function of HSJ1a has also been demonstrated in ALS models: its overexpression in motor neurons of SOD1G93A mutant transgenic mice was found to improve the disease symptoms; the molecular mechanism was related to HSJ1 association to SOD1, with its consequent increased ubiquitylation and lower level of aggregation (Novoselov et al., 2013). More recently HSJ1a was shown to be highly effective at preventing the aggregation of TDP-43 (Chen et al., 2016). The important role played by HSJ1 in neurons is highlighted by the fact that HSJ1-related hereditary neuropathies have been identified: autosomal recessive distal hereditary motor neuropathy (dHMN) was linked to a splice site mutation in the HSJ1 gene (Blumen et al., 2012). The phenotype spectrum of HSJ1-related neuropathies was later broadened by the discovery of two additional mutations of the HSJ1 gene in patients with dHNM and Charcot-Marie-Tooth disease type 2 (CMT2) (Gess et al., 2014); recently, a large HSJ1 gene deletion was found in a family with recessive spinal muscular atrophy and Parkinsonism (Sanchez et al., 2016).

Interestingly, we noticed that the UIM2 motif inside HSJ1 is superimposable to the consensus targeted by CK2 for phosphorylation (see Figure 4.3B and Chapter 3.2.1), therefore we considered high probable that HSJ1 is a CK2 substrate and that this could influence its functions.

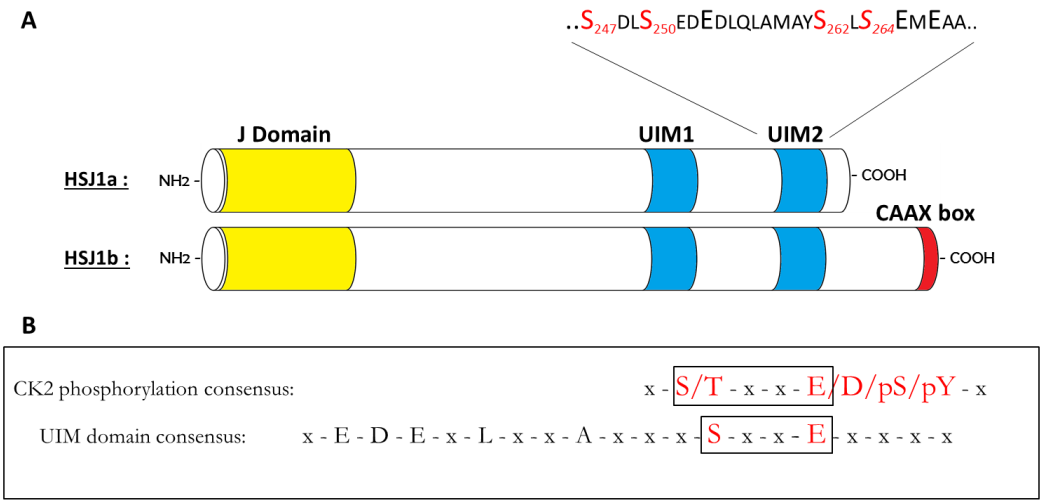

Figure 4.3: **CK2/UIM consensus and HSJ1 structure organization**
(A) The consensuses for phosphorylation by CK2 or for Ub-protein binding by UIM are shown. The overlapping segments are boxed. **(B)** The domains organization of the two HSJ1 isoforms are shown. The sequence of UIM2 is also reported, highlighting the CK2 putative sites.

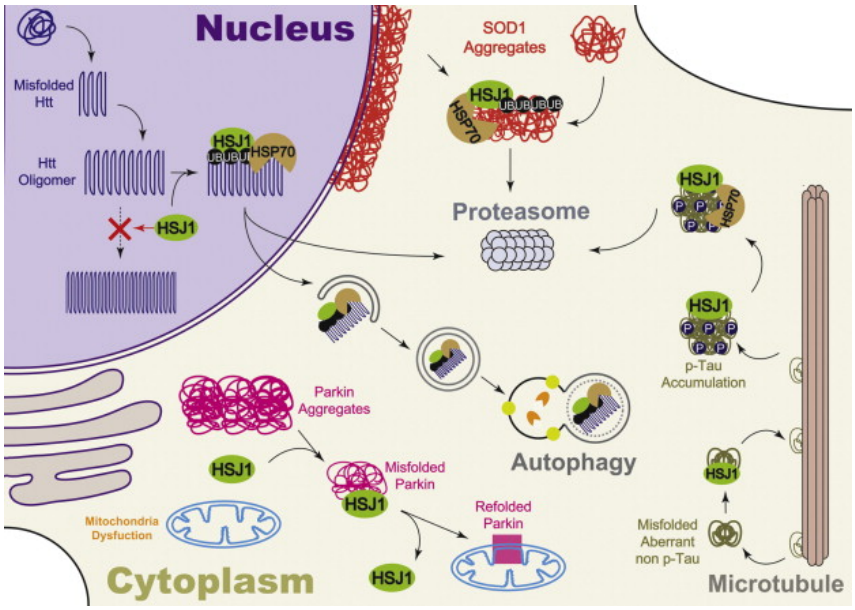

Figure 4.4: **HSJ1 neuroprotective functions**
Scheme showing the effect of HSJ1a on Htt, SOD1, Parkin and Tau in neurons. HSJ1a can bind to ubiquitylated oligomers of Htt in the nucleus blocking the recruitment of more misfolded Htt and further aggregation, leading to increases in soluble Htt and potential autophagic clearance of cytoplasmic Htt oligomers. HSJ1 also facilitates proteasomal degradation of Htt. HSJ1a blocks the aggregation of mutant Parkin and stimulates its refolding, so that Parkin can function in mitochondrial quality control. In ALS, HSJ1a reduces the aggregation of mutant SOD1 and promotes the degradation by proteasome. Adapted from Smith et al. (2015).

Chapter 5

Aim of the study

With this work we aim at investigating a previously uncharacterised crosstalk between protein phosphorylation and ubiquitylated protein signalling. We focused on protein kinase CK2, an enzyme extensively studied and involved in several malignancies. We started from the work of Hofmann and Falquet (Hofmann and Falquet, 2001): they observed that the ubiquitin interacting motif (UIM), which binds ubiquitylated protein clients *en route* to degradation, displays conserved residues essential for its Ub-binding function. We noticed that the conserved motif is superimposable to the consensus targeted by CK2 for phosphorylation (Figure 4.3B). Therefore, we considered high probable that proteins containing UIM domains are CK2 substrates. We focused on the UIM-containing HSJ1, a neuronal chaperone implied in neurodegeneration (Smith et al., 2015). We assumed HSJ1 as paradigmatic example of a possible regulatory mechanism mediated by the phosphorylation of UIMs by CK2. Therefore, we aimed at:

- verifying if HSJ1 is phosphorylated by CK2;
- identifying the HSJ1 sites targeted by CK2;
- analysing the effects of the phosphorylation on the HSJ1 functions.

The more general aim of this work is to disclose a novel mechanism by which CK2 could regulate the ubiquitin signalling played by different UIM-containing proteins.

Part II

Materials and Methods

Chapter 6

Materials and Methods

6.1 Antibodies

Anti-CK2 C-term was raised in rabbit against the sequence of the human protein at C-terminus [376–391], as previously described (Sarno et al., 1996); anti-pSer129 Akt was either produced in rabbit as in (Di Maira et al., 2005) or purchased from Abcam, anti-total Akt and anti-total HSJ1 were from Santa Cruz Biotechnologies, anti-myc, anti-tubulin and anti-actin from Sigma; anti-mono/poly-ubiquitinylated conjugates was from Enzo Life Sciences. Anti-pHSJ1 were produced in rabbits, as described in the next chapter.

6.2 Peptide synthesis

Peptide synthesis was performed by Prof. Oriano Marin and Dr. Michele Sandre. The synthetic peptides PLDSDLSEDED-betaAla-RRR, PLDSDLpSEDED-beta Ala-RRR,PLDSDLSEDED-betaAla-C, PLDSDLpSEDED-betaAla-C, PLDpSDL pSEDED-betaAla-C were synthesized by solid-phase technique using a multiple peptides synthesizer (SyroII, MultiSynTech GmbH) on a pre-loaded Wang resin (100-200 mesh) with Fmoc-Nε-tert-butyloxycarbonyl-L-lysine (Novabiochem). The fluoren-9-ylmethoxycarbonyl (Fmoc) strategy was used throughout the peptide chain assembly, utilizing O-(7-azabenzotriazol-1-yl)-N,N, N´,N´-tetramethyluronium hexafluorophosphate (HATU) as coupling reagent. The side-chain protected amino acid building blocks used were: N-Fmoc-Nω-

(2,2,4,6,7-pentamethyldihydrobenzofuran-5-sulfonyl)-L-arginine, N-α-Fmoc-β-tert-butyl-L-aspartic acid, N-Fmoc-tert-butyl-L-glutamic acid, N-Fmoc-O-tert-butyl-L-serine, N-Fmoc-S-trityl-cystine, and N-Fmoc-O-benzyl-phospho-L-serine. Cleavage of the peptides was performed by incubating the peptidyl resins with trifluoroacetic acid/H2O/triisopropylsilane (95%/2,5%/2,5%) for 2.5 h at 0 °C. Crude peptide were purified by reverse phase HPLC on a preparative column (Prep Nova-Pak HR C18). Molecular masses of the peptide were confirmed by mass spectroscopy on a MALDI TOF-TOF using a Applied Biosystems 4800 mass spectrometer.

6.3 Expression and purification of recombinant HSJ1

His-tagged HSJ1 WT and mutants cloned in pET-14b vectors were kindly provided by Prof. Mike Cheetham and used to transform *E. coli* BL21(DE3) strain. The bacterial culture was grown to reach an Optic Density (OD) of 0.3-0.4 when protein synthesis was induced for 4h by 100mM Isopropil-b-D-1-tiogalattopiranoside (Sigma-Aldrich). Bacteria were then harvested by centrifugation and sonicated in bacterial lysis buffer (50 mM NaH_2PO_4 pH 8, 100 mM NaCl, 0.01% Tween-20 and 2 mM DTT). Cell debris were discarded by centrifugation (35000 x g, 10 min) and HSJ1 was purified from the supernatant by His-selective affinity resin (Sigma-Aldrich) and eluted with 300 mM imidazole pH 8. Aliquots of the purified proteins were stored at -80°C in 10% glycerol, 2 mM DTT.

6.4 In vitro phosphorylation assays of proteins and peptides

Recombinant purified HSJ1 or S5a (Enzo Life Sciences) peptides were incubated for 10min at 30°C with recombinant CK2 (a kind gift from Prof. Stefania Sarno and Dr. Andrea Venerando) and [γ-^{33}P] ATP in an appropriated phosphorylation buffer (50 mM Tris–HCl pH 7.5, 10 mM $MgCl_2$, 50µM [γ-^{33}P] ATP at 2000 cpm/pmol (PerkinElmer) and 0.1 M NaCl). Reactions were stopped by spotting peptides onto phospho-cellulose filters (Perkin Elmer) or by adding Laemmli buffer. Peptides phosphorylation was assessed by washing filters four times in 75 mM phosphoric acid and analysing them by a Scintillation Counter (PerkinElmer). Proteins instead were resolved onto SDS-PAGE, stained with Coomassie blue and analysed by digital autoradiography (CyclonePlus Storage Phosphor System, PerkinElmer).

6.5 HSJ1 phospho-sites identification

Phospho-HSJ1 digestion

Recombinant HSJ1 was incubated with recombinant CK2 for 60 min at 30°C in a phosphorylation buffer suitable for the subsequent protein digestion (Phosphate Buffer pH 7.8, 10 mM $MgCl_2$, 50µM ATP and 0.1M NaCl). Disulfide bonds were then reduced by 5mM DTT for 30 min at 60°C followed by alkylation with 15 mM iodoacetamide for 15 min at room temperature. The final volume was brought to 50 µL and HSJ1 was digested overnight at 37°C by Glu-C protease (Promega) as from manufacturer's instruction. The reaction was then sent to mass spectrometry analysis, kindly performed by Prof. Giorgio Arrigoni and Dr. Cinzia Franchin.

Phospho-peptides enrichment and LC-MS/MS analysis

Enrichment of phosphorylated peptides was carried out as reported in (Salvi et al., 2012). Briefly, samples were subjected to a phospho-peptide enrichment step using home-made TiO_2 micro-columns and analysed by LC-MS/MS using a LTQ-Orbitrap XL mass spectrometer (ThermoFisher Scientific) coupled on-line with a nano-HPLC Ultimate 3000 (Dionex – ThermoFisher Scientific). Samples

were loaded onto a 10 cm pico-frit column (75 μm I.D., 15 μm tip; New Objective) packed with C18 material (Aeris Peptide 3.6 μm XB-C18, Phenomenex) and separated using a 45 min linear gradient of ACN/0.1% formic acid (from 0% to 40% ACN in 25 min), at a flow rate of 250 nL/min. To increase phospho-peptides identification confidence, every sample was analysed three times with three different fragmentation methods (MS2, MS3, and MultiStage Activation), as detailed in (Salvi et al., 2012). Raw data files were analysed with a MudPit protocol against the Human section of the Uniprot database (version 20150107, 89706 sequences) with the software Proteome Discoverer 1.4 (ThermoFisher Scientific) interfaced to a Mascot search engine (version 2.2.4, Matrix Science). Enzyme specificity was set to V8-DE with up to 3 missed cleavages. Mass tolerance window was 10 ppm for parent mass and 0.6 Da for fragment ions. Carbamidomethylation of cysteine was set as fixed modification. Oxidation of methionine residues and phosphorylation of serine, threonine, and tyrosine were set as variable modifications. The algorithm PhosphoRS (Taus et al., 2011) was used to help in the assignment of the correct phosphorylation sites. False Discovery Rate (FDR) was calculated by Proteome Discoverer based on the search against the corresponding randomized database. Phospho-peptides identified with high (99%) confidence, were manually inspected for sequence and phosphorylation site confirmation.

6.6 Site-directed mutagenesis

HSJ1 mutations were introduced by site-directed mutagenesis with the QuikChange II Site-Directed Mutagenesis Kit (Agilent Technologies) in accordance with the manufacturer's protocol. Mammalian and bacterial vectors for HSJ1 were as in (Chapple and Cheetham, 2003; Westhoff et al., 2005). Custom-made primers were made by Sigma-Aldrich as from Table 6.1.

Primer	SEQUENCE (5'-3')
Forward S247A	GCCTCATGCCCCTTGGACGCCGACCTCTCTGAGGATGAGG
Reverse S247A	CCTCATCCTCAGAGAGGTCGGCGTCCAAGGGGCATGAGGC
Forward S250A	CCCCTTGGACAGCGACCTCGCCGAGGATGAGGACCTGCAG
Reverse S250A	CTGCAGGTCCTCATCCTCGGCGAGGTCGCTGTCCAAGGGG
Forward S262A	GCAGCTGGCCATGGCCTACGCCCTGTCAGAGATGGAGGC
Reverse S262A	GCCTCCATCTCTGACAGGGCGTAGGCCATGGCCAGCTGC
Forward S250D	CCCCTTGGACAGCGACCTCGATGAGGATGAGGACCTGCAG
Reverse S250D	CTGCAGGTCCTCATCCTCATCGAGGTCGCTGTCCAAGGGG

Table 6.1: **Custom-made primers.**Sequences of primers exploited for site-directed mutagenesis.

6.7 Cell culture and treatments

All cells were cultured in an atmosphere containing 5% CO_2; HEK293T were maintained in DMEM (Sigma) medium and SK-N-SH in DMEM/ F-12 1:1 nutrient mixture (Sigma); both media were supplemented with 10% (v/v) fetal bovine serum (FBS, Sigma), 2 mM L-glutamine (Sigma), 100 U/mL penicillin, and 100 mg/mL streptomycin (Sigma). Cell treatments with inhibitors were performed in the culture medium. Control cells were treated with equal amounts of the inhibitor solvent which never exceeded 0.5% (v/v). CX-4945 (Cylene Pharmaceuticals), CX-5011 (Glixx Laboratories), and TBB (kindly donated by Dr. Z. Kazimierczuk, Warsaw, Poland) were sodium salts all dissolved in 10 mM stock solutions in DMSO (Sigma).

6.8 Cell transfection, lysis and immunoprecipitation

Transient expression of HSJ1 WT and mutants was induced by transfecting CMV-Myc-Tag3a vectors into mammalian cell lines. Cells were plated into 6-well plates (2.5 × 105 cells/well) the day before transfection and grown to about 70% confluence. HEK-293T cells were transiently transfected with 1 μg of plasmids by a standard calcium-phosphate procedure. The transfection mixture was removed after 16 h and cells were collected 48 h after transfection. Similarly, SK-N-SH

cells were transiently transfected either on plates or 8-wells Permanox microscope slides (Sigma-Aldritch) with 1 μg of plasmids using Lipofectamine LTX Reagent (Life technologies) accordingly to the manufacturer's protocol. 48 h after transfection cells were collected or slides fixed for ICC/IF analysis. Cells were lysed with an ice-cold buffer containing 20 mM Tris–HCl, pH 7.5, 150 mM NaCl, 2 mM EDTA, 2 mM EGTA, 0.5% (v/v) Triton X-100, 2 mM dithiothreitol (DTT), protease inhibitor Complete (Roche) cocktail, 10 mM NaF, 1 μM okadaic acid (Enzo Life Sciences), and 1 mM Na vanadate. After 60 min incubation on ice, the lysates were centrifuged at 16000 x g for 30 min, at 4 °C and the supernatants were subjected to the Bradford protein quantification before SDS-PAGE separation and western blot analysis (WB).

6.9 Stable transfection

CHO inducible cell lines were kindly provided by Dr. Wenwen Li and produced using the Flp-in T-REx system by following the manufacture's instructions (Thermo-Scientific). eGFP-tagged HSJ1a or HSJ1b in the pcDNA5/FRT/TO was received as a gift from Prof. HH Kampinga (Groningen) (Hageman et al., 2007) and used to produce inducible stable cells lines expressing HSJ1 proteins under the control of tetracycline.

6.10 Western blotting

Equal amounts of proteins from cell lysates were analysed by 11% SDS-PAGE and blotting on PVDF membranes (Immobilon-P Millipore) using the Lightning Blotter Transfer System (Perkin Elmer) and buffers as from manufacturer's instructions. Dried membranes were then washed with 1% (w/v) bovine serum albumin (Sigma) in TTBS buffer (Tris–HCl 50 mM pH 7.5, NaCl 50 mM, 0.1% Tween-20) and incubated with the indicated antibodies. Membranes were then incubated with secondary HRP-conjugated antibodies (Perkin Elmer) for 1 h and bands were detected by a chemiluminescence solution composed by 2.25 ml H_2O, 250 μl 1 M Tris, pH 9.35, 1 μl H_2O_2 and 2.5 ml of a luminol solution (prepared

with luminol 78 mg and p-iodophenol 95 mg dissolved in 100 ml 0.1 M Tris pH 9.35) plus 30% (w/v) BSA. Finally, bands were visualized with the Kodak Image Station 4400MM PRO and quantified with the Kodak 1D Image software.

6.11 ^{32}P[phosphate] cell loading

HEK-293T cells were transfected with HSJ1 WT and mutants by a standard calcium phosphate protocol as described above. 44 h after transfection cells were washed twice with PBS (Sigma) and incubated with phosphate-free DMEM (Sigma) supplemented with 50µCi/mL of ^{32}P[phosphate] for 3 h. If required, cells were treated with 10 µM CX-4945 for the same length of time. Cells were then harvested and lysed before being subjected to (co)immunoprecipitation protocol, digital autoradiography and WB analysis.

6.12 Ub-protein binding analysis

Cells were lysed in Co-IP Buffer (25 mM MOPS pH 7.2, 100 mM KCl, 5mM EDTA, 0.5% Tween-20), then 0.5-1 mg of total protein lysate was incubated with anti-myc antibody for 2 h followed by incubation with Protein G PLUS-Agarose resin (Santa Cruz Biotechnology) for 45 min. The resin was then washed twice with wash buffer (25 mM MOPS pH 7.2, 100 mM KCl, 5mM EDTA). Myc-tagged HSJ1 and co-precipitated proteins were eluted with loading buffer and subjected to gel electrophoresis followed by WB analysis with anti-Ub antibody.

6.13 Statistical analysis

Statistical analysis was performed with the Software Graphad Prism and significance determined using the unpaired, two tailed, Student's t-test. All data were collected from at least 3 independent experiments; representative experiments are shown. Graphs show quantification, SEM and significances (*$p \leq 0.05$, ** $p \leq 0.01$, ***$p \leq 0.001$).

6.14 Surface Plasmon Resonance (SPR) analysis

A BiacoreTM T100 (GE Healthcare) instrument was used. HSJ1 pSer250 (P-peptide, PLDSDLpSEDED-A-Cys) or pSer247/pSer250 (PP-peptide, PLDpSDLpSEDED-A-Cys) were immobilized by thiol coupling on a CM5 (series S) sensor chip (carboxymethylated dextran surface) to a final density of 171 (P-peptide) and 174 (PP-peptide) resonance units (RU). A flow cell with no immobilized peptide was used as control. Antibody binding analysis was carried out in a running buffer consisting of 10 mM HEPES, pH 7.4, 150 mM NaCl, 0.001% (v/v) Tween-20, applying a flow rate of 10 µl/min, with 420 s antibody injection time, followed by 420 s dissociation time. For kinetics experiments, a Biacore method program was used. It included a series of three start up injections (running buffer), zero control (running buffer) and 5 different concentrations. Peptide competition experiments were performed by injecting 2 nM antibodies over the sensor chip at a flow rate of 20 µl/min, 180 s injection time, 180 s dissociation time, in the presence of increasing concentrations (1 to 200 nM) of P-peptide or PP-peptide. In all cases, the chip surface was regenerated with 30 s injection of 1 M NaCl plus 30 s injections of 0.1 M HCl; this treatment restored the baseline to the initial RU value. Each sensorgram (time-course of the surface plasmon resonance signal) was corrected for the response obtained in the control flow cell and normalized to baseline. The kinetic data were analysed using the 2.0.3 BIAevaluation software (GE Healthcare). Curves were fitted with the classical Langmuir 1:1 model; the quality of the fits was assessed by visual inspection of the fitted data and their residual, and by chi-square values. Two independent experiments for each analysis were performed.

6.15 Phospho-antibodies production and purification

In silico simulation

The structure of two putative sequences encompassing the main CK2 sites Ser247 and Ser250 of HSJ1 was simulated *in silico* in order to identify the most antigenic peptide to be exploited for rabbit immunization. Results in Figure 6.1A showed that the Pro244 (green) allows the folding of the peptide in a more extended shape (left vs. right panel). Moreover, it maximizes the exposition of the Ser residues to the rabbit immune system. Finally, the cysteine residue (yellow) was moved from the N-term to the C-term, after a β-linker, in order to efficiently conjugate the peptide to the protein carriers Bovine Serum Albumin (BSA) or the Keyhole Limpet Hemocyanin (KLH) (Figure 6.1B). A mixture of them was used for rabbits immunisation. Being KLH smaller in size then BSA, it should likely lead to a better availability of the peptides bound on its surface.

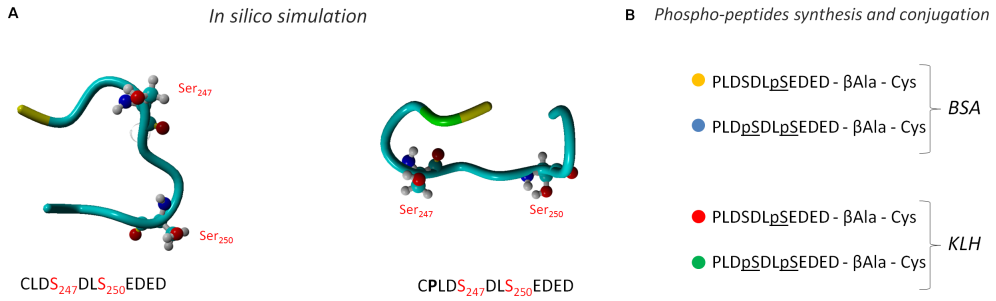

Figure 6.1: **Identification and production of suitable immunizing peptide**
(A) *In silico* simulations of immunizing peptides by Desmond Molecular Dynamics Simulations software and visualized by YASARA software. **(B)** Conjugation of peptides to two different protein carriers.

Rabbits immunization protocol

Antibodies specific to phospho sites Ser-247 and Ser 250 were generated in New Zealand rabbits against the following synthetic epitopes PLDSDLSEDED-betaAla-C, PLDSDLpSEDED-betaAla-C and PLDpSDLpSEDED-betaAla-C as previously described and coupled with maleimide-activated keyhole limpet hemocyanine (KLH) or bovine serum albumin (BSA) (1:1 w/w) through the C-terminal cysteine. Rabbits were injected four times at 3 weeks intervals, with 0,5 mg of peptide-proteins conjugates emulsified with

Freund's adjuvant (1:1 v/v). Antisera were purified using an immobilized peptide affinity resin (Sulfo Link Coupling Gel) according to manufacturer's instructions.
Prof. Oriano Marin Dr. Michele Sandre helped in peptide synthesis and in immunising rabbits that followed a standardized protocol with a 1:1 mixture of mono-phospho and bis-phospho peptides conjugated to the carrier protein BSA or KLH. This would allow the production of antibodies able to recognize the two phosphorylation states of HSJ1 (pSer 250 and pSer247/pSer250). Before every immunization step, siera were collected from rabbits in order to titre the production of the antibodies.

Purification

The first batch of antibodies (pHSJ1) was purified from the serum collected by the animals immunized by BSA-cojugated peptides. It was separated by affinity purification against the same mixture of peptides used for the immunization of the rabbits (pS and pSpS peptides). Then, the antibodies were first validated by WB and Surface Plasmon Resonance (SPR) experiments (see Part III - Results).
Briefly, SPR is a techniques able to detect biological interactions at the mono-molecular level. The instrument has a biosensor, a polarized light source and a detector. Biosensors are analytical devices comprised of a biological element (i.e. an antibody) attached (often covalently) onto the chip surface. Biosensors are covered by a physico-chemical transducer (usually gold), facing opposite to the biological side. In basal condition, the gold particles on the sensorchip are excited by the light source. Then, they return the energy of the exciting ray to a detector that measure it as 'reflection index'. Interactions between analytes injected over the immobilized targets onto the biosensor produce changes in the reflection index. The transducer yields an electronic signal proportional to the amount (concentration) of analytes bounded to the targets hold by the chip surface. This allows to draw concentration- and time- dependent curves and to calculate the kinetic constants of the binding.

6.16 Immunofluorescence experiments

For immunofluorescence staining, coverslips were washed twice with PBS and fixed in 4% paraformaldehyde for 10 min. Cells were then permeabilized with 0.5% Triton X-100 for 10 min, at room temperature. Then, microscope slides were incubated in blocking buffer (3% bovine serum albumin (BSA) and 10% normal donkey serum in PBS) for 1 h before incubation with primary antibodies for 1 h at room temperature. Species-specific anti-IgG Alexa Fluor 488 secondary antibodies were used and nuclei were stained with DAPI (Sigma). Slides were mounted with fluorescence mounting medium (Dako) and images were acquired with the 63X objective of Zeiss LSM700. Scale bars are 50 μM.

6.17 Luciferase assay

SK-N-SH cells were seeded in 96-well plates and transfected at 80% confluence with TransIT-LT1 Transfection Reagent (Mirus). Each well was transfected with 20 ng of HSJ1 WT and mutants, and 10 ng of the pBK-CMV, a cytomegalovirus (CMV)-promoter-driven firefly luciferase reporter vector. Luciferase was expressed in stably HSJ1-transfected CHO cells by 1 μg/mL. HSJ1 synthesis was induced 3 h post transfection by 3 μg/ml tetracycline (Invitrogen). If required, after 21 h cells were treated with 10 μM CX-4945. 24 h after transfection, luciferase activity was measured on an Orion L Microplate Luminometer (Titertek Berthol) with a dual-luciferase reporter assay system (Dual-Glo Luciferase Assay System, Promega) in accordance with the manufacturer's protocol.

Part III

Results

Chapter 7

Results

The UIM motifs of HSJ1 display canonical CK2 consensus sites and this characteristic is shared by diverse UIM-containing proteins. We chose the HSJ1 and S5a (or Rpn10) proteins, among the many exploited by Hofmann and colleagues (Hofmann and Falquet, 2001), to define the UIM motif (see Chapter 3.2.1). As described in the introduction, the first is a molecular chaperone and the latter is a component of the regulatory 19S caps of the proteasome. We first aimed at demonstrating that HSJ1 and S5a are phosphorylated by CK2. Then, we mainly focused on HSJ1 to better characterized its phosphorylation and functional significance.

7.1 HSJ1 and S5a are phosphorylated by CK2

To test the hypothesis that HSJ1 and S5a are phosphorylated by CK2, recombinant proteins were analysed *in vitro* as substrates in radioactive assays. They were incubate in a reaction buffer containing cofactors, ATP, and [γ-^{33}P] ATP, in the presence of monomeric CK2 (catalytic α subunit) or CK2 holoenzyme ($\alpha 2 \beta 2$). The phosphorylation of both S5a (Figure 7.1) and HSJ1 (Figure 7.2) was detected by autoradiography of SDS-PAGE gels. Further studies on HSJ1 followed, due to its pivotal roles in neuronal proteostasis and NDs.

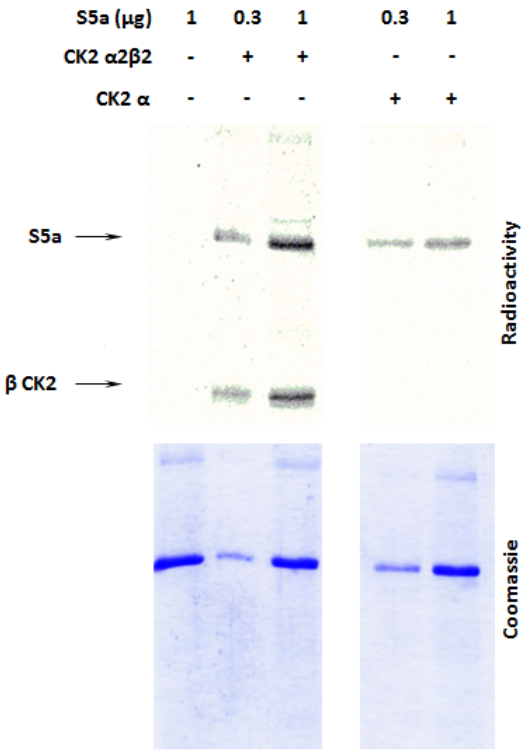

Figure 7.1: **S5a phosphorylation by CK2 in vitro**
Different amounts of recombinant S5a were incubated with a radioactive phosphorylation mixture in the presence of CK2 α2β2 (50 ng) or α (50 ng), as indicated.

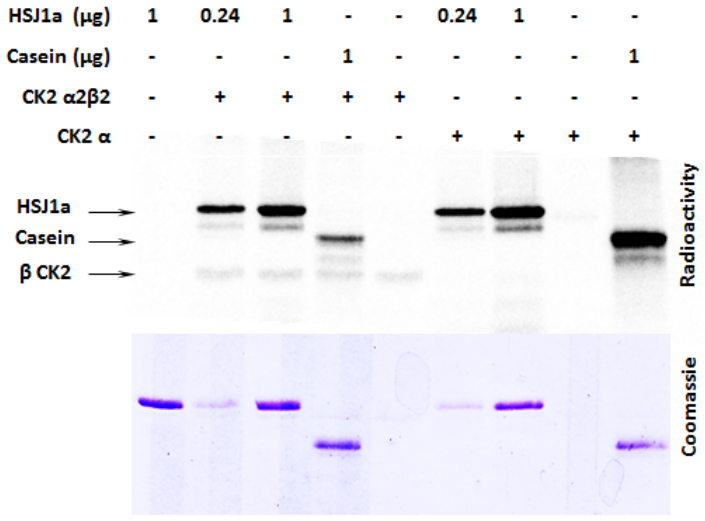

Figure 7.2: **HSJ1 phosphorylation by CK2 *in vitro***
Different amounts of recombinant HSJ1 were incubated with a radioactive phosphorylation mixture in the presence of CK2 α2β2 (50 ng) or α (50 ng), as indicated. Casein was used as a control substrate for CK2 activity..

7.2 In vitro characterization of HSJ1 phosphorylation

As delineated in Chapter 4.3, HSJ1 is spliced in two isoforms, a and b, displaying different subcellular localizations. Figure 7.2 shows the phosphorylation of HSJ1a by CK2. As expected, the other HSJ1 isoform, HSJ1b, which shares the same CK2 putative sites with HSJ1a, was also readily phosphorylated by CK2 *in vitro* (Figure 7.3). We also found that the two CK2 catalytic subunits, α and α', had a similar activity towards HSJ1 (both a or b isoforms) (Figure 7.3).

Then, we evaluated the concentration and time dependence of the *in vitro* HSJ1 phosphorylation. Figure 7.4 shows the increase of the autoradiographic signal displayed by the protein at different incubation times. HSJ1 phosphorylation was also concentration-dependent (Figure 7.4). However, we observed that the concentration-dependent curves for the HSJ1 phosphorylation displayed different slopes. For this reason it was not possible to calculate a K_m (although data suggested a value in the nM range, not shown). These results are consistent with the presence of multiple phosphosites on HSJ1 (see chapter 7.4).

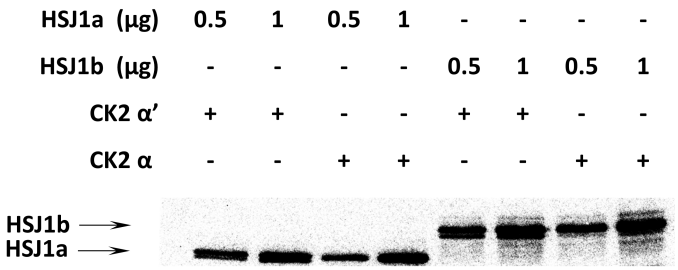

Figure 7.3: **Phosphorylation of both HSJ1 isoforms**
Different amounts of recombinant HSJ1a or HSJ1b were phosphorylated by CK2 α (50 ng) or α' (ng), as indicated. The radioactivity is shown.

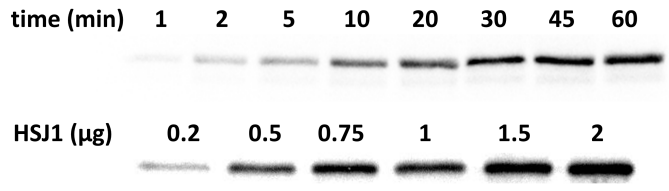

Figure 7.4: **Concentration and time dependence of HSJ1 phosphorylation**
Phosphorylation of HSJ1a by CK2 α2β2 (50 ng) was performed at increasing times (upper panel, 0.5 µg HSJ1a) or with increasing HSJ1a amounts (lower panel, 5 min incubation). The radioactivity is shown.

7.3 In cell phosphorylation of HSJ1

To confirm HSJ1 phosphorylation in the cellular milieu, we transiently expressed myc-tagged HSJ1a in HEK-293T cells, then loaded with [^{32}P]phosphate in order to generate an intracellular pool of radioactive ATP. The immunoprecipitation of HSJ1 followed. We observed a strong reduction of phosphate incorporation upon cell treatment with the CK2 specific inhibitor CX-4945, suggesting that CK2 is a prominent HSJ1 phosphorylating kinase (Figure 7.5).

We also observed that the HSJ1 mobility on SDS-PAGE was increased in response to CX-4945. This can be due to the prevention of phosphorylation, since the presence of phospho-residues often reduces protein mobility. This produces a so-called up-shift of the phospho-protein compared to the unphosphorylated one. This result suggests that the protein, in untreated cells, is phosphorylated and that the inhibition of CK2 prevents the mobility shift.

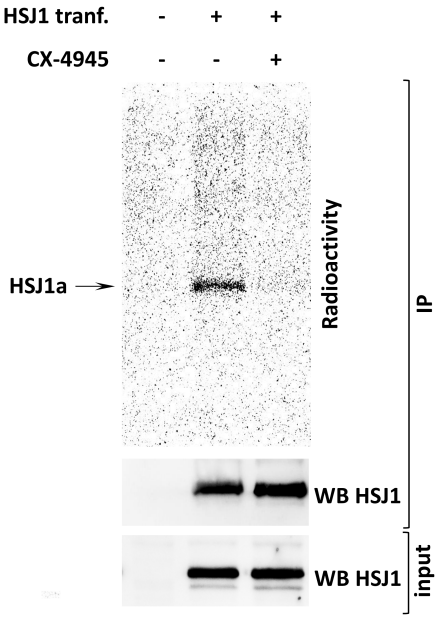

Figure 7.5: **HSJ1 phosphorylation by CK2 *in vitro***
HEK-293T cells were transfected with myc-HSJ1a (+) or empty vector (-), then loaded with (^{32}P)phosphate, and treated with 10 μM CX-4945, as indicated. Anti-myc IP was performed, followed by analysis of radioactivity and of the amount of HSJ1a immunoprecipitated. The lower panel (input) shows 20 μg of total protein lysate, analysed by WB for HSJ1 before IP. Radioactive phospho-proteins were separated by SDS-PAGE/blot and analysed for radioactivity using Cyclone Plus (PerkinElmer) and by WB, as indicated in each panel.

7.4 Mass spectrometry identification of HSJ1 phosphosite(s)

A

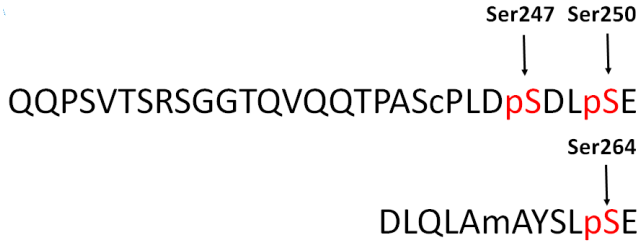

B

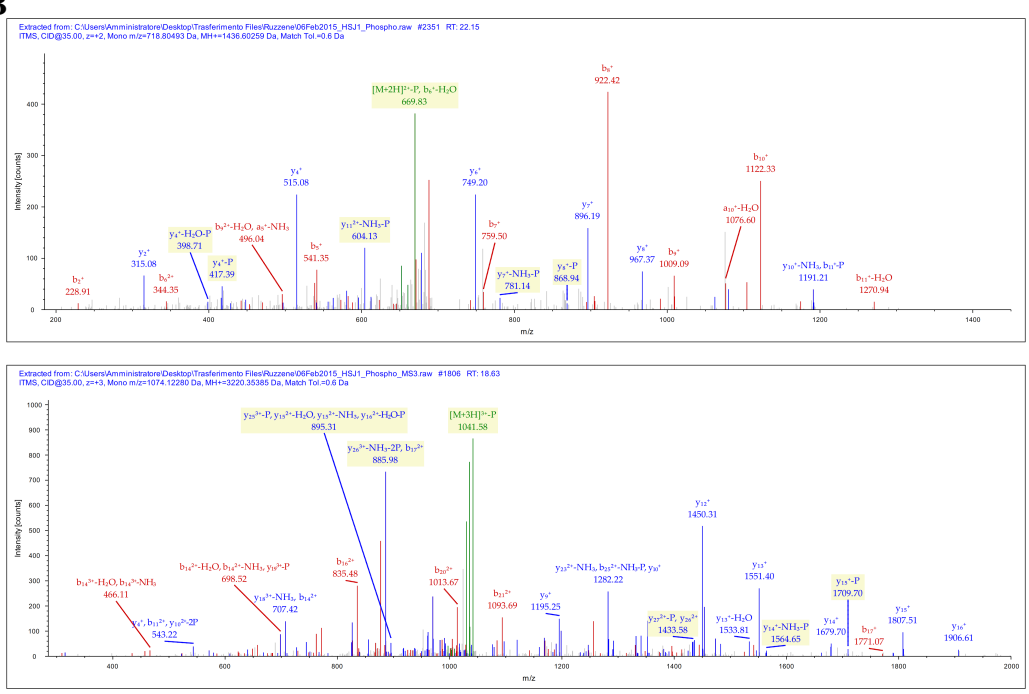

Figure 7.6: **Mass spectrometry identification of CK2 sites on HSJ1**
A. HSJ1a sequences of the peptides in which MS/MS identified phosphorylated residues. Phosphoresidues are reported in red together with their position on HSJ1a. **B.** Annotated MS/MS spectra relative to the phospho-peptides identified in the peptides reported above: DLQLAmAYSLpSE (Above panel) and QQPSVTSRSGGTQVQQTPAScPLDpSDLpSE (Below Panel).

HSJ1a was phosphorylated *in vitro* by CK2 and digested with V8 protease, in order to identify the precise phosphorylated residue(s). The sample was then sent to collaborators (see Materials and Methods section) and the proteolytic peptides analysed by mass spectrometry (MS/MS). This identified Ser247, Ser250, and Ser264 as phospho-amino acids (Figure 7.6).

7.5 Phospho-site mutations

In vitro

To validate the MS/MS findings, we produced Ser-to-Ala single-site mutants of all the identified sites, and also of the putative additional CK2 site Ser262 (within the second UIM), although it was not identified by MS/MS. *In vitro* phosphorylation of the recombinant purified HSJ1a mutants was consistent with the MS outcomes (Figure 7.7): Ser262 mutation did not affect phosphorylation, and Ser264 very weakly contributed to the overall phosphorylation. In contrast, Ser250 appeared to be the main phosphorylation site, as its mutation almost completely abrogated phosphorylation. In apparent contradiction to this, Ser247 mutation to Ala caused an about 50% drop on the total HSJ1a radioactivity. A plausible explanation is the following: Ser247 does not fulfil the CK2 minimal consensus sequence, because it does not have an acidic residue in +3 position. However, once Ser250 is phosphorylated, it becomes acidic and generates the consensus sequence for Ser247. This implies that a hierarchical phosphorylation can occur in HSJ1, where the previous phosphorylation of Ser250 primes Ser247 for subsequent phosphorylation.

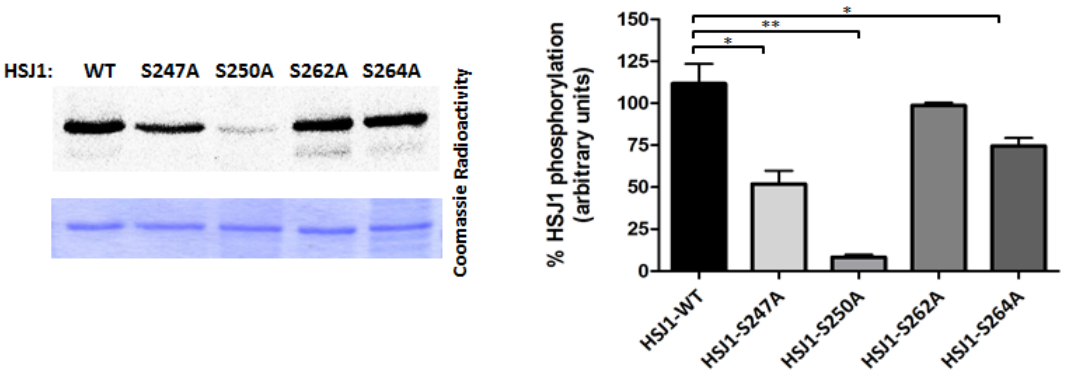

Figure 7.7: **HSJ1 mutants phosphorylation by CK2 *in vitro***
Phosphorylation of HSJ1 WT and mutants by CK2 Recombinant WT or mutant HSJ1a proteins were phosphorylated by CK2 $\alpha 2\beta 2$ (25 ng) and separated by SDS-PAGE. Radioactivity and Coomassie staining of representative experiments are shown. The bar graph shows quantification of radioactivity (mean of n=3 experiments ± SEM. *p=0.03 **p=0.002, unpaired, two-tailed, Student's t-test).

To confirm this hypothesis, we synthesized peptides reproducing the HSJ1 sequence 244-254 in two variants, differing by the presence or absence of phosphate at Ser250. We then checked for their phosphorylation by CK2. As shown in Figure 7.8, both peptides are readily phosphorylated: the one presenting both Ser247 and Ser250 as available sites is better phosphorylated but the phospho S250 one is also a CK2 target, confirming that S247 can be primed by pS250.

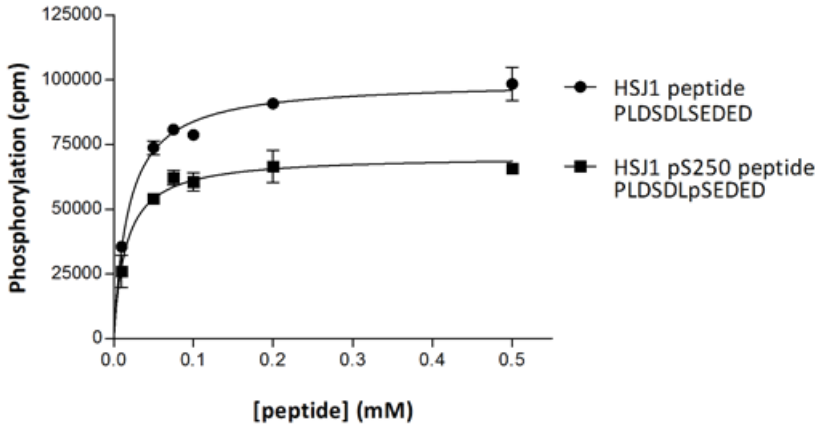

Figure 7.8: **Hierarchical phosphorylation of HSJ1 by CK2**
Increasing concentrations of the indicated peptides were phosphorylated by CK2 $\alpha 2\beta 2$ (25 ng) and analysed for the incorporated radioactivity. More details under Materials and Methods.

In cells

The results obtained *in vitro* with the recombinant mutants were confirmed in cells: expression of the mutants in HEK-293T followed by their immunoprecipitation from [^{32}P]phosphate pre-loaded cells, revealed that the Ser250Ala mutant was not phosphorylated. This demonstrates that this site is the crucial one for the overall phosphorylation of the HSJ1 protein (Figure 7.9). It is also conceivable that a different turnover might occurs between the phospho-sites we identified (i.e. different accessibility to phosphatases). To address this point we increased the loading time of [^{32}P]phosphate from 3 to to 6 hours. This would let phospho-sites with a slow turnover to be better labelled by the radioactive probe. We did not observed significant changes between these two conditions (Figure 7.10). Collectively, data indicate that there are two major phospho-sites in the entire HSJ1 protein, Ser250 and the hierarchical site Ser247, with minimal contribution of other sites.

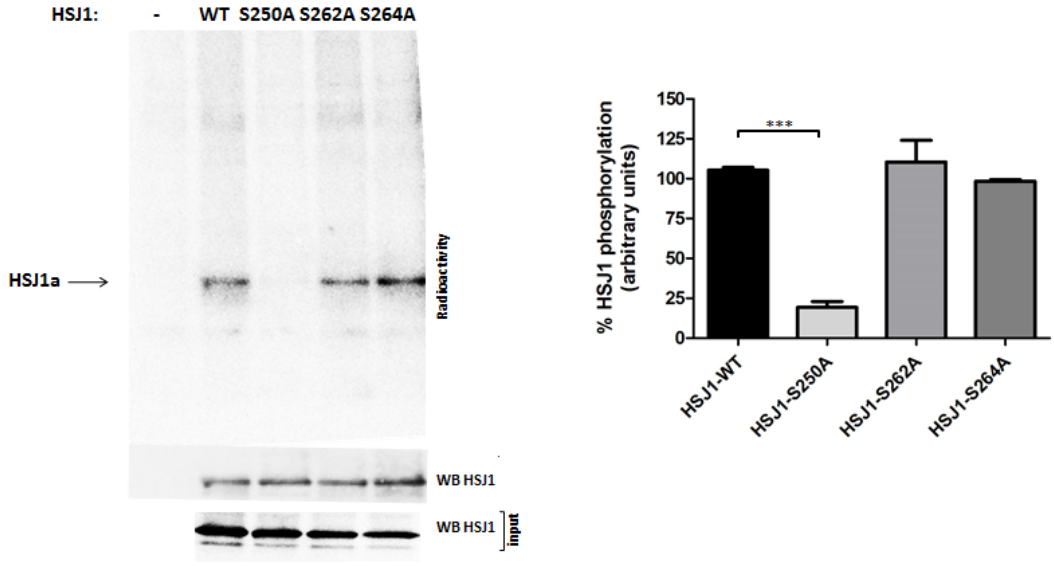

Figure 7.9: **HSJ1 mutants phosphorylation by CK2 in cells**
HEK-293T cells were transfected with myc-HSJ1a (+) or empty vector (-), then loaded with (^{32}P)phosphate for **3 hours**, and treated with 10 µM CX-4945, as indicated. Anti-myc IP was performed, followed by analysis of radioactivity and of amount of HSJ1a immunoprecipitated. The lower panel (input) shows 20 µg of total protein lysate, analysed by WB for HSJ1 before IP. Radioactive phospho-proteins were separated by SDS-PAGE/WB and analysed for radioactivity using Cyclone Plus (PerkinElmer). A Representative experiments are shown. Mean of n=4 experiments ± SEM. ***p≤0.0001, unpaired, two-tailed, Student's t-test.

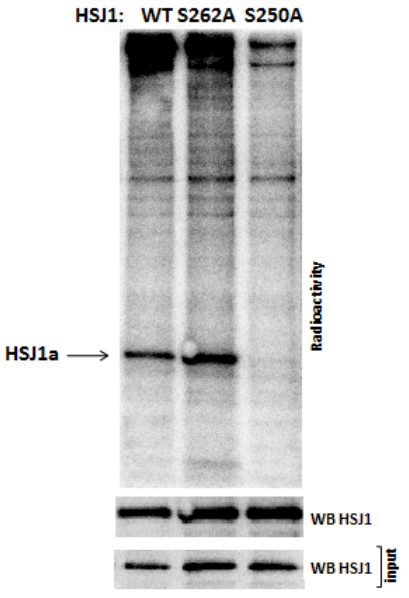

Figure 7.10: **HSJ1 mutants phosphorylation by CK2 in cells**
HEK-293T cells were transfected with myc-HSJ1a (+) or empty vector (-), then loaded with (^{32}P)phosphate for **6 hours instead of 3 hours**, and treated with 10 µM CX-4945, as indicated. Anti-myc IP was performed, followed by analysis of radioactivity and of amount of HSJ1a immunoprecipitated. The lower panel (input) shows 20 µg of total protein lysate, analysed by WB for HSJ1 before IP. Radioactive phospho-proteins were separated by SDS-PAGE/WB and analysed for radioactivity using Cyclone Plus (PerkinElmer). Representative experiments are shown.

7.6 HSJ1 phospho-specific antibodies

We decided to developed phospho-specific antibodies towards the identified sites, choosing a strategy that allows the detection of the protein either when mono-phosphorylated at Ser250 or bis-phosphorylated at Ser250 and Ser247 (see Materials and Methods). Finally antibodies were purified and their specificity was analysed by western blot (WB) and surface plasmon resonance (SPR) techniques. All animals positively responded to the immunization and successfully produced antibodies against the sites phosphorylated by CK2 on the chaperone HSJ1. The antibodies recognize either the mono-phospho and bis-phospho HSJ1 states with affinities in the nM range. They represented fundamental tools to confirm the phosphorylation of HSJ1 *in cells* and to allow further studies on the physiological significance of this novel HSJ1/CK2 connection.

Western Blot analysis

The antibodies were validated *in vitro* toward the protein phosphorylated by recombinant CK2 and transferred onto WB membranes after SDS-PAGE separation. Autoradiography was used to check where phosphorylation occurred (Figure 7.11). It was evident that our antibodies recognized only the phosphorylated form of HSJ1 in a manner that is dependent on phosphorylation levels. Then, the phospho-specific antibodies were used to assess the HSJ1 phosphorylation *in cells*.

First, we expressed either the wild-type (WT) protein or the Ser250 mutant (S250A) of HSJ1a or b in HEK-293T cells. The WT protein was strongly detected by the phospho-specific antibody, while the mutation of the Ser250 completely abrogated the signal (Figure 7.12). A major decrease in the phospho-antibody signal was observed in cells expressing WT HSJ1a and treated with a panel of CK2 inhibitors (Figure 7.13). The reduction in HSJ1 phosphorylation in response to CX-4945, TBB, or CX-5011 was consistent with the reduction of immunoreactivity for the well-known CK2 target Akt pSer129 (Di Maira et al., 2005), and was even more pronounced. Furthermore, staurosporine, which inhibits most protein kinases, but not CK2 (Meggio et al., 1995), had no effect on pHSJ1 immunoreactivity. This

confirmed that CK2 is the major kinase responsible of HSJ1 phosphorylation in these cells.

Then, we tested the phospho-HSJ1 antibodies on a CHO cell line with inducible HSJ1 expression. Also in this case we observed a significant level of phosphorylation, which was sensitive to CK2 inhibition (Figure 7.14). We also performed experiments with CX-4945 that was then washed-out and cells let recover in complete medium (devoid of the inhibitor). As expected, the removal of the compound rapidly restored the HSJ1 phosphorylation. This was probably due to the low persistence of the CX4945-CK2 complex, as described in a parallel project in which I was involved (see Part V, Girardi et al., 2015).

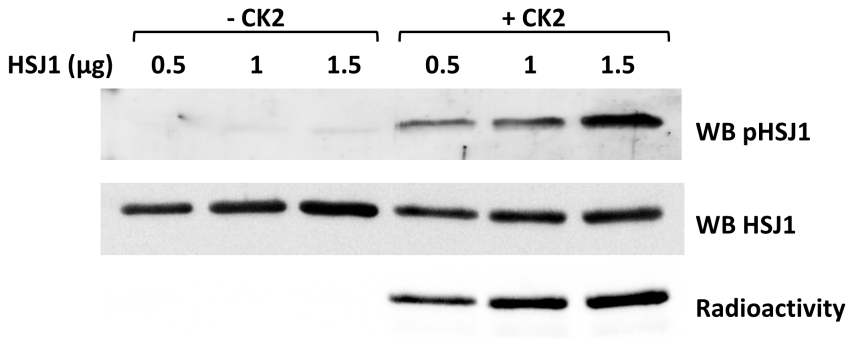

Figure 7.11: **CK2-dependent HSJ1 phosphorylation detected *in vitro***
Increasing amounts of recombinant HSJ1a were incubated in the absence or in presence of CK2 $\alpha 2\beta 2$ (25 ng) and a radioactive phosphorylation mixture. Samples were analysed by WB with the phospho-specific antibody or with total HSJ1 antibody. The radioactivity of the bands is also shown.

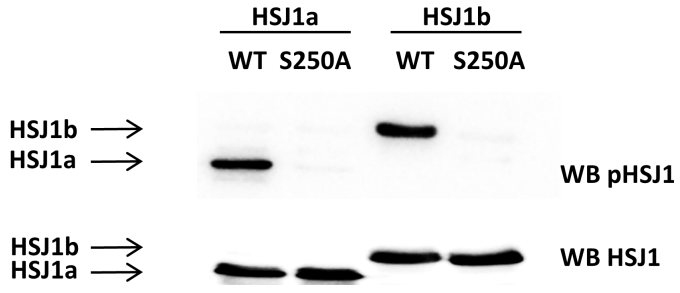

Figure 7.12: **CK2-dependent HSJ1 phosphorylation detected *in cells***
WT or mutant HSJ1 isoforms were expressed in HEK-293T cells. 20 µg of total lysate proteins were analysed by WB with the phospho-specific antibody or with total HSJ1 antibody.

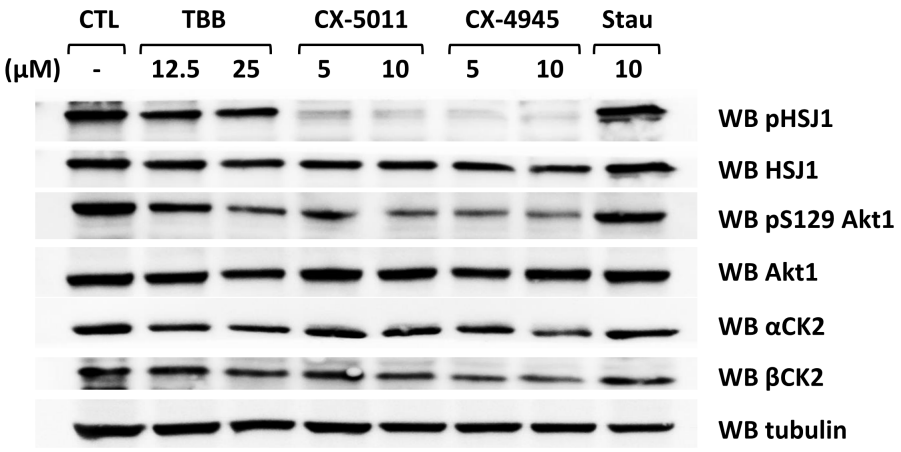

Figure 7.13: **Dephosphorylation of HSJ1 in response to CK2 inhibition**
HEK-293T cells transfected with WT HSJ1a were treated for 3 h with the indicated concentrations of kinase inhibitors; 20 μg of total lysate proteins were analysed by WB, as indicated.

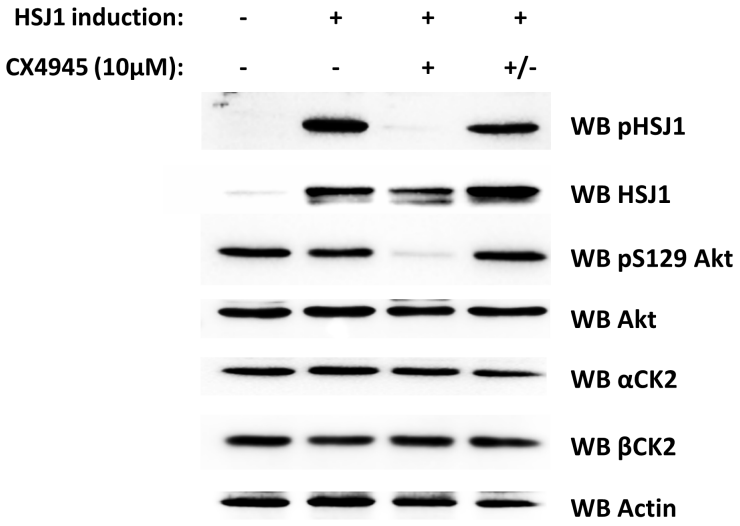

Figure 7.14: **HSJ1 phosphorylation in response to the removal of the CK2 inhibition**
HSJ1a expression was induced in CHO cells by 3 μg/ml tetracycline. Where indicated (+) cells were treated for 3 h with CX-4945; +/- refers to cells that where incubated with CX-4945 for 3 h, then the inhibitor was removed and cells incubated for further 3 h before lysis. 20 μg of total lysate proteins were analysed by WB as indicated.

Biacore analysis

We applied the SPR technology to assess the recognition of the phospho-HSJ1 antibodies toward the mono- and bis-phosphorylated peptides reproducing pSer250 and pSer250/pSer247 HSJ1 sequences, respectively. The peptides were immobilized on a chip surface, and increasing concentration of the pHSJ1 antibody (μM values indicated) flowed in solution over the sensorchip where the pSer250 peptide or pSer247/pSer250 peptide were immobilized in a Biacore T100 instrument (See Materials and Methods).

Results clearly showed that the pSer250 peptide was strongly recognized, with a calculated K_D of $7.65x10^{-9}$ M + $5.77x10^{-10}$; on the contrary, the signal towards pSer250/pSer247 peptide was much weaker, and the K_D was $8.29x10^{-8}$ + $4.92x10^{-9}$ M (Figure 7.15A). Similar results were obtained with the KLH-cojugated phospho-specific antibodies (Figure 7.15B)

Since the peptide immobilization could affect the affinity (Peter et al., 2003), we also applied a competition protocol. Antibodies were injected over the chip in the presence of increasing concentrations of the pSer250 peptide, or pSer250/pSer247 peptides, to assess their ability to prevent the binding to the pSer250 peptide. This analysis allowed the determination of the IC_{50} value for each peptide, which confirmed that the mono-phosphorylated peptide is the best recognized, while the bis-phosphorylated peptide has lower affinity (Fig 7.15C).

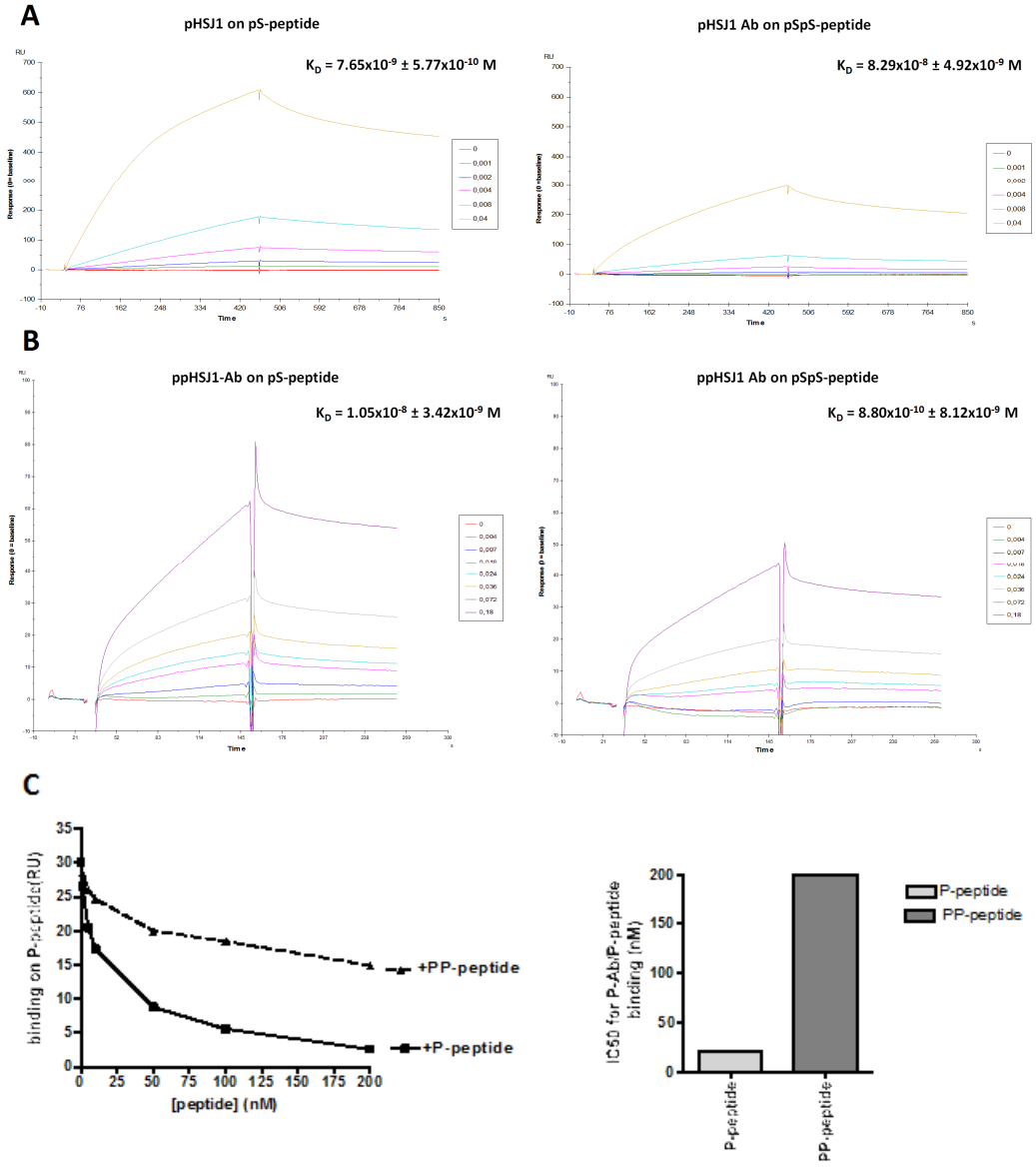

Figure 7.15: **Kinetics of the phospho-HSJ1 antibody (pHSJ1) interactions by means of SPR signal**

A. The first batch (pHSJ1) of antibodies was purified by affinity against mono- and bis-phospho peptides while the second batch (ppHSJ1) **(B)** was purified by affinity against bis-phospho peptides only.

Increasing concentration of the pHSJ1 antibody (M values indicated) were injected over a sensor chip where pSer250 peptide (left panel) or pSer247/pSer250 peptide (right panel) were immobilized in a Biacore T100 instrument (see the Methods for details). Surface plasmon resonance (SPR) signal is shown as sensorgram (time course of the response) reported in resonance units (RU). Each sensorgram has been subtracted from the corresponding signal produced on a control surface and normalized to baseline. 0 concentrations corresponded to dilution buffer.

C. 0.002 M phospho-HSJ1 antibody was injected over the pSer250 peptide immobilized on the chip, in the presence of increasing concentrations of pSer250 peptide or pSer247/pSer250 peptide. The RU signals at the end of the binding time (relative response subtracted of the control signal) for each condition were plotted and the calculation of the IC_{50} was performed by GraphPad software.

7.7 Effects of phosphorylation on HSJ1 function

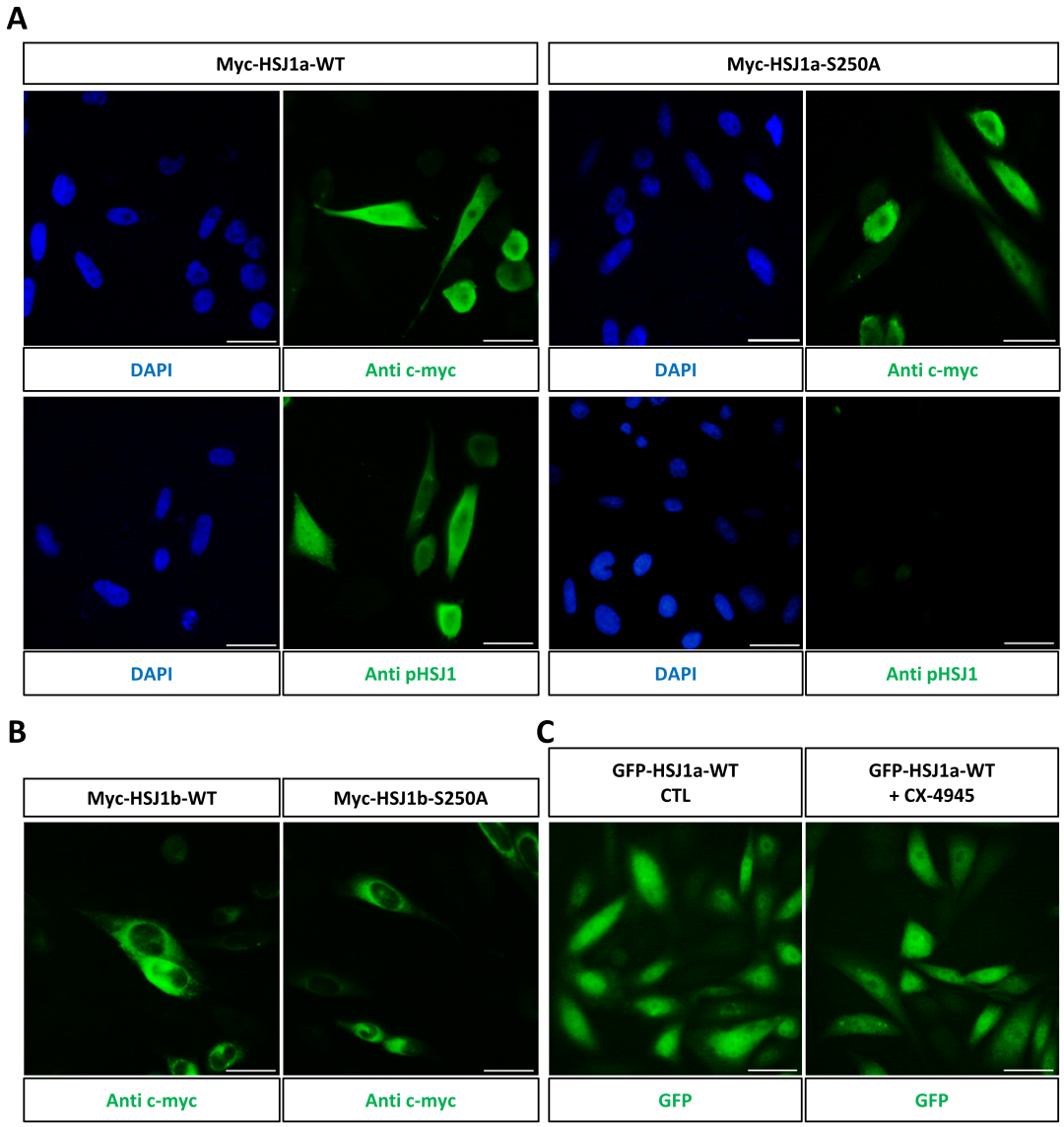

Figure 7.16: **Subcellular localization of HSJ1 and phospho-HSJ1**
A. SK-N-SH cells transfected with myc-HSJ1a WT or Ser250Ala mutant were stained with anti-c-myc or anti-phospho HSJ1 antibody, as indicated, and detected by the Alexa Fluor 488 secondary antibody. Nuclei are stained with DAPI. **B.** SK-N-SH cells transfected with myc-HSJ1b WT or Ser250Ala (S250A)_mutant were stained with anti-c-myc antibody and revealed by the Alexa Fluor 488 secondary antibody. **C.** GFP-HSJ1a expressing CHO cells were treated for 3 h with 10 µM CX-4945 and analysed for fluorescence localization. Scale bars = 50 µm.

We wanted to test whether the phosphorylation of HSJ1 could alter its subcellular localization, as reported for the Ub-binding protein ataxin-3 (Mueller et al., 2009). To this purpose, immunofluorescence analysis was performed with the phospho-HSJ1 antibodies in the neuronal cell line SK-N-SH. we observed a very similar pattern for total HSJ1a or phospho-HSJ1a signal (Figure 7.16). Furthermore, transfection of the Ser250Ala instead of WT HSJ1 did not alter the localization observed by an antibody raised against total HSJ1, while abrogating the phospho-specific signal (Figure 7.16A). In all cases the HSJ1a signal was predominantly in the cytosol and nucleus, as previously reported (Chapple and Cheetham, 2003). Even in the case of HSJ1b, the mutation of the phosphorylation site did not alter the localization of the WT protein, which was consistent with its published localization on the cytoplasmic face of the ER (Chapple and Cheetham, 2003) (Figure 7.16B). The lack of effect of phosphorylation on subcellular HSJ1 localization was also confirmed by treatment of HSJ1-inducible cells with CX-4945, which had no overt effect (Figure 7.16C). The collected data show that HSJ1 is phosphorylated within its second UIM domain which has been reported to be the most important in the binding of ubiquitylated proteins (Westhoff et al., 2005). Therefore, we wanted to test the hypothesis that the phosphorylation could alter the recognition of HSJ1 client proteins (Westhoff et al., 2005). Co-immunoprecipitation was used to analyse the amount of HSJ1a-associated ubiquitylated-proteins (Ub-proteins) and if this was affected by HSJ1 phosphorylation state. Initially, we assessed the effect of CK2 inhibition in HSJ1a stable-inducible cells (Figure 7.17). We found that more Ub-proteins co-precipitated with HSJ1a when cells were treated with CX-4945, which in turn did not change the total amount of Ub-proteins.

To test whether this was due to the reduced HSJ1 phosphorylation or to other effects of CK2 inhibition, we immunoprecipitated HSJ1 from HEK-293T cells overexpressing HSJ1a WT or phospho-mutant forms (Figure 7.18). I also exploited the mutant of Ser262, which is not a CK2 site, but is known to impair UIM functionality (Westhoff et al., 2005), and therefore was used as negative control. The Ser262Ala mutant, as expected, co-precipitated with the lowest amount of Ub-proteins while the phospho-null mutant Ser250Ala showed enhanced binding

to Ub-clients compared to WT HSJ1. By contrast, the same site Ser250 mutated to Asp, that we produced to mimic phosphorylation, was similar to WT or even less effective for Ub-clients association, while the Ser247Ala mutation produced an intermediate level of coIP Ub signal. All together, these results indicate that the phosphorylation of HSJ1 by CK2 reduced its ability to bind ubiquitylated clients. Therefore, we wanted to test if it could also affect HSJ1 chaperone activity. It has been shown that HSJ1 associates with luciferase, and promotes a decrease of the luciferase level/activity in a UIM dependent manner (Howarth et al., 2007). With this in mind, I expressed luciferase in control (uninduced) cells and in HSJ1 induced cells, and I treated them with CX-4945. We found that luciferase activity was reduced in cells expressing HSJ1a. This was probably due to the increased ability of HSJ1 in binding ubiquitylated luciferase trough its second UIM, when dephosphorylated. This was mediated by the inhibition of CK2 via CX-4945 treatment which instead had negligible effect in cells not expressing HSJ1a.

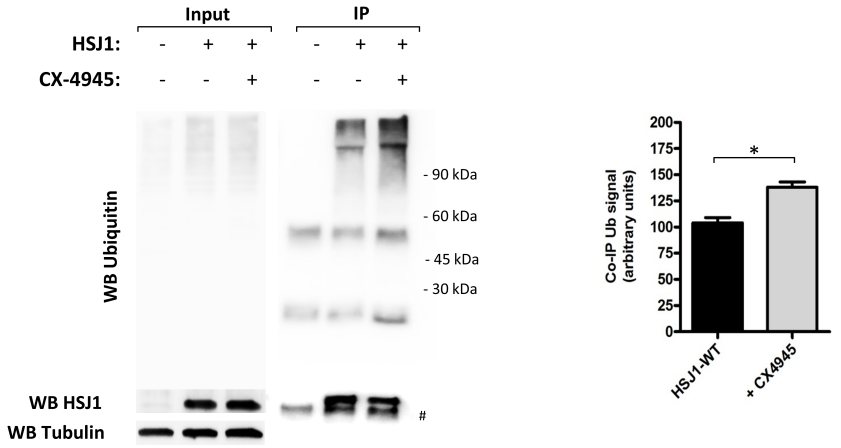

Figure 7.17: **Effects of HSJ1 phosphorylation on Ub-client binding**
1 mg of protein lysates from CHO cells stably transfected with HSJ1 (+) or not (-) were used for HSJ1 immunoprecipitation. Where indicated, cells were treated with 10 µM CX-4945 for 3 h before lysis. 20 µg lysate proteins were loaded for input analysis. Bar graph in A shows the quantification of the Ub signals assigning 100 to the signal of Ub-proteins co-IP with WT HSJ1. Data are presented as mean of n=3 experiments ± SEM. *p<0.05 **p<0.01 ***p<0.001, n.s., not significant, unpaired, two-tailed, Student's t-test.

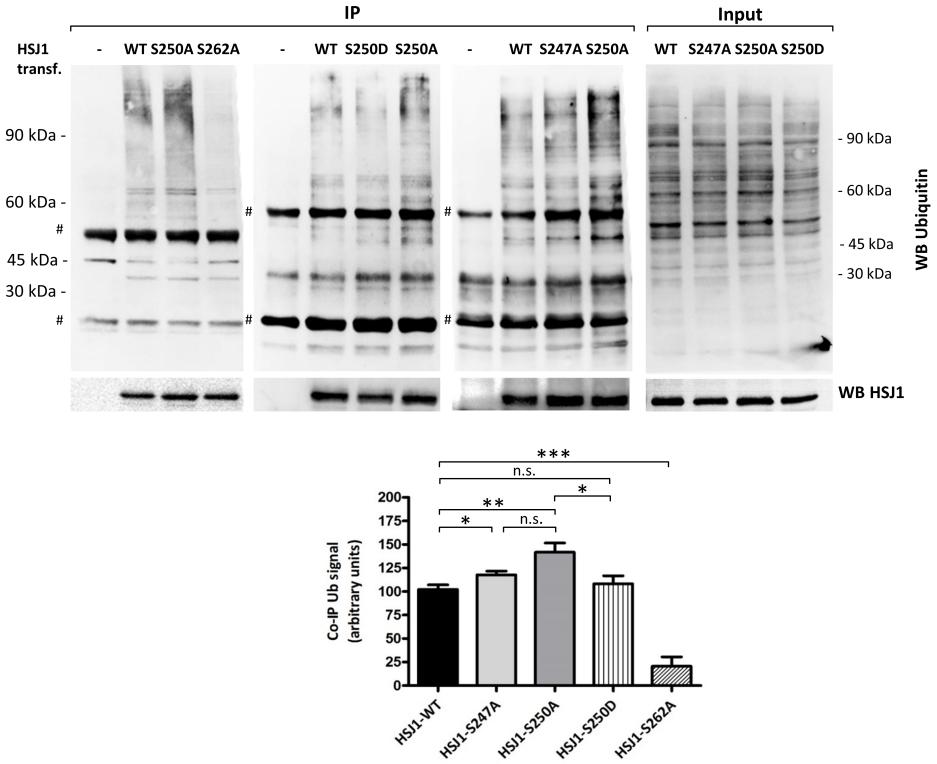

Figure 7.18: **Effects of HSJ1 mutations on Ub-client binding**
HEK-293T cells were transiently transfected with empty vector (-) or HSJ1 WT or mutants, as indicated; 600 µg proteins from cell lysate were used for HSJ1a immunoprecipitation. Analysis was performed by WB for Ubiquitin and for HSJ1. # indicates immunoglobulin bands. Bar graphs in B shows the quantification of the Ub signals assigning 100 to the signal of Ub-proteins co-IP with WT HSJ1a. Data are presented as mean of n=4 experiments ± SEM. *p<0.05 **p<0.01 ***p<0.001, n.s., not significant, unpaired, two-tailed, Student's t-test.

As a net effect, the targeting of the enzyme to proteasomal degradation was enhanced (Figure 7.19A). In a similar experiment, cells expressing the HSJ1 phospho-site mutants Ser247Ala and Ser250Ala displayed the lowest luciferase activity, while the phospho-mimetic Ser250Asp mutant produced an effect quite similar to the WT (Figure 7.19B).

Collectively, these data indicate that the phosphorylation by CK2 prevents the full functionality of HSJ1 chaperone activity. Our findings indicate that CK2 inhibition can be exploited in all those conditions where a higher activity of HSJ1 would be beneficial. Being HSJ1 overexpression involved in the clearance of amyloid aggregates, there are potential therapeutic implications for NDs.

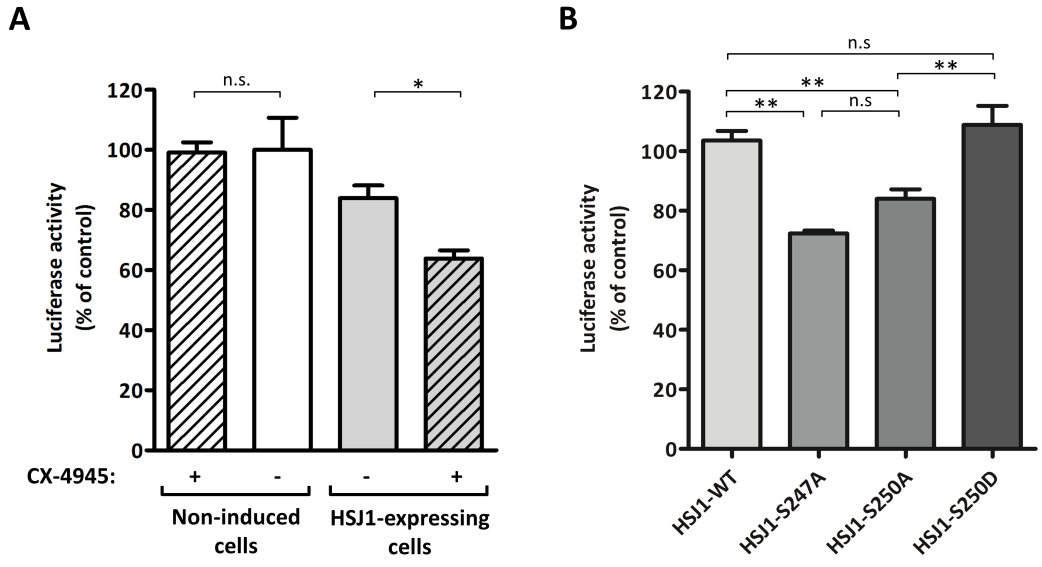

Figure 7.19: **Effects of HSJ1 phosphorylation on its chaperone activity**

A. Luciferase was expressed in HSJ1a stable transfected CHO cells; HSJ1 expression was induced as indicated. Where indicated, cells were treated for 3 h with 10 μM CX-4945. **B.** SK-N-SH cells were co-transfected with HSJ1 WT or mutants and luciferase before activity measurements. Data are presented as mean of n=3 experiments ± SEM. *p<0.05 **p<0.01 ***p<0.001, n.s., not significant, unpaired, two-tailed, Student's t-test.

Part IV

Discussion

Chapter 8

Discussion

Signal transduction is mediated by several types of post-translation modifications. Coordination of this network of interconnections among the different systems is essential to better tune the signal. An emerging theme is represented by the multiple connections between phosphorylation and ubiquitylation (Hunter, 2007). Here we disclose a novel crosstalk between CK2 signalling and Ub system. CK2 has been frequently connected to protein degradation pathways. It has a well-defined role in the regulation of caspases, mainly through the phosphorylation of crucial sites in caspase substrates that become refractory to proteolysis (Duncan et al., 2010). CK2 involvement in the regulation of other proteolytic pathways has been also reported. Interestingly, it has been demonstrated that the SUMO interacting motifs (SIMs), when phosphorylated by CK2, display a higher affinity for the Ub-like molecule SUMO. This was initially reported for the tumour suppressor PML, the exosome component PMSCL1, and the E3 SUMO ligase PIAS1 (Stehmeier and Muller, 2009), and recently for the RAP80 protein, a key component of double-strand DNA break repair mediated by the BRCA1 complex (Anamika and Spyracopoulos, 2016). CK2 also phosphorylates p62, an autophagy-related Ub-binding protein; the phosphorylation occurs at several sites, also within the UBA (Ub-associated) domain of p62, and promotes a shift of specificity that allows the binding to both K63-linked and K48-linked poly-Ub (Matsumoto et al., 2011). CK2 has been also reported to regulate the clearance of misfolded proteins by recruiting them to aggresomes in response to stress (Watabe and Nakaki, 2011). Moreover, the Ub-interacting protein Ataxin-3 was found

phosphorylated by CK2 at several sites; although phosphorylation did not affect protein interactions, it affected its subcellular localization and stabilization (Mueller et al., 2009). To the best of my knowledge, it has never been reported before that CK2 phosphorylates a protein within a UIM sequence, with functional consequences for Ub-client binding. Here we show that HSJ1, a protein involved in the delivery of Ub-proteins for proteasomal degradation, is phosphorylated by CK2 on its second UIM, both *in vitro* and *in cells*, and this inhibits its function. Other findings have previously connected CK2 to the proteasome function. Tsuchiya and coworkers showed that CK2, by inhibiting the transcriptional activity of Nrf1, down-regulates the expression of proteasome subunit genes, and that CK2 knock-down alleviates the accumulation of Ub-proteins upon proteasome inhibition (Tsuchiya et al., 2013). Moreover, CK2 controls the stability of 26S proteasome by phosphorylating the 20S proteasome alpha subunit C8 (Bose et al., 2004). A recent proteomics study from our laboratory showed that cell treatment with the CK2 inhibitor quinalizarin is accompanied by a dramatic increase of all the components of the proteasomal catalytic core (Franchin et al., 2015). Other studies have correlated the activity of CK2 to the proteasomal degradation of specific proteins. It is worth mentioning the direct phosphorylation of PML by CK2 at Ser517, which promotes the proteasome-dependent degradation of PML, thus preventing its tumour-suppressive activity (Scaglioni et al., 2006). More recently, it was demonstrated that the SUMOylation of PML is required for its interaction with CK2 and subsequent proteasome-mediated degradation (Rabellino et al., 2012). PTEN is another tumour suppressor protein degraded by proteasome and phosphorylated by CK2; in this case, the phosphorylation protects the protein from degradation, although, at the same time it inhibits its function (Barata, 2011). Similarly, Pax7, a transcription factor with important functions in muscle regeneration, is protected from proteasome-dependent degradation when phosphorylated by CK2 (González et al., 2016). Here we add HSJ1 to the list of the CK2 targets that are related to the proteasome function.

We identified the HSJ1 sites where phosphorylation occurs by a hierarchical mechanism, and demonstrated that the presence of phosphate within the second UIM of HSJ1 reduces its binding to Ub-clients and its chaperone activity, without

affecting the protein subcellular distribution. The effects of UIM phosphorylation in HSJ1 is the opposite of what reported for the SIM, where the CK2-dependent phosphorylation enhances the affinity for SUMO (Stehmeier and Muller, 2009; Anamika and Spyracopoulos, 2016), and for UBA, the Ub-binding domain of p62 that increases its affinity for clients when phosphorylated by CK2 (beside displaying altered specificity) (Matsumoto et al., 2011). However, the binding of SUMO to SIM (Hecker et al., 2006), and of Ub to UBA (Long et al., 2008) are due to a combination of hydrophobic and electrostatic interactions, while Ub typically interacts to UIMs mainly through hydrophobic bonds (Shekhtman and Cowburn, 2002; Hicke et al., 2005). It should be also considered that p62 is phosphorylated in many other sites that can modulate the final outcome. The complex correlation between Ub-binding and phosphorylation is further highlighted by the observation that phosphorylation of ataxin-3 produces variable effects, depending on the UIM domain considered (Mueller et al., 2009). Further studies will be necessary to fully understand the functional effects of HSJ1 phosphorylation by CK2 and the exact mechanism of UIM regulation.

The addition of HSJ1 among the numerous CK2 substrates has a relevance to neurodegenerative diseases. The importance of CK2 to neuronal functions and disease is supported by several findings. Already in 2000, Blanquet and colleagues reviewed data supporting a potential role of CK2 in neuronal function and implicated it in degenerative disorders (Blanquet, 2000) and this was extended later (Guerra and Issinger, 2008). More recently, it was found that CK2 phosphorylates and promotes stabilization and aggregation of ataxin3 (ATXN3), the pathogenic protein of spinocerebellar ataxia type 3 (SCA3) (Mueller et al., 2009). HSJ1, here identified as a novel CK2 substrate, is related to protein aggregation and neurodegeneration, since it exerts a neuroprotective function by processing aggregation-prone proteins and promoting their delivery to the proteasome (Westhoff et al., 2005), preventing the seeding of aggregation (Labbadia et al., 2012) or refolding of mutant proteins (Rose et al., 2011; Chen et al., 2016). Our results, showing that CK2 inhibits HSJ1 function, suggest that CK2 inhibition might help enhance HSJ1 function in the clearance of Ub-protein aggregates and deserve attention in a therapeutic perspective. CK2 inhibitors,

already under investigation as anticancer drugs, might in future also be applied to neurodegenerative conditions to prevent or reduce protein aggregation. Overexpression of HSJ1a has been shown to be protective in several models of neurodegeneration both in cells and in *vivo* by UIM dependent mechanisms (Labbadia et al., 2012; Novoselov et al., 2013). Data suggest that simultaneous HSJ1a overexpression and CK2 inhibition could synergise the chaperone activity and further prolong neuronal survival.

With this study, we disclosed an unanticipated HSJ1/CK2 connection with important implications for the molecular mechanisms of neurodegeneration and hopefully for the development of associated therapies. Since the HSJ1 co-chaperone function is critical in preventing neurodegeneration and is enhanced by the dephosphorylation of the sites targeted by CK2, treatments with CK2 inhibitors could be explored in the future as novel therapeutical compounds. Moreover, we observed that residues inside UIMs are superimposable to the consensus targeted by CK2 for phosphorylation and that they are evolutionary conserved. Therefore, we consider highly probable that other UIM-containing proteins could be phosphorylated by CK2. Our results possibly suggest a broader regulation mechanism in cellular proteostasis able to influence the processing of ubiquitylated clients. Further work will be dedicated to unveil the meaning of this CK2/UIM connection as we already started by showing the phosphorylation of the UIM-containing protein S5a.

Part V

Related Projects

Chapter 9

Novel strategies to inhibit CK2

Protein kinase CK2 appeared to be a prominent druggable target after the discovery of its deregulated activity in cancer. Moreover, cancer cells rely on abnormal levels of CK2 for their viability leading to the concept of 'addiction' to CK2 (Ruzzene and Pinna, 2010) (see Chapter 2.2). Therefore, cancer cells were demonstrated to be more sensitive to the inhibition of the CK2 activity whereas their healthy counterparts have appeared to better tolerate the reduction of the enzyme (Ruzzene and Pinna, 2010). This promoted the design and test of several inhibitory molecules some of which are currently patented and or in clinical trials (as described in Chapter 2.3).

However, the use of inhibitors was of invaluable support also in helping understanding the role of CK2 in other pathologies. The main work of this thesis suggests that CK2 inhibition can be considered in a therapeutic perspective for different diseases, such as neurodegeneration. Despite the wide use and availability of CK2 inhibitory compounds, the characterization of their mechanism of action and tolerability are still under intensive investigations.

Several studies have been deeply focused in developing molecules targeting the ATP cavity of CK2 (Cozza et al., 2013). We designed, developed and characterized two inhibition strategies as novel approaches to possibly increase the therapeutic efficacy. They are hereafter described as two related projects respect to the main focus of this thesis.

9.1 Chimeric peptides as modulators of CK2-dependent signalling: Mechanism of action and off-target effects

I have been involved in a parallel project focused on the work of Perea and collaborators, who exploited a new CK2 inhibition strategy. They design a molecule able to bind the CK2 consensus on substrates and to hamper their phosphorylation, rather than directly affect the enzyme activity (Perea et al., 2008). Perea's inhibitor was developed looking for sequences able to block the phosphorylation of the human papilloma virus protein HPV-16 E7. They exploited a sequence, named p15, derived from a screening of random cyclic peptide phage display libraries. It was then fused to a cell-penetrating peptide: a portion of the Tat protein which mediates the invasion of the HIV virus. Authors named this chimeric compound CIGB-300 (Perea et al., 2008). CIGB-300 was shown to have antitumoural effects in cancer cell lines and in test animals (Perera et al., 2008; Martins et al., 2014; Farina et al., 2011; Perera et al., 2014; Cirigliano et al., 2016; Benavent et al., 2016). Similarly to CX-4945, CIGB-300 entered clinical trials for the treatment of cervical malignancies (Perea et al., 2008; Solares et al., 2009).
Given the complementary of CIGB-300 to the CK2 phospho-consensus and the pleiotropicity of the enzyme, it is conceivable that a broad number of proteins can be potentially hit by the compound. To better test this hypothesis and exploit the potential of this new inhibition strategy, we developed a Tat-conjugated p15 chimeric peptide we named CK2-MCP, similar in sequence to CIGB-300. I specifically contributed to this project by performing Biacore experiments and proteasome activity assays. Results showed that CK2-MCP was also able to directly bind to CK2. Moreover, we found that CK2-MCP inhibits CK2 activity *in vitro* towards those substrates that specifically require the presence of the beta-subunit (class III substrates, see Chapter 2.1). It is also able to impair the CK2 auto-phosphorylation at its β subunit thus suggesting a direct interaction with the enzyme. This was confirmed by Biacore experiments, where we found that the CK2-MCP peptide interacts with the CK2 holoenzyme, but also with the separate α and β subunits (please refer to the following reprint for more details).

While analysing CK2-MCP effects in cells, we observed an unexpected, abundant accumulation of ubiquitylated proteins as a consequence of cell treatment with the inhibitor. Therefore, we decided to check if this effect was related to proteasome dysfunctions. Indeed, we measured the proteasome activity in cells treated with the chimeric compound and found an impaired proteasomal activity. Possibly, it was due to a direct inhibition of the proteasome activity by CK2-MCP. Therefore, we performed an analysis of the sequences of the proteasome components, looking for possible interacting sites for CK2-MCP. We found that the protein S5a, one of the accessory particles of the proteasome, displays two typical CK2 consensuses onto the CK2-MCP might act, having been designed to block CK2 sites. These consensuses were located inside UIMs. This suggested a possible effect of the inhibitor in blocking the binding of ubiquitylated clients to S5a and their delivery to proteasomal degradation. Then, a more detailed study revealed an entire class of proteins containing UIM domains and displaying sites possibly phosphorylated by CK2 (as detailed in Chapter 3.2.1). We specifically focused on the UIM-containing protein HSJ1 due to its relevance in neurodegeneration (Chapter 4.3).

Biochimica et Biophysica Acta 1854 (2015) 1694–1707

Contents lists available at ScienceDirect

Biochimica et Biophysica Acta

journal homepage: www.elsevier.com/locate/bbapap

Chimeric peptides as modulators of CK2-dependent signaling: Mechanism of action and off-target effects☆

Sofia Zanin [a], Michele Sandre [b], Giorgio Cozza [a], Daniele Ottaviani [a], Oriano Marin [a,b,*], Lorenzo A. Pinna [a,c], Maria Ruzzene [a,**]

[a] Department of Biomedical Sciences, University of Padova, Padova, Italy
[b] CRIBI Biotechnology Centre, University of Padova, Padova, Italy
[c] CNR Institute of Neurosciences, Padova, Italy

ARTICLE INFO

Article history:
Received 22 January 2015
Received in revised form 17 April 2015
Accepted 21 April 2015
Available online 30 April 2015

Keywords:
CK2
CKII
Inhibitors
Chimeric peptides
Casein kinase
ClGB-300

ABSTRACT

Protein kinase CK2 is a tetrameric enzyme composed of two catalytic (α/α′) and two regulatory (β) subunits. It has a global prosurvival function, especially in cancer, and represents an attractive therapeutic target. Most CK2 inhibitors available so far are ATP-competitive compounds; however, the possibility to block only the phosphorylation of few substrates has been recently explored, and a compound composed of a Tat cell-penetrating peptide and an active cyclic peptide, selected for its ability to bind to the CK2 substrate E7 protein of human papilloma virus, has been developed [Perea et al., Cancer Res. 2004; 64:7127–7129]. By using a similar chimeric peptide (CK2 modulatory chimeric peptide, CK2-MCP), we performed a study to dissect its molecular mechanism of action and the signaling pathways that it affects in cells. We found that it directly interacts with CK2 itself, counteracting the regulatory and stabilizing functions of the β subunit. Cell treatment with CK2-MCP induces a rapid decrease of the amount of CK2 subunits, as well as of other signaling proteins. Concomitant cell death is observed, more pronounced in tumor cells and not accompanied by apoptotic events. CK2 relocalizes to lysosomes, whose proteases are activated, while the proteasome machinery is inhibited. Several sequence variants of the chimeric peptide have been also synthesized, and their effects compared to those of the parental peptide. Intriguingly, the Tat moiety is essential not only for cell penetration but also for the in vitro efficacy of the peptide. We conclude that this class of chimeric peptides, in addition to altering some properties of CK2 holoenzyme, affects several other cellular targets, causing profound perturbations of cell biology. This article is part of a Special Issue entitled: Inhibitors of Protein Kinases.

1. Introduction

CK2 is a ubiquitous and constitutively active Ser/Thr protein kinase, expressed in all cells but particularly abundant in cancer cells [1–3]. It is a tetrameric holoenzyme composed of two catalytic (α and/or α′) and two regulatory (β) subunits; the catalytic subunits alone are active even in the absence of the β subunits, whose major role is in stabilizing the holoenzyme and affecting substrate selectivity. In fact, among the huge number of CK2 substrates [4], some of them are exclusively phosphorylated by the catalytic subunit in the absence of β, others are phosphorylated only by the tetrameric holoenzyme, others by both [5]. CK2 is involved in practically all cellular process, but its major function is recognized in counteracting apoptosis and promotes cell survival [6,7].

Inhibition of pro-survival kinases is a successful strategy to induce apoptosis of cancer cells. Also CK2 inhibitors are becoming promising pharmacological tools; after the initial diffidence in targeting a ubiquitous and pleiotropic kinase such as CK2, it turned out that cancer cells are more dependent on CK2 for their survival than normal cells, and are consequently more affected by its inhibition [3]. This can explain

Abbreviations: Akt, protein kinase Akt (PKB); B23, nucleophosmin; BSA, bovine serum albumin; CaM, calmodulin; CK2-MCP, CK2 modulatory chimeric peptide; CK2, protein kinase CK2, (casein kinase 2); CM5, carboxymethylated dextran 5; CML, chronic myeloid leukemia; DC_{50}, concentration inducing 50% cell death; DMEM, Dulbecco's Modified Eagle's Medium; DTT, dithiothreitol; eiF2β, elongation initiation factor 2β; FBS, fetal bovine serum; HATU, O-(7-azabenzotriazole-1-yl)-N,N,N,N′-tetramethyluronium hexafluorophosphate; HPV, human papilloma virus; Hsp90, heat shock protein 90; LAMP1, lysosomal associated membrane protein 1; MTT, 3-(4,5-dimethylthiazol-2-yl)-3,5-diphenyltriazolium bromide; Mtt, methyltrityl group; PARP, poly (ADP-ribose) polymerase; PBS, phosphate buffered saline; PVDF, polyvinylidene difluoride; rpS6, ribosomal protein S6; RU, resonance unit; SDS-PAGE, sodium dodecyl sulfate polyacrylamide gel electrophoresis; SPR, surface plasmon resonance; TBS, Tris buffered saline; WB, western blot

☆ This article is part of a Special Issue entitled: Inhibitors of Protein Kinases.

* Correspondence to: Department of Biomedical Sciences, University of Padova, Via Ugo Bassi 58b, 35131 Padova, Italy. Tel.: +39 049 8276151.

** Correspondence to: Department of Biomedical Sciences, University of Padova, Via Ugo Bassi 58b, 35131 Padova, Italy. Tel.: +39 049 8276112.

E-mail addresses: oriano.marin@unipd.it (O. Marin), maria.ruzzene@unipd.it (M. Ruzzene).

http://dx.doi.org/10.1016/j.bbapap.2015.04.026
1570-9639/

why systemic treatments of animals with CK2 inhibitors are safe and well-tolerated (as reviewed in [8]) and accounts for the preliminary encouraging results of a powerful ATP-competitive inhibitor of CK2, CX-4945, employed in clinical trials in humans [9]. While most CK2 inhibitors, CX-4945 included, are ATP-competitive molecules, a peptidic-compound was developed by Perea and coworkers to "block CK2 phosphorylation" [10]. The peptide was designed by screening a random cyclic peptide phage display library, looking for sequences able to block the phosphorylation of the human papilloma virus HPV-16 E7 protein by CK2. The identified sequence was a cyclic peptide, initially termed p15, which was fused to a cell-penetrating peptide derived from the HIV Tat protein. The resulting compound, later renamed CIGB-300 [11], was shown to have cytotoxic effect in cancer cell lines, and to reduce solid tumor growth in mice upon systemic administration [12]. The peptide was also reported to display antitumor efficacy in mouse xenograft models of human chronic lymphocytic leukemia [13], to exhibit anti-angiogenesis activity in a chicken embryo model [14], and to produce synergistic effects with antitumor drugs in lung and cervical cancer models [15]. It has also entered clinical trials for patients with cervical malignancies, proving to be well tolerated and able to induce clinical benefits [11,16].

As far as the CIGB-300 mechanism of action is concerned, a number of studies have been published attempting to identify its cellular targets. Although the compound has been developed to selectively block the phosphorylation of the HPV-16 E7 protein by CK2, several other effects have been reported. A proteomic study in non-small cell lung cancer cells has revealed an effect of CIGB-300 on the abundance of several proteins, especially evident on those proteins involved in the translation process [17]. However, the main cellular target of CIGB-300 seems to be B23/nucleophosmin [18]. This is a nucleolar protein, whose phosphorylation by CK2 [19] is prevented by CIGB-300 with concomitant nucleolar disassembly. Indeed the peptide, after cellular uptake, rapidly localizes to the nucleolus, to subsequently reach the lysosomes, which are involved in its degradation [20].

The complexity of the cellular effects reported so far suggests that the action of CIGB-300, improperly often defined as a "CK2 inhibitor", could be mediated by alternative mechanisms in addition to targeting specific phosphoacceptor sites in CK2 substrates. We performed this study with the aim to investigate in more details the direct effect of this kind of chimeric peptides on CK2 activity, and to better understand the molecular events and the pathways involved in response to cell treatment with these compounds.

2. Materials and methods

2.1. Materials

For peptide synthesis, all N-α-fluorenylmethyloxycarbonyl (Fmoc) L-amino acids, p-benzyloxybenzyl alcohol resin (Wang resin), 4-(2′,4′-dimethoxyphenyl-Fmoc-aminomethyl)-phenoxyacetamido-norleucyl-MBHA resin (Rink Amide MBHA resin) were obtained from Novabiochem (Darmstadt, Germany). Coupling reagent O-(7-azabenzotriazole-1-yl)-N,N,N',N'-tetramethyluronium hexafluorophosphate (HATU) was purchased from ChemPep (Wellington, FL, USA). D-Biotin was obtained from Sigma-Aldrich. Chemical reagents were purchased from Sigma-Aldrich and Iris Biotech (Marktredwitz, Germany).

Glu-C protease was from Promega.

Anti-α CK2 was raised in rabbit against the sequence of the human protein at C-terminus [376–391] and N-terminus [2–15,21], total anti-Akt, total anti-Cdc37, anti-Hsp90, anti-LAMP1 and anti-rpS6 antibodies were from Santa Cruz Biotechnology, anti-β-actin, anti-α-tubulin and anti-p62 antibodies were from Sigma, anti-ubiquitin antibody was from Millipore, anti-PARP antibody was from Roche, anti-procaspase 3 antibody was from Cell Signaling Technology, anti-CK2 β antibody was from Epitomic; and B23 antibody was from Invitrogen. Secondary antibodies towards rabbit and mouse IgG, conjugated to horse radish peroxidase, were from PerkinElmer.

CK2-tide, eiF2β-tide, E7-tide1, E7-tide2, B23-tide and REV-tide synthetic substrates were made available by the Peptide Facility at CRIBI.

Recombinant human α and $\alpha_2\beta_2$ CK2 were purified and kindly provided by Dr. S. Sarno and Dr. A. Venerando (University of Padova, Italy). Recombinant His-B23 was from AbCam. Total casein, α-casein and β-casein were from Sigma. Recombinant Akt2 was from Active Motif.

2.2. Synthesis of peptides

The synthetic peptide CK2-MCP and its derivatives (see Table 1) were synthesized by solid-phase technique using a multiple peptides synthesizer (SyroII, MultiSynTech GmbH) on a Wang resin or alternatively Rink Amide MBHA resin. The fluoren-9-ylmethoxycarbonyl (Fmoc) strategy [22] was used throughout the peptide chain assembly, utilizing HATU as coupling reagent [23].

Table 1
Primary structures of peptides synthesized and used in this work.
Tat sequence is in italic, bold underlined residues indicate variations compared to p15 sequence. C, cyclic; L, linear; and β-Ala (β-Alanine) was used as non-α-amino acid flexible spacer. The sequence between the two Cys in Emo-Tat peptide corresponds to sequence 22-30 of human hemoglobin α subunit, while in the scramble peptide corresponds to the sequence used in [40]. CK2-MCP-Biotin is CK2-MCP biotinylated at the C-terminus via the primary ε amino group on a C-terminal inserted lysine. The bottom part of the table displays the sequence of the peptides used as in vitro CK2 substrates.

Name	Sequence	C/L
CIGB-300	*GRKKRRQRRRPPQ*-β-Ala-CWMSPRHLGTC	C
CK2-MCP	CWMSPRHLGTC-β-Ala-*GYGRKKRRQRRRG*-NH_2	C
CK2-MCP-Lin	CWMSPRHLGTC-β-Ala-*GYGRKKRRQRRRG*-NH_2	L
p15	CWMSPRHLGTC	C
Tat	*GYGRKKRRQRRRG*-NH_2	L
CK2-MCP scramble	C**HPGSTWMRL**C-β-Ala-*GYGRKKRRQRRRG*-NH_2	C
Emo-Tat	C**AGEYGAEAL**C-β-Ala-*GYGRKKRRQRRRG*-NH_2	C
CK2-MCP-C1C11	**A**WMSPRHLGT**A**-β-Ala-*GYGRKKRRQRRRG*-NH_2	L
CK2-MCP-C11	CWMSPRHLGT**A**-β-Ala-*GYGRKKRRQRRRG*-NH_2	L
CK2-MCP-Biotin	CWMSPRHLGTC-β-Ala-*GYGRKKRRQRRRG*K(Biotin)-NH_2	C
CK2-tide	RRRADDSDDDDD	
eiF2β-tide	MSGDEMIFDPTMSKKKKKKKKP	
REV-tide	MAGRSGDSDEELIRTVRLIKLLYQSN	
B23-tide	RLKCGSGPVHISGQHLVAVEEDAESEDEEEEDVK	
E7-tide1	HGDTPILHEYMLDLQPETTDLYCYEQLNDSSEEEDEIDGPAGQAEPDRA	
E7-tide2	ETTDLYCYEQLNDSSEEEDEIDGPAGQAEPD	

The side-chain protected amino acid building blocks used were: N-α-Fmoc-Nω-(2,2,4,6,7-pentamethyldihydrobenzofuran-5-sulfonyl)-L-arginine, N-α-Fmoc-O-tert-butyl-L-serine, N-α-Fmoc-Nε-(tert-butyloxycarbonyl)-L-lysine, N-α-Fmoc-N(im)-trityl-L-histidine, N-α-Fmoc-N-γ-trityl-L-glutamine, N-α-Fmoc-S-trityl-cystine, N-α-Fmoc-N-β-trityl-L-glutamine, and N-α-Fmoc-N(in)-(tert-butyloxycarbonyl)-L-tryptophan.

For anchoring the biotin probe, an additional lysine residue side-chain protected with the methyltrityl group (Mtt) was introduced at C-terminal position. After synthesis of the fully protected peptide, the Mtt group was selectively removed by treatment of the peptidyl resins with 1% trifluoroacetic acid, 10% trifluoroethanol in dichloromethane. Then, the free ε-amine of lysine was reacted with biotin, in the presence of HATU as coupling reagent.

Cleavage of the peptides was performed by reacting the peptidyl resins with a mixture containing trifluoroacetic acid and ethanedithiol (95:5) for 2.5 h.

Crude peptides were purified by reverse phase HPLC on a preparative column (Prep Nova-Pak HR C18, Waters, USA).

Cyclization of peptides containing two cysteine moieties was achieved by oxidizing the purified peptide (0.1 mg/ml) in 100 mM NH_4HCO_3 buffer (pH 8.2) for 72 h. The formation of disulfide bridges and the masses of the peptides were confirmed by mass spectrometry using a MALDI TOF/TOF instrument (ABI 4800, Applied Biosystems, USA).

All the peptides synthetized and used in this work are listed in Table 1.

2.3. CK2 activity assays

Recombinant $\alpha_2\beta_2$ CK2 (10–40 ng) or recombinant α CK2 (10–50 ng) were incubated with peptides or protein substrates in a phosphorylation buffer containing 50 mM Tris–HCl pH 7.5, 10 mM $MgCl_2$, 10 μM [γ-^{33}P] ATP (1000–2000 cpm/pmol) and 0.1 M NaCl, in a final volume of 20 μl. When α CK2 was used, NaCl was omitted. The following peptide substrates were used: CK2-tide, eiF2β-tide, REV-tide and B23-tide at 0.1 mM; and E7-tide1, E7-tide2 at 0.3 mM. The protein substrates were used at the following concentrations: α-casein and total casein 0.5 μg, calmodulin 2 μg, His-B23 and β-casein 1 μg. When $\alpha_2\beta_2$ and α CK2 activities were compared, the same units were used (0.01), defining 1 unit as the amount of enzyme which catalyzed the introduction of 1 nmol of phosphate into CK2-tide/min under our experimental conditions. Phosphorylation reactions were performed at 30 °C for 10 min. In the case of the peptide phosphorylation, reactions were stopped by sample absorption on phospho-cellulose P81 paper. Papers were washed three times with 75 mM phosphoric acid and counted in a scintillation counter (Perkin Elmer). In the case of protein substrates or CK2 autophosphorylation assays, phospho-reactions were stopped adding Laemmli buffer and proteins were resolved onto SDS-PAGE, stained with Coomassie blue and analyzed by digital autoradiography (CyclonePlus Storage Phosphor System, PerkinElmer).

CK2 activity in total cell lysates was assayed by incubating 0.5–2 μg of lysate proteins in the same phosphorylation buffer described above in the presence of 0.1 mM CK2-tide peptide. Control samples were performed in the absence of CK2-tide peptide.

2.4. CK2 partial proteolysis assay

In vitro proteolysis experiments were performed on recombinant tetrameric CK2 (80 ng) dissolved in 50 mM Tris–HCl, pH 8.0 employing the Glu-C protease (enzyme to substrate ratio of 1:3, by weight) at 37 °C in the presence or absence of different peptides and varying incubation time. The reactions were stopped by cooling on ice and adding Laemmli sample buffer. The proteolysis mixtures were then separated by SDS-PAGE, blotted and analyzed by western blot.

2.5. Surface plasmon resonance (SPR) experiments

For SPR analysis, a Biacore™ T100 (GE Healthcare) system was used. CK2-MCP was biotinylated at the C-terminus as described above, then diluted in running buffer consisting of 10 mM Hepes, pH 7.4, 150 mM NaCl, 0.001% (v/v) Tween-20, and immobilized on a SA sensor chip, series S, to a final density of 400 resonance units (RU), following the SA-biotin capture method of Biacore T100 control software. A flow cell with no immobilized peptide was used as control.

Binding analysis was carried out in running buffer applying a flow rate of 10 μl/min. Each sensorgram (time course of the SPR signal) was corrected for the response obtained in the control flow cell and normalized to baseline. After each injection the surface was regenerated by a 30 s injection of 1 M NaCl; this treatment restored the baseline to the initial resonance unit value. For kinetics experiments, a Biacore method program was used that included a series of three start up injections (running buffer), zero control (running buffer) and 6 different concentrations (ranging between 1 and 300 nM, two of which in double). High performance injection parameters were used; the contact time was of 150 s followed by a 150 s dissociation phase. The kinetic data were analyzed using the 2.0.3 BIA evaluation software (GE Healthcare). Curves were fitted with the classical Langmuir 1:1 model; the quality of the fits was assessed by visual inspection of the fitted data and their residual, and by chi-square values. In the case of α CK2 a two-state binding model was also applied, giving a better fitting. Two independent experiments were performed.

For the opposite experimental design (α CK2 on the chip surface and peptides injected in solution) we immobilized CK2 to a CM5 (series S) sensor chip (carboxymethylated dextran surface) by amine-coupling chemistry, to a final density of 4700 units (RU), as described elsewhere [24]. All other Biacore experimental conditions were the same described above.

2.6. CK2-MCP pull-down assay

Biotinylated CK2-MCP (25 μg in 15 μl of water) was incubated with 50 μl of streptavidine-agarose beads (Sigma-Aldrich) for 30 min at room temperature on rotation. After three washings with TBS, beads were added to total CEM cell lysate and incubated for 2 h at 4 °C on rotation. Beads were isolated by centrifugation and washed several times with 50 mM Tris–HCl, pH 7.5. The bound proteins were eluted by adding Laemmli sample buffer, boiled for 10 min, subjected to SDS-PAGE and analyzed by western blot.

2.7. Cell culture and treatment

Human cell lines were maintained in a 5% CO_2 atmosphere at 37 °C. The following lines were maintained in RPMI 1640 medium (Sigma): T lymphoblastoid CEM cells (normally sensitive, S-CEM, and their multidrug-resistant variant, R-CEM, selected with 0.1 μg/ml vinblastine [25]), acute promyelocytic leukemia HL60 cells, acute T lymphoblastic Jurkat cells and chronic myeloid leukemia (CML) LAMA84 [26]. Osteosarcoma U2OS cells [27], liver carcinoma HepG2 cells, cervix adenocarcinoma HeLa cells, embryonic kidney HEK-239T cells and lung CCD34Lu cells were grown in DMEM medium (Sigma). Both media were supplemented with 10% (v/v) fetal bovine serum (FBS), 2 mM L-glutamine, 100 U/ml penicillin, and 100 μg/ml streptomycin.

For treatments, cells growing in suspension were seeded at 3×10^6 cells/ml, while adherent cells at about 70% of confluence; during the treatments FBS was at 1% (v/v). Controls were treated with equal amounts of distilled sterile H_2O.

2.8. Cell lysis and western blot analysis

Cells were lysed with an ice-cold buffer containing 20 mM Tris–HCl, pH 7.5, 150 mM NaCl, 2 mM EDTA, 2 mM EGTA, 0.5% (v/v) Triton X-100,

2 mM dithiothreitol (DTT), protease inhibitor cocktail complete (Roche), 10 mM NaF, 1 μM okadaic acid, and 1 mM Na vanadate. After 30 min incubation on ice, the lysates were centrifuged at 13,200 rpm for 10 min, at 4 °C. Equal amount of proteins (10–20 μg) were resolved onto 11% SDS-PAGE and blotted on PVDF membranes (Immobilon-P Millipore) using a buffer containing 10 mM CAPS-NaOH (3-(Cyclohexylamino)-1-propanesulfonic acid) pH 10, DTT 3 mM and 1% (v/v) methanol. Dried membranes were then washed with TBS buffer (Tris–HCl 50 mM pH 7.5, NaCl 50 mM) with 1% (w/v) bovine serum albumin (BSA, Sigma) and incubated with the indicated antibodies, diluted in the same buffer, for a variable time, ranging from 2 h at room temperature to 16 h at 4 °C. Then membranes were incubated with a secondary HRP-conjugated antibody solution for 30 min in the same buffer. Protein bands were detected with a chemiluminescence reaction solution composed of 2.25 ml H_2O, 250 μl 1 M Tris, pH 9.35, 1 μl H_2O_2 and 2.5 ml of a luminol solution (prepared with luminol 78 mg and p-iodophenol 95 mg dissolved in 100 ml 0.1 M Tris pH 9.35) plus 30% (w/v) BSA, and visualized with Kodak Image Station 4400MM PRO; quantification of bands were performed with the Kodak 1D Image software.

2.9. Cell viability and apoptosis assays

Cell viability was assessed by means of MTT assay, as described in [28]. Plates were read at 590 nm in a Titertek Multiskan Plus plate reader (Flow Laboratories) and DC_{50} (concentrations inducing 50% of cell death) values were calculated with Prism 4.0c software (GraphPad Software). Apoptosis occurrence was evaluated by western blot to detected cleavage of PARP or procaspase 3. DNA laddering analysis on agarose gel [28] or nucleosome formation detection by means of a commercial kit [25] was also performed.

2.10. Confocal microscopy immunofluorescence experiments

LAMA84 cells (about 500,000) were plated on poly-L-lysine-coated coverslips while U2OS cells (about 200,000) were seeded on glass cover-slips and allowed to adhere overnight. Cells were washed three times with warm PBS, fixed with 4% (w/v) paraformaldehyde (Sigma) for 20 min at room temperature in the dark, permeabilized with 0.1% (v/v) Triton X-100 in PBS for 10 min at 4 °C, and incubated with the primary antibody from a time variable, ranging from 2 h (anti-CK2

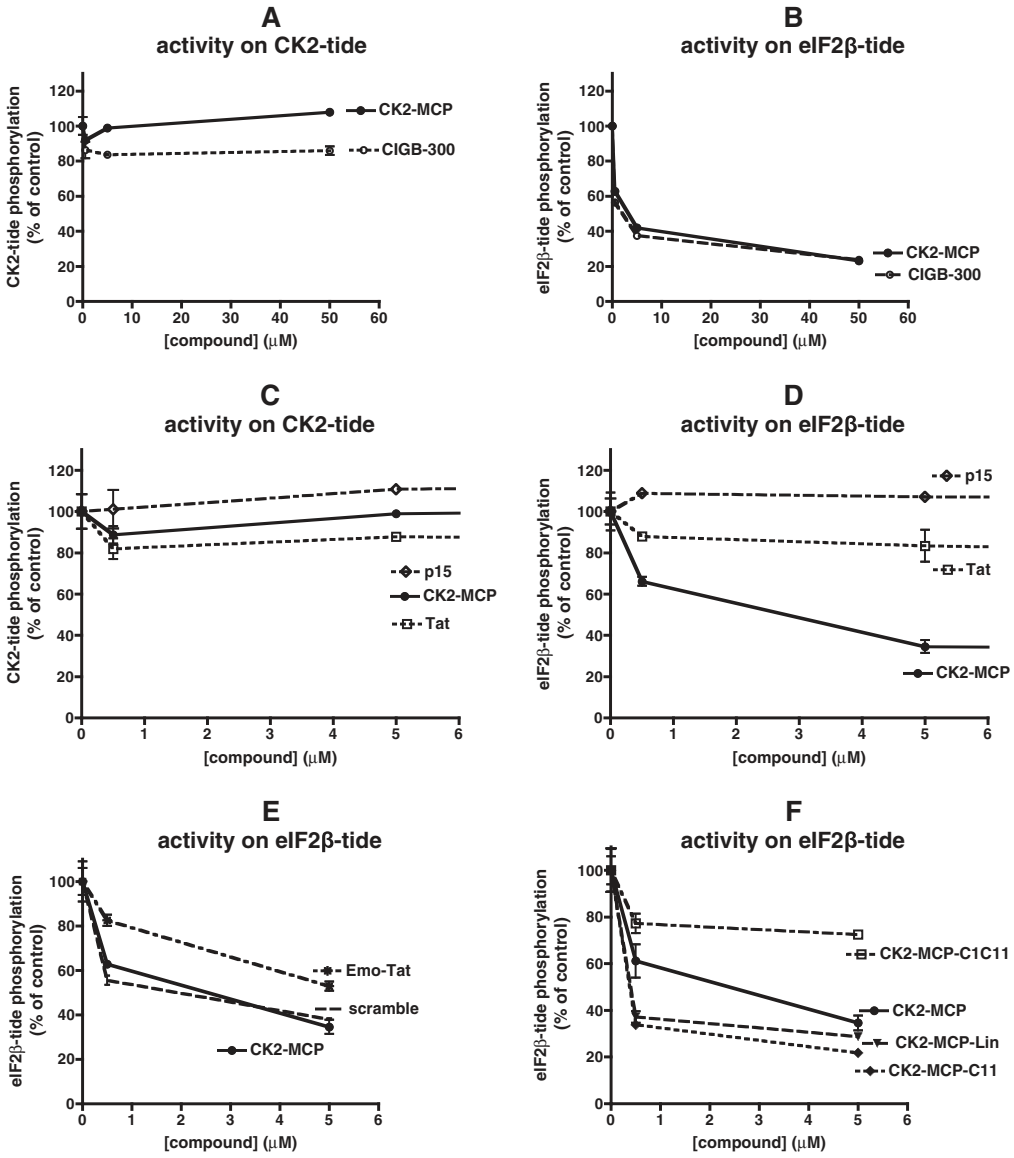

Fig. 1. Effects of chimeric peptides on CK2 activity towards peptide substrates. Holomeric CK2 was assayed on the indicated substrate peptides (CK2-tide, panels A and C; eIF2β-tide, panels B, D, E, and F) as described in Materials and methods, in the presence of increasing concentrations of the indicated different variants of chimeric peptides. In panels A and B, solid lines refer to CK2-MCP and dotted lines to CIGB-300. Activity is reported as % of controls (means ± SEM of at least two experiments in duplicate).

antiboby, 1:50) at room temperature to overnight at 4 °C (anti-LAMP1 antibody, 1:20) in PBS containing 1% BSA. After 3 washes with warm PBS, cells were incubated with the secondary antibody Alexa Fluor 633-conjugated goat anti-rabbit IgG (Life Science) (1:400) and FITC conjugated anti-mouse IgG secondary antibody (Dako) (1:50) for 1 h in PBS with 1% BSA at 37 °C in the dark. Controls were performed with the same protocols but in the absence of the primary antibody. For nuclear staining coverslips were incubated with Hoechst 33342 (1:10000; Sigma) for 10 min at room temperature in the dark. The coverslips were mounted with fluoromount solution (Sigma) and the immunofluorescence images were acquired with LEICA TCS SP5 confocal microscope equipped with HCX PL APO l blue 63x1.4 oil immersion objective. LAS IF software was used for image processing.

2.11. Proteasome activity assay

The proteasome activity in LAMA84 cell line was assessed with the Proteasome-Glo™ Chymotrypsin-Like Cell-Based Assay (Promega), based on luminescence detection. LAMA84 cells were plated in 100 μL of growing medium but with 1% (v/v) FBS, in 96-well white opaque plates optimized for luminescence detection (Perkin Elmer). Cells were treated as indicated; media-only wells were set to allow non-specific luminescence subtraction. The manufacturer's instructions were followed; the detection mixture was added to each well and incubated 10 min at room temperature to stabilize the signal. Luminescence emission was finally measured with a luminometer (Fluoroskan, Thermo Scientific Fisher).

3. Results

3.1. Effects of chimeric peptides on CK2 activity and stability in vitro

We synthetized a CIGB-300 analog, termed CK2 Modulator Chimeric Peptide (CK2-MCP) because it is composed of both an N-terminal "active" cyclic peptide (p15 in [10]) originally designed to interact with CK2 phospho-acceptor sites, and a C-terminal Tat peptide conferring cell permeability [29]. We used a Tat sequence slightly different from that present in CIGB-300 [11], and we placed it on the opposite side of the p15 peptide (C instead of N terminal) (see Table 1).

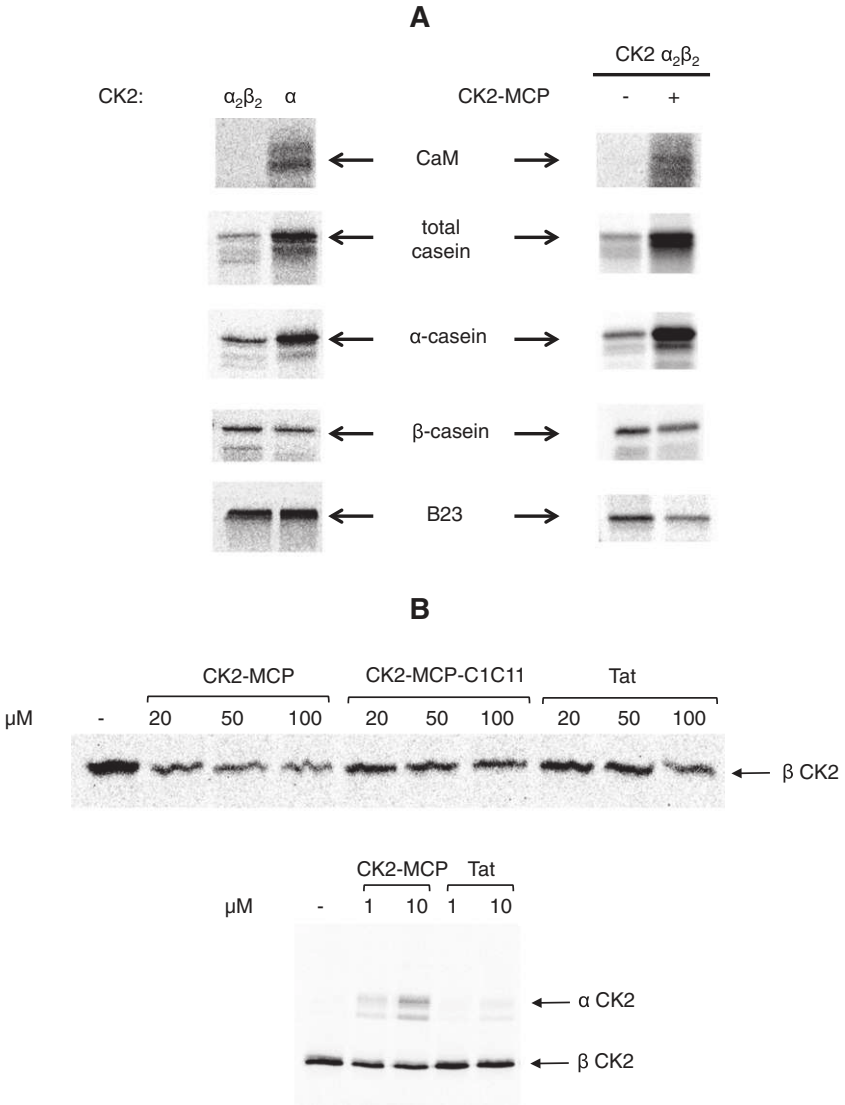

Fig. 2. Effects of chimeric peptides on CK2 activity towards protein substrates and in autophosphorylation assays. A. Left panels show a comparison between tetrameric $\alpha_2\beta_2$ and monomeric α CK2 (in both cases 0.01 U towards CK2-tide) in the phosphorylation of different proteins. In the right panels, the same proteins were phosphorylated by $\alpha_2\beta_2$ CK2, in the absence or presence of 10 μM CK2-MCP. Digital autoradiographies are shown of radioactively phosphorylated proteins separated on SDS-PAGE. B. Autophosphorylation of CK2 was performed in the presence of increasing concentration of the indicated peptides; digital autoradiographies of β (upper panel) or of both α and β (lower panel) subunits separated on SDS-PAGE are shown. See Materials and methods for more details. Images are representative of at least three independent experiments.

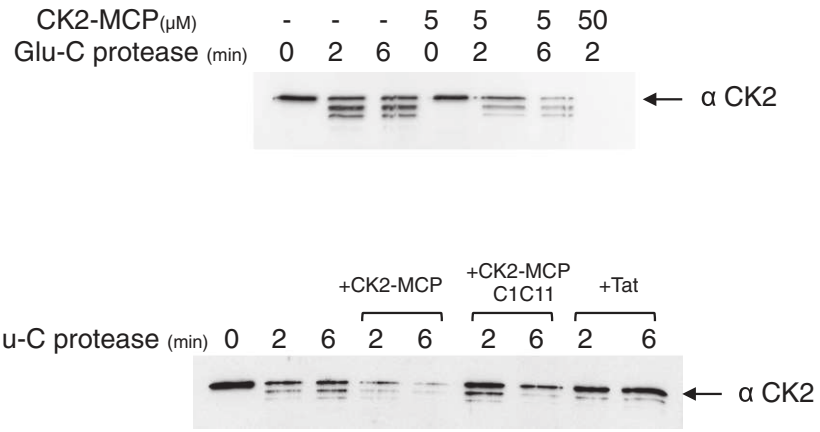

Fig. 3. Effects of chimeric peptides on α CK2 stability in limited proteolytic assays. Tetrameric CK2 was incubated with Glu-C protease as described under Materials and methods, for the indicated times and in the presence of the indicated peptides. Partial proteolysis was assessed by WB analysis with anti-α CK2 C-terminal antibody. Representative images are shown of at least three independent experiments.

We first measured the in vitro activity of recombinant CK2 towards synthetic peptides. We found that CK2-MCP, up to a 50 μM concentration, does not affect the phosphorylation of the canonical CK2 peptide substrate "CK2-tide" (Fig. 1A) and of several other CK2 peptide substrates (see Table 1 for sequences), including two different HPV-16 E7-derived peptides, a REV-derived [30] peptide and a B23-derived peptide (not shown), all of which are phosphorylated with comparable efficiency by either CK2 holoenzyme or its isolated catalytic subunit. A notable exception is provided by a peptide, denoted as "eiF2β-tide", designed for being phosphorylated by the tetrameric $\alpha_2\beta_2$ holoenzyme but not by its monomeric catalytic subunit [31]. This is the only peptide among the many tested so far whose phosphorylation, as shown in Fig. 1B, is markedly inhibited in a dose-dependent manner. Fig. 1 also shows that the parental peptide CIGB-300, synthetized for comparison, has very similar effects, as also mentioned elsewhere [32]. Intriguingly, the inhibitory effect towards eiF2β-tide requires the presence of both the p15 and the Tat portion of CK2-MCP, since the individual components are almost ineffective (Fig. 1C/D). Surprisingly, a scramble Tat-fused peptide, where the aminoacidic composition but not the sequence of the p15 moiety is conserved, has a similar inhibitory potency on eiF2β-tide phosphorylation; on the contrary, when the p15 sequence is substituted by a completely different peptide of the same length (Emo-Tat), we observed a reduced effect (Fig. 1E). We therefore decided to synthetize a number of peptides, all presenting the Tat sequence at the C-terminus, but with individual aminoacidic substitutions in the p15 sequence (see Table 1). The effects of some CK2-MCP variants on eiF2β-tide phosphorylation by CK2 are shown in Fig. 1F. It is worth to note that the cyclization of the p15 peptide, performed by the oxidation of the N- and C-terminal cysteine residues, is not required for the inhibitory effect, since the linear peptide (CK2-MCP-Lin) is even more effective. However, the substitution of the two Cys with Ala is significantly detrimental (CK2-MCP-C1C11), while the maintenance of a single Cys mutation is still compatible with a significant inhibitory efficacy (CK2-MCP-C11). To note that all these peptides, similar to the parent one (CK2-MCP), were ineffective, either using monomeric α or tetrameric $\alpha_2\beta_2$ CK2, when the phosphoacceptor substrate was the canonical "CK2-tide" whose phosphorylation is not dependent on the β subunit (not shown).

The effect of CK2-MCP on CK2 activity when full proteins are used as substrates, instead of peptides, is shown in Fig. 2. The phosphorylation of these substrates was first compared by using equivalent units of either $\alpha_2\beta_2$ or α CK2 (Fig. 2A, left panel). Under our experimental conditions, three of them (CaM, total casein and α-casein) were phosphorylated more efficiently by the monomeric form, with the limit case of CaM, whose phosphorylation is completely suppressed by the presence of β, as already known [33]. With these substrates, CK2-MCP displays a stimulatory effect on $\alpha_2\beta_2$ (Fig. 2A, right panel). On the contrary, its effect is somewhat inhibitory with those substrate whose phosphorylation is not significantly affected by the β subunit, such as β-casein and B23 protein, the major intracellular target of CIGB-300 identified so far [18] (Fig. 2A). These observations suggest that CK2-MCP acts by preventing the function of the β subunit. Accordingly, the effect of CK2-MCP was invariably negligible whenever α instead of $\alpha_2\beta_2$ CK2 was used as a catalyst (not shown). A further clue that CK2-MCP may disrupt the oligomeric structure of CK2 comes from the analysis of CK2 autophosphorylation (Fig. 2B): in the presence of the chimeric peptide, the regular autophosphorylation of the β subunit decreases, with a concomitant induction of autophosphorylation of the α subunit. This effect resembles that produced on CK2 autophosphorylation by polybasic compounds [33], which are also able to promote the phosphorylation of calmodulin by $\alpha_2\beta_2$ CK2, similarly to CK2-MCP (Fig. 2A). A priori, it was reasonable to suspect that the basic sequence of Tat could be responsible for these effects of CK2-MCP; however, Tat sequence alone has an only marginal effect (Fig. 2B), and was also ineffective on all the protein phosphorylation assays described above (not shown). Fig. 2B also shows that a CK2-MCP derivative (CK2-MCP-C1C11), poorly effective on CK2 activity towards peptide substrates (Fig. 1F), is also unable to affect CK2 autophosphorylation.

Since the β subunit of CK2 protects α from partial proteolysis [34], we performed in vitro proteolysis assays to check whether CK2-MCP has an effect on the rate of α proteolysis, as expectable if it is able to loosen the holoenzyme structure. As shown in Fig. 3, the limited proteolysis of α subunit is in fact fastened by the addition of CK2-MCP (5–50 μM). Again, this effect is not promoted by the Tat sequence alone, nor by CK2-MCP derivatives which are much less effective on CK2 activity, such as CK2-MCP-C1C11 (Fig. 3, lower panel).

3.2. Physical interaction between CK2 and CK2-MCP

The results presented so far prove that the chimeric peptides, initially developed as compounds able to interact with CK2 substrates, are also able to directly affect CK2. To confirm the direct interaction between CK2-MCP and CK2, we performed SPR (surface plasmon resonance) experiments exploiting Biacore technology. We found that CK2-MCP is able to bind to CK2 holoenzyme and to its α and β isolated subunits (Fig. 4A). Moreover, since this approach is also suitable to determine the kinetic constants, we compared the affinity of these associations to that of B23, the known cellular target of CIGB-300: they are reported in Fig. 4, and indicate that CK2-MCP has similar affinity for α, β or $\alpha_2\beta_2$ CK2, which is only slightly lower than that calculated for B23. Other proteins tested, such as Akt,

A

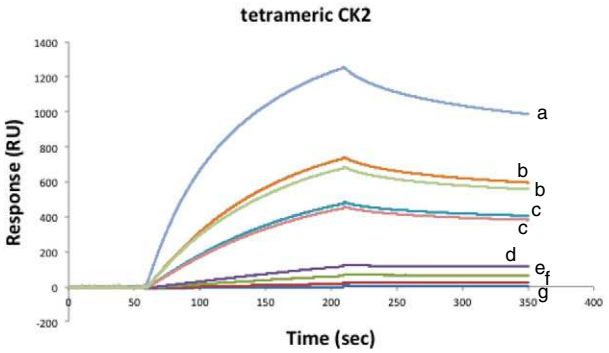

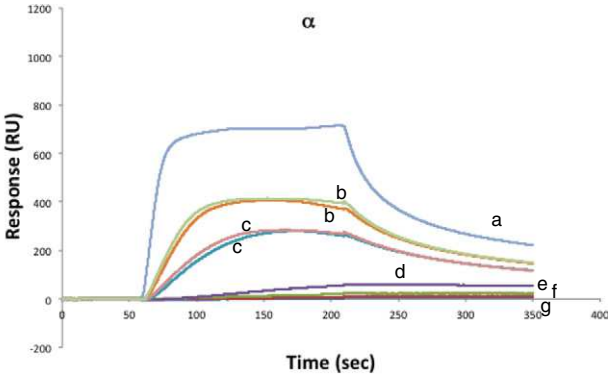

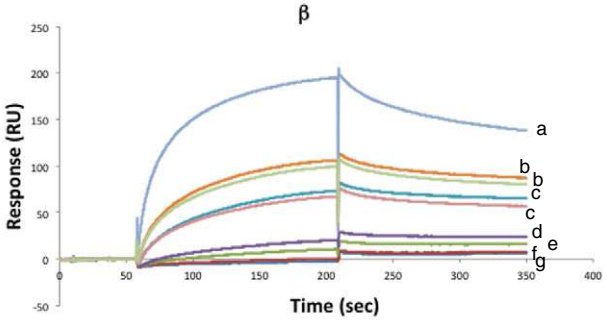

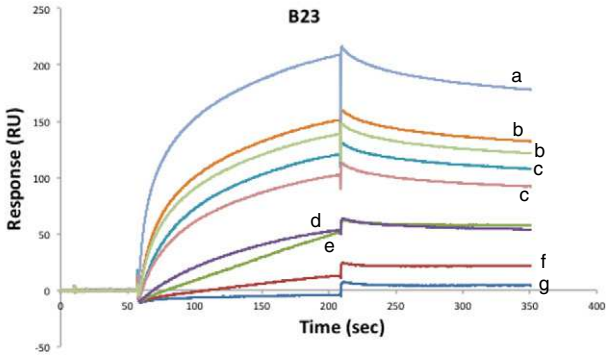

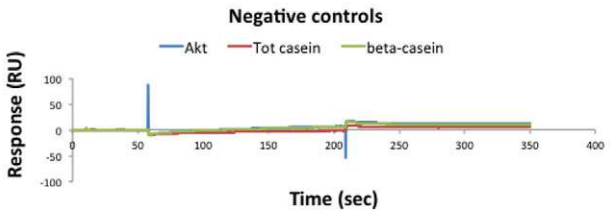

	K_D (M)	SE
Tetrameric CK2	2.7×10^{-8}	1.6×10^{-10}
α CK2	5.3×10^{-8}	7.8×10^{-10}
β CK2	2.6×10^{-8}	3.4×10^{-10}
B23	7.1×10^{-9}	2.2×10^{-10}
α CK2*	1.8×10^{-8}	6.3×10^{-9}

*two-state reaction analysis

B

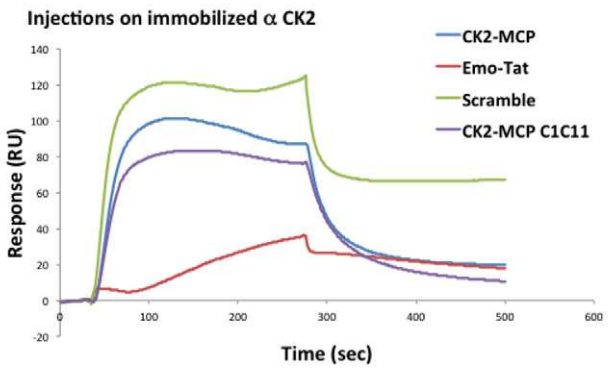

C

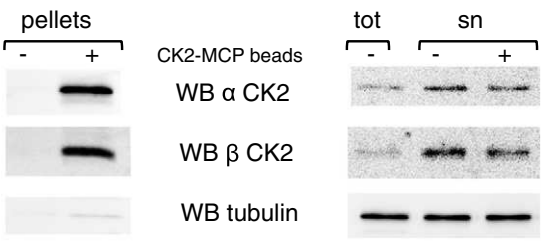

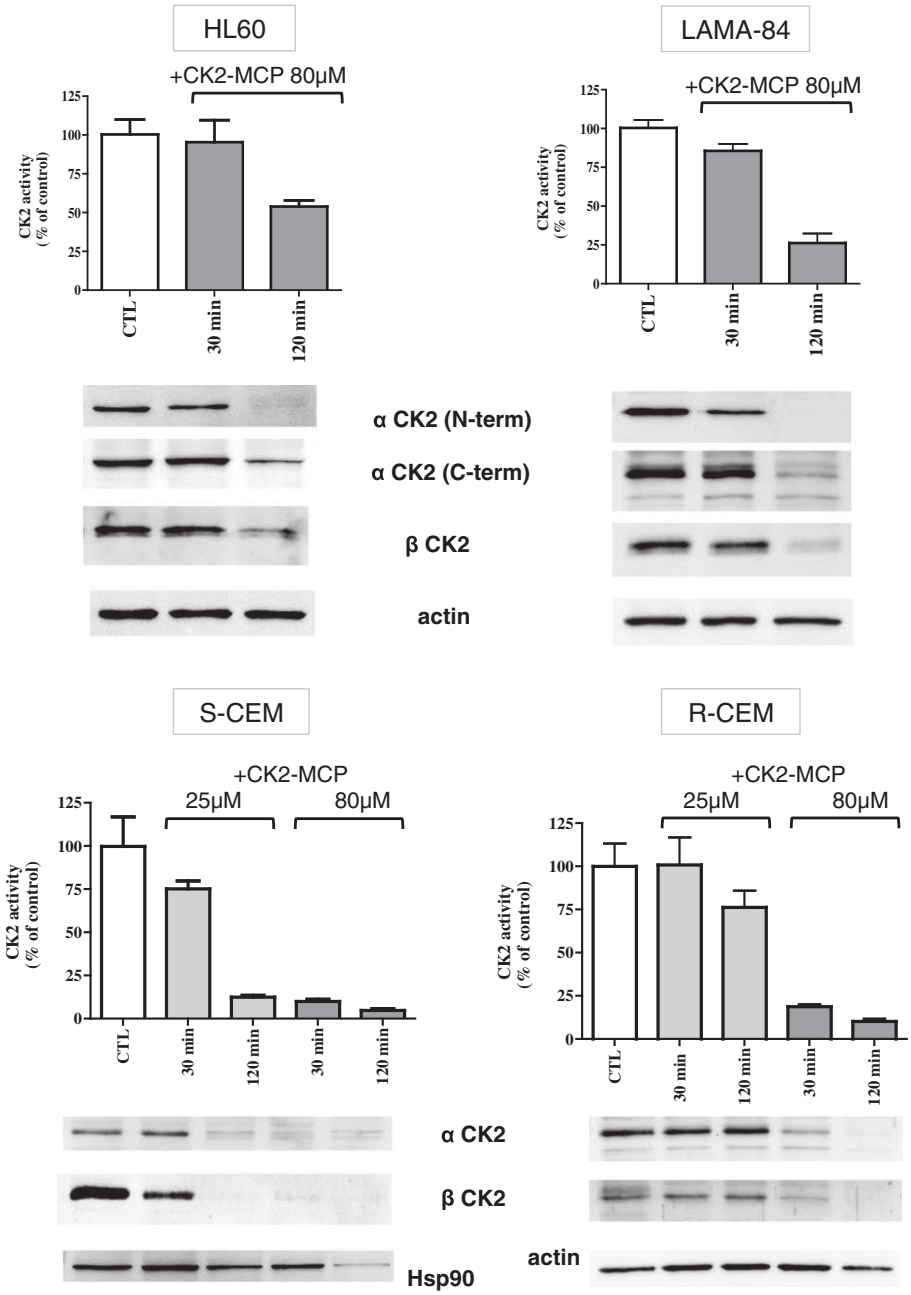

Fig. 5. Effects of CK2-MCP on cellular CK2. Cells were incubated with 25 or 80 μM CK2-MCP for 30 or 120 min, as indicated. Then cells were lysed and 1–2 μg of lysate protein used for measuring CK2 activity towards CK2-tide, while 10 μg loaded on SDS-PAGE and blotted for WB analysis. For each cell type, the upper graph shows CK2 activity under the different conditions, while the corresponding WB for α or β CK2 are reported below the graph. In the case of HL60 and LAMA84 cells, two different anti-α CK2 antibodies were tested, with similar results. Images are representative of at least three independent experiments. Actin or Hsp90 were analyzed as loading control.

total casein or β-casein, are not able to interact with CK2-MCP as judged from our Biacore experiments (Fig. 4A), despite the fact that they are CK2 substrates.

We also applied the opposite experimental design on the Biacore system, thus immobilizing α CK2 and injecting peptides in solution (Fig. 4B): this approach confirmed the association of CK2-MCP, and

Fig. 4. Interaction between CK2-MCP and CK2 or B23. A. The panels show the sensorgrams obtained with Biacore T100 instrument. CK2-MCP was immobilized on the chip surface while tetrameric CK2, α CK2, β CK2 or B23 (and Akt, β-casein or total casein as negative controls) were injected in solution and flowed over the surface. In each panel, the concentrations of the injected protein solutions are indicated by letters, as follows: a, 500 nM; b, 100 nM; c, 50 nM; d, 10 nM; e, 5 nM; f, 1 nM; g, 0 nM (some concentrations were in duplicate); and the negative controls Akt2, β casein and total casein were injected at a 100 nM concentration. In the box, the K_D values for each interaction are reported, calculated by means of Biacore Evaluation software, adopting a 1:1 Langmuir interaction model, except for α CK2, where the two-state reaction model fitted better and whose results are also reported (*); SE, standard error. B. Sensorgrams obtained with Biacore T100, by injecting 500 nM solutions of the indicated peptides over a chip surface where α CK2 was covalently immobilized. All Biacore experiments were performed at least twice. C. 175 μg proteins from CEM cell lysate were incubated with biotinylated CK2-MCP conjugated to streptavidine-agarose beads; control was performed with the unconjugated streptavidine-agarose beads. After beads pull-down, the presence of CK2 subunits in the pellets was assessed by WB (left panels); 2 μg proteins from total lysate (tot) or from supernatants (sn) were also loaded as controls (right panels). Anti-tubulin was used as loading control.

showed that the scramble peptide acts similarly to the parental one, while the Emo-Tat peptide, much less effective on CK2 activity, gives only a negligible binding. Interestingly, the CK2-MCP-C1C11, which has poor effects on CK2 activity and stability (see Figs. 1, 2 and 3), gave instead a positive signal in this kind of experiment. However, our Biacore experimental design only allows analyzing the association between the peptides and α CK2, while important differences between peptides are possibly due to their interaction with the CK2 holoenzyme.

The interaction between CK2-MCP and CK2 was also confirmed by pull-down experiments, showing that the chimeric peptide is able to bind CK2 subunits in a cell lysate environment (Fig. 4C).

3.3. Effects of chimeric peptides on CK2 activity and stability in cells

Next we analyzed the effects of CK2-MCP in cells. We found that the endocellular activity of CK2 measured in cell lysates towards CK2-tide (Fig. 5, bar graphs) or different substrates (not shown) very rapidly decreased upon cell treatment with CK2-MCP. However, a parallel disappearance of the CK2 protein (both α and β subunits) was also observed (Fig. 5, western blots). Very similar results were obtained with different cell lines; Fig. 5 shows the results obtained with HL60, LAMA84 and CEM cells, this latter tested in both their apoptosis sensitive (S) or resistant (R) variants. These observations allow concluding

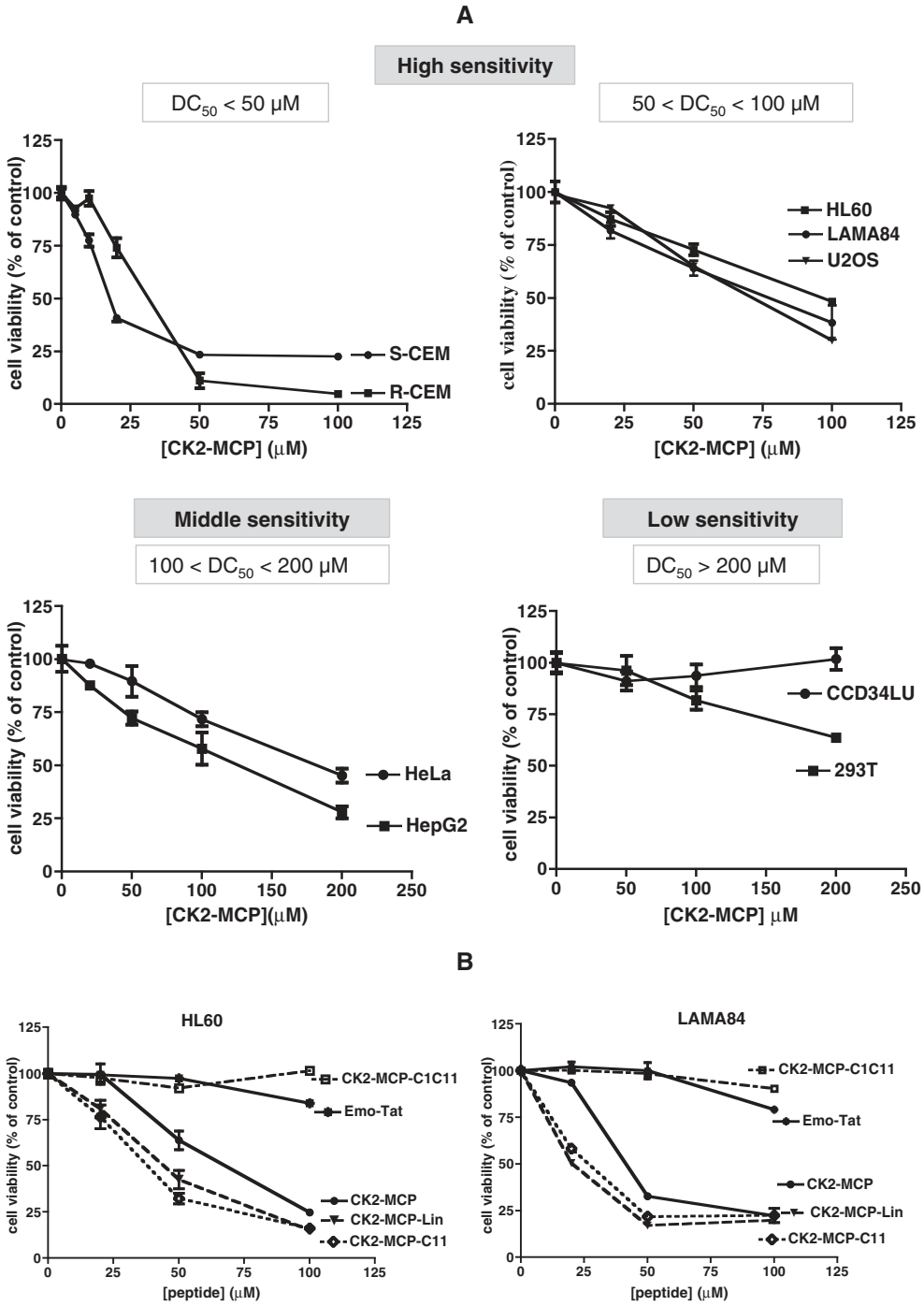

Fig. 6. Effects of chimeric peptides on cell viability. Cells were treated for 24 h with increasing concentration of chimeric peptides, then cell viability was assessed by the MTT method. A. The effect of CK2-MCP is shown on different cell lines that are grouped in different graphs according to their sensitivity. B. Graphs show a comparison of the effects of different chimeric peptide variants on HL60 and LAMA84 viability. Cell viability is reported as % of controls (means + SEM of at least two experiments in duplicate).

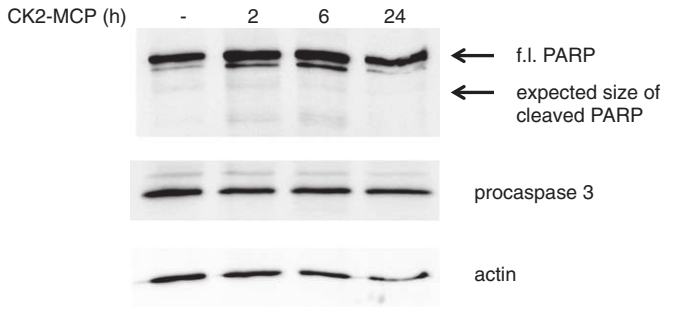

Fig. 7. Absence of caspase activation in cells treated with CK2-MCP. LAMA84 cells were treated with 80 μM CK2-MCP for the indicated times, then cells were lysed and 10 μg of lysate proteins loaded on SDS-PAGE and blotted for evaluation of PARP and procaspase 3 cleavage by WB analysis. WB for actin was used as loading control. Images are representative of five independent experiments.

that the apparent inhibition of cellular CK2 by CK2-MCP is instead due to the reduced amount of the enzyme available.

3.4. Effects of chimeric peptides on cell viability

As expected in response to a drop in CK2 activity/amount, cell viability is rapidly and heavily affected by CK2-MCP (Fig. 6A). However, as already reported for CIGB-300 [20], the sensitivity to CK2-MCP treatment significantly differs depending on the cell type, blood tumor and U2OS cell lines being the most responsive (DC_{50} < 100 μM), with other solid tumor cells having an intermediate sensitivity (100 μM < DC_{50} < 200 μM), and the two non-tumor cell lines being almost insensitive. This parallels the effect observed on the decrease of CK2 levels, which is negligible in not tumor cells (not shown). In all cases, Tat alone or p15 alone have no cytotoxic effect (not shown). On HL60 and LAMA84 cells, we performed a comparison of different CK2-MCP derivatives for their effects on cell viability, finding a correlation between their effects on CK2 in vitro and their ability to induce cell death (Fig. 6B). In particular, it can be noticed that CK2-MCP-C1C11, significantly less effective than CK2-MCP as in vitro inhibitor (Fig. 1F) and proteolysis inducer (Fig. 3), is also less effective in the cell viability assay; on the contrary, CK2-MCP-C11 and CK2-MCP-Lin are even more effective, both in vitro and in cells. Emo-Tat, a peptide with the same Tat component but the complete substitution of the p15 sequence, is almost ineffective also in the cell viability assays (Fig. 6B).

We then analyzed whether CK2-MCP induces cell death by apoptosis, as usually happens in response to CK2 down-regulation. Surprisingly we were unable to detect any signal of apoptosis in cell treated with CK2-MCP. Fig. 7 shows that no signal of PARP or pro-caspase 3 cleavage was found in LAMA84 cells treated with 80 μM CK2-MCP (which in these cells induces more than 50% cell death in 24 h, see Fig. 6A). Similar results were observed in all cell lines tested (not shown). Other methods for apoptosis evaluation, such as DNA laddering analysis on agarose gel, or nucleosome formation detection by means of commercial kits, also failed to reveal apoptosis induction by CK2-MCP (not shown).

3.5. Effects of chimeric peptides on CK2 subcellular localization

Given the unanticipated findings of CK2 amount reduction and cell death not due to apoptosis, and in order to better understand the

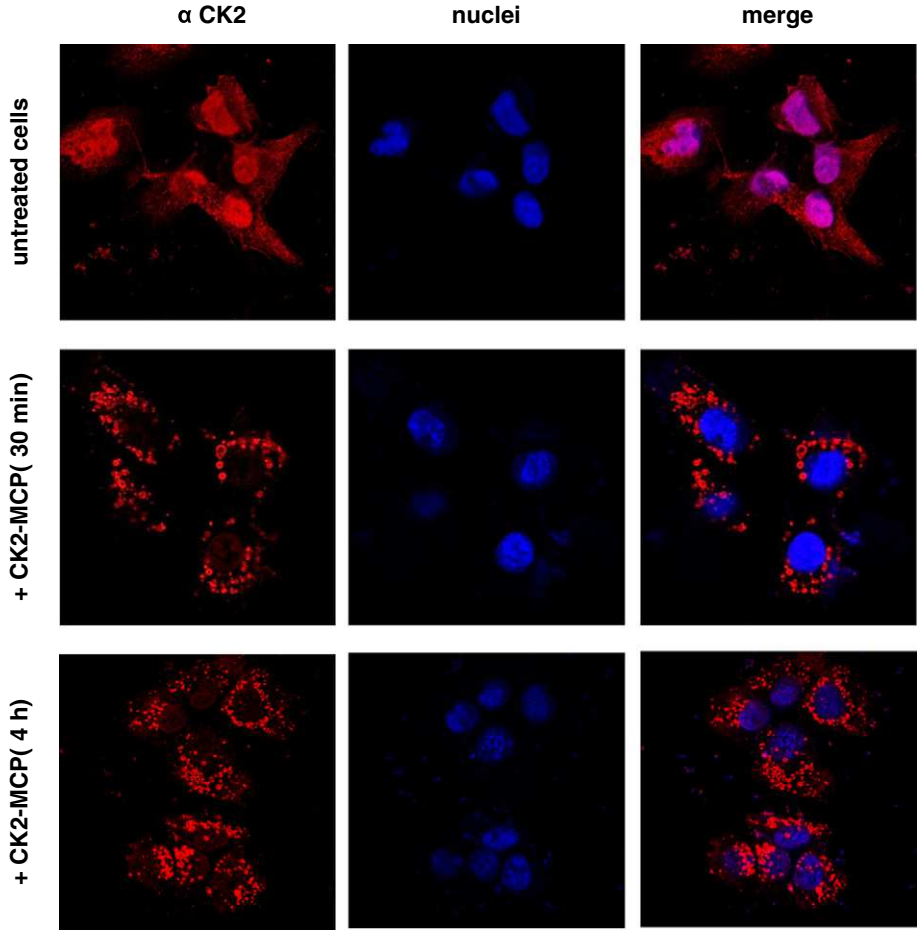

Fig. 8. Effects of CK2-MCP on cellular CK2 localization. U2OS cells were treated with 80 μM CK2-MCP for the indicated times, then stained with anti-α CK2 and secondary antibody conjugated to Alexa 633 (red), while nuclei were stained with Hoechst 33342 (blue). Fluorescence images were captured with confocal microscopy; merge images are also shown. The secondary antibody alone gave negligible signal (not shown). Images are representative of six independent experiments.

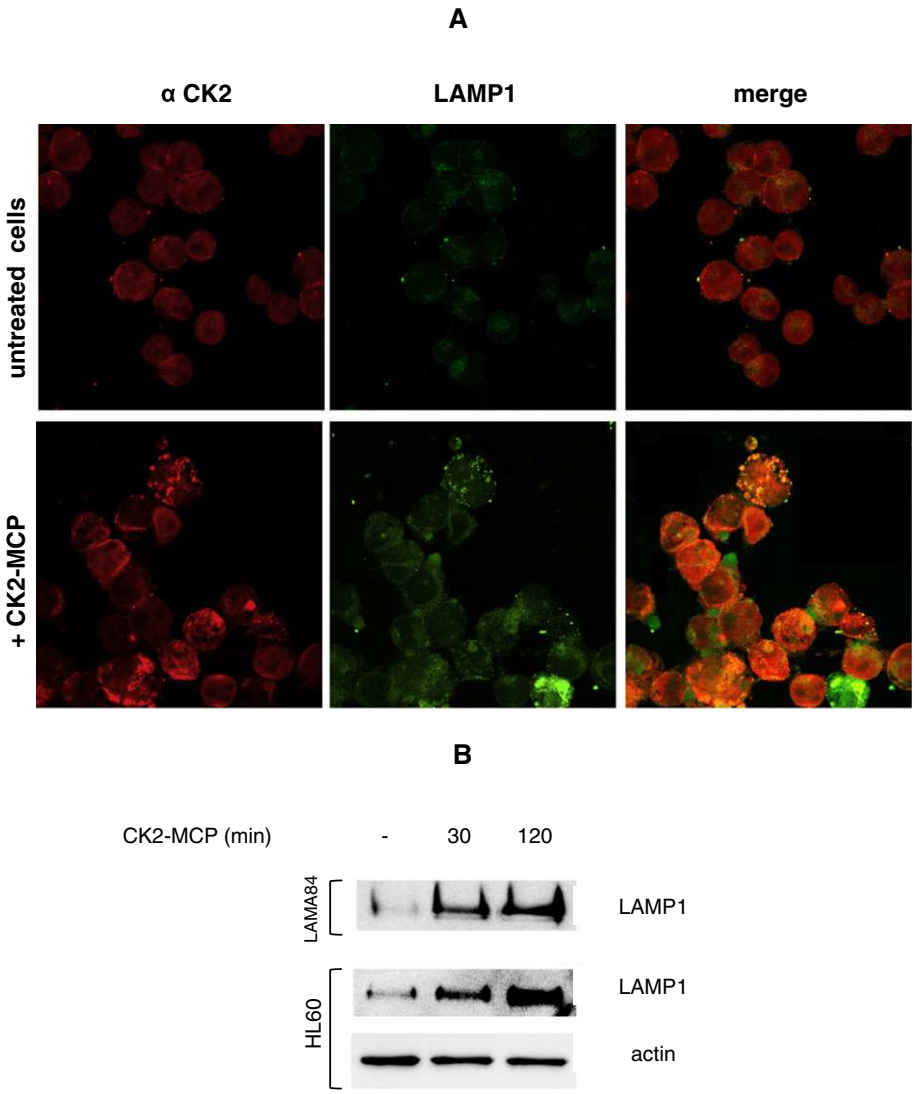

Fig. 9. Effects of CK2-MCP on lysosomes. A. LAMA84 cells were treated for 30 min with 80 μM CK2-MCP, then stained with anti-α CK2 plus anti-rabbit IgG secondary antibody conjugated to Alexa 633 (red) and anti-LAMP1 plus anti-mouse IgG secondary antibody conjugated to FITC (green). Fluorescence images were captured with confocal microscopy; merge images are also shown. The secondary antibodies alone gave negligible signal (not shown). Images are representative of three independent experiments. B. HL60 or LAMA84 cells were treated with 80 μM CK2-MCP for 30 or 120 min, then lysed. 20 μg of lysate proteins were loaded on SDS-PAGE and blotted for LAMP1 WB. Actin was used as loading control.

cellular events occurring in response to CK2-MCP, we performed confocal microscopy immunofluorescence experiments, initially focusing on CK2. The study was performed in S-CEM, R-CEM, LAMA84 and U2OS cells. We found that CK2, mainly present in the cytosol and the nucleus of control cells, moves out of the nucleus very rapidly in response to CK2-MCP, and localizes in punctate structures. Fig. 8 shows images obtained with U2OS cells, but similar results, albeit in some cases less evident, were also observed in S-CEM, R-CEM (not shown), and LAMA84 cells (see Fig. 9A). By contrast, the punctate pattern of CK2 immunostaining was not induced by cell treatment with Emo-Tat or other ineffective Tat-containing peptides (not shown).

3.6. Effects of chimeric peptides on cellular proteolytic systems

Since the punctate structures where CK2 localizes (Fig. 8) were reminiscent of lysosomes, we performed immunofluorescence experiments for the lysosome marker LAMP1 protein, finding that indeed CK2 and LAMP1 co-localize in response to CK2-MCP (Fig. 9A). In addition, these experiments revealed a marked increase of LAMP1 signal in treated cells, that was also confirmed by WB analysis (Fig. 9B), suggestive of an up-regulated activity of lysosomal proteases in CK2-MCP-treated cells. [35]. Consistently, the amount of other proteins, besides CK2, was reduced in cells treated with CK2-MCP (Fig. 10). These proteins include B23 and rpS6, that have been described as direct targets of CIGB-300 [17,18], but also other signaling proteins, such as Cdc37 and Akt. Interestingly, those CK2-MCP variants with reduced efficacy on CK2 activity and on cell viability (such as emo-Tat or CK2-MCP-C1C11), as well as non-chimeric Tat peptide, were ineffective also on the decrease of protein amounts (not shown).

As a major mechanism of protein degradation, cells exploit the ubiquitin-proteasome system; therefore we wanted to assess whether, besides the lysosome pathway, also the proteasome function is affected by cell treatment with CK2-MCP. For this purpose, since a crucial step in the proteasome-mediated degradation is the poly-ubiquitination, we performed WB experiments to detect the poly-ubiquitinated proteins present in lysates from control or treated cells. Fig. 11A shows that their amount is greatly increased after 12 h of cell treatment with CK2-MCP, while the poly-ubiquitin signal goes down with longer treatment times. This is consistent with a blockage of the proteasome function producing an accumulation of unprocessed poly-ubiquitinated proteins, which are possibly then cleared by the activated lysosomal system [36,37]. In fact, the proteasome activity is greatly reduced by CK2-

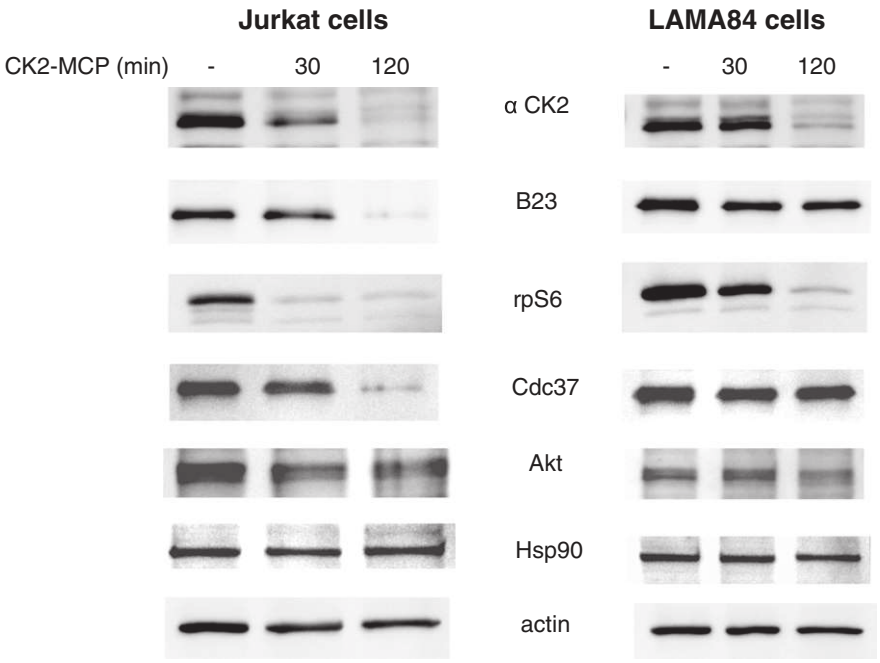

Fig. 10. Analysis of different signaling proteins in cells treated with CK2-MCP. Jurkat or LAMA84 cells were treated with 80 μM CK2-MCP for 30 or 120 min, as indicated, then cells were lysed and 10 μg of lysate proteins loaded on SDS-PAGE and blotted for WB analysis with the indicated antibodies. Images are representative of at least four independent experiments.

MCP, in a dose- and time-dependent manner, and similarly to what observed in the presence of the well-known proteasome inhibitor MG132 (Fig. 11B); again, also in this context, CK2-MCP-C1C11 or non-chimeric Tat peptide were ineffective. To note that the proteasome blockage and the lysosomal protease activation are events compatible with the induction of the autophagic pathway, a possibility also supported by a reduced amount of p62 (Fig. 11C), a protein whose amount is generally considered to inversely correlate with autophagic activity [37].

4. Discussion

In this paper we analyze the complicated mechanism of action of chimeric peptides that were originally designed to prevent the phosphorylation of specific CK2 substrates [10]. They were expected to bind to the phospho-acceptor site on the protein targets, and not to the kinase itself. However, as partially anticipated by others for the prototype of these compounds, CIGB-300 [32], our chimeric peptide, CK2-MCP, is also able to directly bind to CK2 (Fig. 4) and to inhibit its activity in vitro (Figs. 1 and 2), provided that the phosphorylatable target belongs to the class III of CK2 substrates [5], whose phosphorylation relies on the β subunit. On the contrary, CK2-MCP exerts a positive effect in the case of class II CK2 substrates, whose phosphorylation is inhibited by β, such as calmodulin [33], and is flatly ineffective with class I substrates, whose phosphorylation is poorly influenced by β. CK2 autophosphorylation at its β subunit, which is symptomatic of supramolecular organization, is reduced by our chimeric peptide, while that of the α subunit is increased (Fig. 2B). Surprisingly, the p15 portion of the chimeric peptide, which was expected to be its active moiety (the Tat portion being present only to ensure cell permeability), is instead almost ineffective on CK2 activity in vitro, and the same applies to the Tat sequence alone. This could simply indicate that a certain size is necessary for the peptide to be effective; indeed, a scramble peptide, composed of Tat fused to a peptide with the same composition of p15 but different sequence, is as good as CK2-MCP in producing its effects on CK2. However, other peptides with the same number of residues but different composition cannot effectively replace p15 (e.g. the Emo-Tat chimeric peptide and the substituted CK2-MCP-C1C11 peptide, Figs. 1, 2, and 3). What we can safely conclude is that the exact p15 sequence and its cyclization are not essential, but that the abrogation of both Cys residues at the p15 termini is completely detrimental. The requirement of Tat can be explained assuming that its basic sequence mediates the association of CK2-MCP to the acidic stretch of the β subunit that is crucial for its interaction with the α subunit [38]. This hypothesis is consistent with the observation that CK2-MCP is inhibitory only with class III CK2 substrates [5], requiring β for their phosphorylation, with special reference to the eIF2β peptide whose high affinity binding to the active site of the catalytic subunit of CK2 holoenzyme has been shown to exceptionally rely also on the N-terminal segment of the β-subunit. Indeed, from the Biacore experiments (Fig. 4) we have to assume that α CK2, β CK2 and the tetrameric enzyme all interact with CK2-MCP; we do not know the exact mechanism of the interaction, and further studies will be necessary to investigate whether the two individual moieties of CK2-MCP, p15 and Tat, interact with different CK2 subunits. For the time being, we can only conclude that the chimeric peptide seems to antagonize the functions of β in the holoenzyme. This hypothesis is also supported by the observation that it induces a faster in vitro proteolysis of α CK2 (Fig. 3), apparently preventing the well-known protective function of the β subunit [34]. Also in cells CK2-MCP promotes a rapid and substantial reduction of CK2 amount (Fig. 5). However, in the case of cells, the degradation of CK2 can be also related to other effects of CK2-MCP, bearing in mind that this chimeric peptide alters CK2 localization (Fig. 8), and induces the activation of the lysosome functions (Fig. 9). In our analysis, we found that several other signaling proteins are also rapidly degraded in response to cell treatment with CK2-MCP (Fig. 10), and this could be associated to an increased lysosome activity. Significantly, however, when we compared different sequence variants of CK2-MCP, we observed that those forms less effective on CK2 activity and stability in vitro were also less effective on cell viability (compare for example Fig. 1E/F and Fig. 6B). This parallelism suggests that CK2 is one of the major direct targets of CK2-MCP. Interestingly, the chimeric peptide CIGB-300 developed by Perea and co-workers, in our hands produced effects very similar to CK2-MCP both in vitro (Fig. 1) and in cells (not shown), indicating that the properties of CK2-MCP are not critically dependent on its differences in Tat sequence and position as compared to CIGB-300.

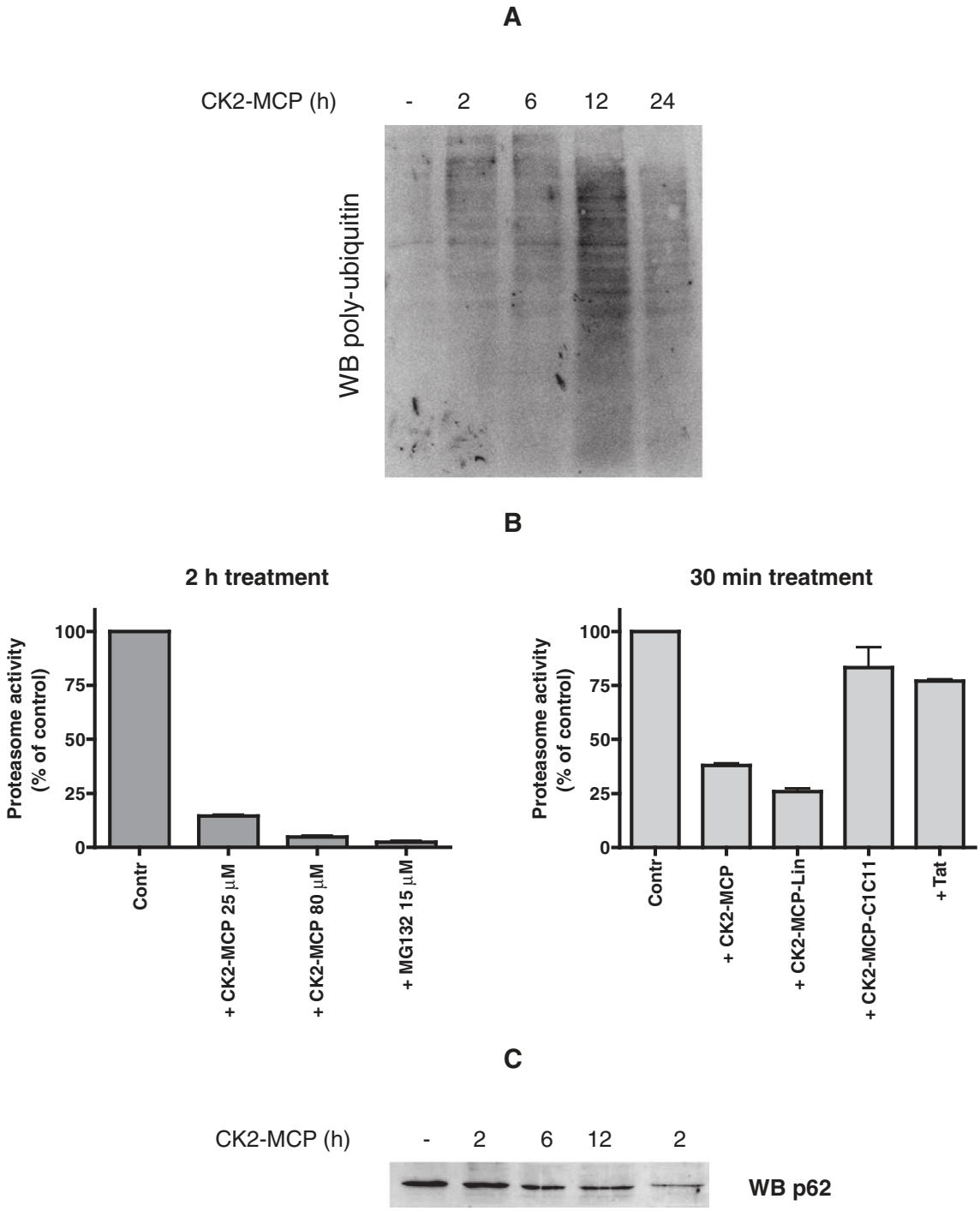

Fig. 11. Effects of CK2-MCP on proteasome activity. A. LAMA84 cells were treated for increasing times with 80 μM CK2-MCP, then 20 μg of lysate proteins were loaded on SDS-PAGE, blotted and analyzed for the accumulation of poly-ubiquitinated proteins by WB. Images are representative of at least four independent experiments. B. LAMA84 cells were treated with CK2-MCP for 2 h (left) or 30 min (right), then the activity of the proteasome system was evaluated by means of a commercial kit. The effect of CK2-MCP is compared to that of the proteasome inhibitor MG132 (left panel), or to different peptide variants, all used at 80 μM (right panel). Proteasome activity is reported as % of that measured in untreated cells (means ± SEM of two independent experiments). C. The reduced proteasome activity was correlated to the activation of the autophagic pathway by checking the p62 cleavage: LAMA84 cells were treated with 80 μM CK2-MCP for increasing times and 20 μg of lysate proteins were used for WB analysis with anti-p62 (representative image of three experiments).

Despite the conclusion that CK2 is a CK2-MCP target also in cells, it is unlikely that all the dramatic cellular perturbations induced by this chimeric peptide can be mediated by CK2. For example, in the case of proteasome inhibition (Fig. 11) a direct effect of CK2-MCP would be expectable. This in turn could cause major consequences, among them the upregulation of lysosomal and autophagic pathways, in a compensatory manner, as frequently occurs (for reviews see [36,39]), and could explain why the cytotoxic effect of CK2-MCP is devoid of any symptom of apoptosis occurrence (Fig. 7 and not shown).

In conclusion, here we show that cell treatment with this class of chimeric peptides generates an intricate network of events which suggests reconsidering their simple and inappropriate definition as CK2 inhibitors, and, at the same time, warns that caution should be applied when their clinical usage is planned. Nevertheless, the circumstance

that non-tumor cells seem to be much less sensitive to the treatment (Fig. 6 and [40]), encourages to take advantage of this alternative approach to develop new therapeutic strategies, even though some molecular aspects of their modus operandi are still enigmatic.

5. Conclusions

Altogether, our results demonstrate that the dramatic cellular alterations promoted by the chimeric peptides described here and by CIGB-300 described in [10] are mediated by both a direct effect on CK2 and the perturbation of several signaling pathways, ultimately triggering the lysosomal autophagic machinery and driving tumor cells to death.

Transparency Document

The Transparency document associated with this article can be found, in the version.

Acknowledgments

We thank Stefania Sarno and Andrea Venerando (Padova) for providing recombinant CK2, and the Peptide Facility at CRIBI (Padova) for the support in synthesizing peptides. This work was supported by grants from the AIRC (Italian Association for Cancer Research), Project IG14180.

References

[1] J.H. Trembley, G. Wang, G. Unger, J. Slaton, K. Ahmed, Protein kinase CK2 in health and disease: CK2: a key player in cancer biology, Cell. Mol. Life Sci. 66 (2009) 1858–1867.
[2] J.S. Duncan, D.W. Litchfield, Too much of a good thing: the role of protein kinase CK2 in tumorigenesis and prospects for therapeutic inhibition of CK2, Biochim. Biophys. Acta 1784 (2008) 33–47.
[3] M. Ruzzene, L.A. Pinna, Addiction to protein kinase CK2: a common denominator of diverse cancer cells? Biochim. Biophys. Acta 1804 (2010) 499–504.
[4] F. Meggio, L.A. Pinna, One-thousand-and-one substrates of protein kinase CK2? FASEB J. 17 (2003) 349–368.
[5] L.A. Pinna, Protein kinase CK2: a challenge to canons, J. Cell Sci. 115 (2002) 3873–3878.
[6] K.A. Ahmad, G. Wang, G. Unger, J. Slaton, K. Ahmed, Protein kinase CK2—a key suppressor of apoptosis, Adv. Enzym. Regul. 48 (2008) 179–187.
[7] N.A. St-Denis, D.W. Litchfield, Protein kinase CK2 in health and disease: from birth to death: the role of protein kinase CK2 in the regulation of cell proliferation and survival, Cell. Mol. Life Sci. 66 (2009) 1817–1829.
[8] A. Venerando, M. Ruzzene, L.A. Pinna, Casein kinase: the triple meaning of a misnomer, Biochem. J. 460 (2014) 141–156.
[9] A. Siddiqui-Jain, D. Drygin, N. Streiner, P. Chua, F. Pierre, S.E. O'Brien, J. Bliesath, M. Omori, N. Huser, C. Ho, C. Proffitt, M.K. Schwaebe, D.M. Ryckman, W.G. Rice, K. Anderes, CX-4945, an orally bioavailable selective inhibitor of protein kinase CK2, inhibits prosurvival and angiogenic signaling and exhibits antitumor efficacy, Cancer Res. 70 (2010) 10288–10298.
[10] S.E. Perea, O. Reyes, Y. Puchades, O. Mendoza, N.S. Vispo, I. Torrens, A. Santos, R. Silva, B. Acevedo, E. Lopez, V. Falcon, D.F. Alonso, Antitumor effect of a novel proapoptotic peptide that impairs the phosphorylation by the protein kinase 2 (casein kinase 2), Cancer Res. 64 (2004) 7127–7129.
[11] S.E. Perea, O. Reyes, I. Baladron, Y. Perera, H. Farina, J. Gil, A. Rodriguez, D. Bacardi, J.L. Marcelo, K. Cosme, M. Cruz, C. Valenzuela, P.A. Lopez-Saura, Y. Puchades, J.M. Serrano, O. Mendoza, L. Castellanos, A. Sanchez, L. Betancourt, V. Besada, R. Silva, E. Lopez, V. Falcon, I. Hernandez, M. Solares, A. Santana, A. Diaz, T. Ramos, C. Lopez, J. Ariosa, L.J. Gonzalez, H. Garay, D. Gomez, R. Gomez, D.F. Alonso, H. Sigman, L. Herrera, B. Acevedo, CIGB-300, a novel proapoptotic peptide that impairs the CK2 phosphorylation and exhibits anticancer properties both in vitro and in vivo, Mol. Cell. Biochem. 316 (2008) 163–167.
[12] Y. Perera, H.G. Farina, I. Hernandez, O. Mendoza, J.M. Serrano, O. Reyes, D.E. Gomez, R.E. Gomez, B.E. Acevedo, D.F. Alonso, S.E. Perea, Systemic administration of a peptide that impairs the protein kinase (CK2) phosphorylation reduces solid tumor growth in mice, Int. J. Cancer 122 (2008) 57–62.
[13] L.R. Martins, Y. Perera, P. Lucio, M.G. Silva, S.E. Perea, J.T. Barata, Targeting chronic lymphocytic leukemia using CIGB-300, a clinical-stage CK2-specific cell-permeable peptide inhibitor, Oncotarget 5 (2014) 258–263.
[14] H.G. Farina, F. Benavent Acero, Y. Perera, A. Rodriguez, S.E. Perea, B.A. Castro, R. Gomez, D.F. Alonso, D.E. Gomez, CIGB-300, a proapoptotic peptide, inhibits angiogenesis in vitro and in vivo, Exp. Cell Res. 317 (2011) 1677–1688.
[15] Y. Perera, N.D. Toro, L. Gorovaya, D.E.C.J. Fernandez, H.G. Farina, S.E. Perea, Synergistic interactions of the anti-casein kinase 2 CIGB-300 peptide and chemotherapeutic agents in lung and cervical preclinical cancer models, Mol. Clin. Oncol. 2 (2014) 935–944.
[16] A.M. Solares, A. Santana, I. Baladron, C. Valenzuela, C.A. Gonzalez, A. Diaz, D. Castillo, T. Ramos, R. Gomez, D.F. Alonso, L. Herrera, H. Sigman, S.E. Perea, B.E. Acevedo, P. Lopez-Saura, Safety and preliminary efficacy data of a novel casein kinase 2 (CK2) peptide inhibitor administered intralesionally at four dose levels in patients with cervical malignancies, BMC Cancer 9 (2009) 146.
[17] A. Rodriguez-Ulloa, Y. Ramos, J. Gil, Y. Perera, L. Castellanos-Serra, Y. Garcia, L. Betancourt, V. Besada, L.J. Gonzalez, J. Fernandez-de-Cossio, A. Sanchez, J.M. Serrano, H. Farina, D.F. Alonso, B.E. Acevedo, G. Padron, A. Musacchio, S.E. Perea, Proteomic profile regulated by the anticancer peptide CIGB-300 in non-small cell lung cancer (NSCLC) cells, J. Proteome Res. 9 (2010) 5473–5483.
[18] Y. Perera, H.G. Farina, J. Gil, A. Rodriguez, F. Benavent, L. Castellanos, R.E. Gomez, B.E. Acevedo, D.F. Alonso, S.E. Perea, Anticancer peptide CIGB-300 binds to nucleophosmin/B23, impairs its CK2-mediated phosphorylation, and leads to apoptosis through its nucleolar disassembly activity, Mol. Cancer Ther. 8 (2009) 1189–1196.
[19] A. Szebeni, K. Hingorani, S. Negi, M.O. Olson, Role of protein kinase CK2 phosphorylation in the molecular chaperone activity of nucleolar protein b23, J. Biol. Chem. 278 (2003) 9107–9115.
[20] F.R. Benavent Acero, Y. Perera Negrin, D.F. Alonso, S.E. Perea, D.E. Gomez, H.G. Farina, Mechanisms of cellular uptake, intracellular transportation, and degradation of CIGB-300, a Tat-conjugated peptide, in tumor cell lines, Mol. Pharm. 11 (2014) 1798–1807.
[21] S. Sarno, P. Vaglio, F. Meggio, O.G. Issinger, L.A. Pinna, Protein kinase CK2 mutants defective in substrate recognition. Purification and kinetic analysis, J. Biol. Chem. 271 (1996) 10595–10601.
[22] G.B. Fields, R.L. Noble, Solid phase peptide synthesis utilizing 9-fluorenylmethoxycarbonyl amino acids, Int. J. Pept. Protein Res. 35 (1990) 161–214.
[23] L.A. Carpino, H. Imazumi, A. El-Faham, F.J. Ferrer, C. Zhang, Y. Lee, B.M. Foxman, P. Henklein, C. Hanay, C. Mugge, H. Wenschuh, J. Klose, M. Beyermann, M. Bienert, The uronium/guanidinium peptide coupling reagents: finally the true uronium salts, Angew. Chem. Int. Ed. Engl. 41 (2002) 441–445.
[24] M. Ruzzene, L.A. Pinna, Assay of protein kinases and phosphatases using specific peptide substrates, Protein Phosphorylation2nd ed., Hardie, 1999. 221–253.
[25] G. Di Maira, F. Brustolon, J. Bertacchini, K. Tosoni, S. Marmiroli, L.A. Pinna, M. Ruzzene, Pharmacological inhibition of protein kinase CK2 reverts the multidrug resistance phenotype of a CEM cell line characterized by high CK2 level, Oncogene 26 (2007) 6915–6926.
[26] P. le Coutre, E. Tassi, M. Varella-Garcia, R. Barni, L. Mologni, G. Cabrita, E. Marchesi, R. Supino, C. Gambacorti-Passerini, Induction of resistance to the Abelson inhibitor STI571 in human leukemic cells through gene amplification, Blood 95 (2000) 1758–1766.
[27] V. Cenni, N.M. Maraldi, A. Ruggeri, P. Secchiero, R. Del Coco, A. De Pol, L. Cocco, S. Marmiroli, Sensitization of multidrug resistant human ostesarcoma cells to Apo2 Ligand/TRAIL-induced apoptosis by inhibition of the Akt/PKB kinase, Int. J. Oncol. 25 (2004) 1599–1608.
[28] M. Ruzzene, D. Penzo, L.A. Pinna, Protein kinase CK2 inhibitor 4,5,6,7-tetrabromobenzotriazole (TBB) induces apoptosis and caspase-dependent degradation of haematopoietic lineage cell-specific protein 1 (HS1) in Jurkat cells, Biochem. J. 364 (2002) 41–47.
[29] J.S. Wadia, S.F. Dowdy, Protein transduction technology, Curr. Opin. Biotechnol. 13 (2002) 52–56.
[30] O. Marin, S. Sarno, M. Boschetti, M.A. Pagano, F. Meggio, V. Ciminale, D.M. D'Agostino, L.A. Pinna, Unique features of HIV-1 Rev protein phosphorylation by protein kinase CK2 ('casein kinase-2'), FEBS Lett. 481 (2000) 63–67.
[31] M. Salvi, S. Sarno, O. Marin, F. Meggio, E. Itarte, L.A. Pinna, Discrimination between the activity of protein kinase CK2 holoenzyme and its catalytic subunits, FEBS Lett. 580 (2006) 3948–3952.
[32] S.E. Perea, O. Filhol, C. Cochet, CIGB-300 Anticancer Peptide Impairs the Casein Kinase 2 (CK2) Beta-Dependent Phosphorylation In Vitro, Oral Presentation at 7th International Conference on Protein Kinase CK2, Lublin, Poland, 2013.
[33] F. Meggio, B. Boldyreff, O. Marin, F. Marchiori, J.W. Perich, O.G. Issinger, L.A. Pinna, The effect of polylysine on casein-kinase-2 activity is influenced by both the structure of the protein/peptide substrates and the subunit composition of the enzyme, Eur. J. Biochem. 205 (1992) 939–945.
[34] F. Meggio, B. Boldyreff, O. Marin, L.A. Pinna, O.G. Issinger, Role of the beta subunit of casein kinase-2 on the stability and specificity of the recombinant reconstituted holoenzyme, Eur. J. Biochem. 204 (1992) 293–297.
[35] M. Fukuda, Lysosomal membrane glycoproteins. Structure, biosynthesis, and intracellular trafficking, J. Biol. Chem. 266 (1991) 21327–21330.
[36] V.I. Korolchuk, F.M. Menzies, D.C. Rubinsztein, Mechanisms of cross-talk between the ubiquitin-proteasome and autophagy–lysosome systems, FEBS Lett. 584 (2010) 1393–1398.
[37] M. Lippai, P. Low, The role of the selective adaptor p62 and ubiquitin-like proteins in autophagy, Biomed. Res. Int. 2014 (2014) 832704.
[38] F. Meggio, B. Boldyreff, O.G. Issinger, L.A. Pinna, Casein kinase-2 down-regulation and activation by polybasic peptides are mediated by acidic residues in the 55-64 region of the beta-subunit — a study with calmodulin as phosphorylatable substrate, Biochemistry 33 (1994) 4336–4342.
[39] D.M. Benbrook, A. Long, Integration of autophagy, proteasomal degradation, unfolded protein response and apoptosis, Exp. Oncol. 34 (2012) 286–297.
[40] Y. Perera, H.C. Costales, Y. Diaz, O. Reyes, H.G. Farina, L. Mendez, R.E. Gomez, B.E. Acevedo, D.E. Gomez, D.F. Alonso, S.E. Perea, Sensitivity of tumor cells towards CIGB-300 anticancer peptide relies on its nucleolar localization, J. Pept. Sci. 18 (2012) 215–223.

9.2 Different Persistence of the Cellular Effects Promoted by Protein Kinase CK2 Inhibitors CX-4945 and TDB

PKs multi-targeting is emerging as a novel strategy aimed at hitting pathologies sustained by more than one enzyme. The designing of compounds able to selectively target two kinases is a challenging task recently addressed by the compound called TDB. TDB is an ATP-competitive CK2 inhibitor with promising therapeutic features (Cozza et al., 2014) since able to target also PIM-1, an anti-apoptotic kinase often overexpressed in cancer cells, as CK2 (Blanco-Aparicio and Carnero, 2013).

I was involved in this collaborative parallel project, aimed at comparing the efficacy of TDB and CX-4945 in cells. We compared the compounds in term of their ability to inhibit the CK2 activity and to reduce cancer cells viability. Our results, in different treatments times and protocols, revealed that TDB displays a higher persistence of the inhibitory effect on CK2. This peculiarity produced a more pronounced toxicity for cancer cells, despite the superiority of CX-4945 efficacy *in vitro*. Such a superiority was not expected, since the IC_{50} for CK2 of TDB (32 nM) is many fold higher than that of CX-4945 (2 nM) *in vitro*. We found that the most relevant difference between them is the persistence of TDB on CK2. Indeed, in CX-4945 treated cells CK2 activity is rapidly restored to basal levels after the removal of the inhibitor, while in TDB-treated cells the inhibition lasts for several days. This implies important consequences on cellular processes affected by CK2, such as cell survival, proliferation, and migration (please refer to the following reprint for more details).

We hypothesized that a possible difference between TDB and CX-4945 could be related to the stability of their complex with CK2 in cells. We suggest that the cellular persistence of the CK2-inhibitor complex is a crucial aspect that should be considered during the optimization of inhibitory compounds.

Hindawi Publishing Corporation
BioMed Research International
Volume 2015, Article ID 185736, 9 pages
http://dx.doi.org/10.1155/2015/185736

Research Article

Different Persistence of the Cellular Effects Promoted by Protein Kinase CK2 Inhibitors CX-4945 and TDB

Cristina Girardi, Daniele Ottaviani, Lorenzo A. Pinna, and Maria Ruzzene

Department of Biomedical Sciences and CNR Institute of Neuroscience, University of Padova, 35131 Padova, Italy

Correspondence should be addressed to Maria Ruzzene; maria.ruzzene@unipd.it

Received 27 May 2015; Accepted 6 August 2015

Academic Editor: Sung-Hoon Kim

We compare the cellular efficacy of two selective and cell permeable inhibitors of the antiapoptotic kinase CK2. One inhibitor, CX-4945, is already in clinical trials as antitumor drug, while the other, TDB, has been recently successfully employed to demonstrate the implication of CK2 in cellular (dis)regulation. We found that, upon treatment of cancer cells with these compounds, the extent of inhibition of endocellular CK2 is initially comparable but becomes significantly different after the inhibitors are removed from the cellular medium: while in CX-4945 treated cells CK2 activity is restored to control level after 24 h, in the case of TDB it is still strongly reduced after 4 days from removal. The biological effects of the two inhibitors have been analyzed by performing clonogenic, spheroid formation, and wound-healing assays: we observed a permanent inhibition of cell survival and migration in TDB-treated cells even after the inhibitor removal, while in the case of CX-4945 only its maintenance for the whole duration of the assay insured a persisting effect. We suggest that the superiority of TDB in maintaining kinase activity inhibited and perpetuating the consequent effects is an added value to be considered when planning new therapies based on CK2 targeting.

1. Introduction

CK2 is a Ser/Thr protein kinase ubiquitously expressed and constitutively active, which phosphorylates hundreds of substrates and is involved in different cellular processes [1, 2]. Its activity is especially relevant for cancer cells [3], which not only express higher amount of CK2 compared to normal cells, but also rely more on it for their survival, being often dependent on tumor-specific prosurvival pathways which are potentiated by CK2 [4]. For these reasons, and despite its expression also in healthy cells, CK2 is presently considered a valuable anticancer therapeutic target. Several CK2 inhibitors have been developed so far [5, 6], but the most promising results have been obtained with CX-4945. This compound, initially discovered by Cylene Pharmaceuticals Inc. [7], is an ATP-competitive inhibitor, which is very selective for CK2 and is presently the only CK2 inhibitor under clinical trials in humans for cancer therapy [8, 9]. CX-4945 displays a very strong efficacy towards CK2 in vitro, with a IC_{50} of 1-2 nM [10]. However, when used to treat cancer cells, the concentrations required to induce apoptosis are not proportionally low; for example, in one of the initial studies, published by Pierre and coworkers [8], the calculated Ki for the CK2 catalytic subunit α in vitro was 1 nM, while the concentrations required to induce 50% cell death (DC_{50}) varied between 1 and 9 μM. We found very similar results in a study on different pairs of apoptosis sensitive/resistant variants of tumor cell lines [11] (DC_{50} 2–9 μM), and many other similar examples can be found in the literature, from where it is evident that CX-4945 is commonly used in the μM range to inhibit CK2 in cells.

We have recently developed a compound called TDB, which is another ATP-competitive CK2 inhibitor with promising therapeutic features [12]. We found that TDB is more effective than CX-4945 in inducing cell death. Such a superiority was not expected, since the IC_{50} for CK2 of TDB (32 nM) is manyfold higher than that of CX-4945. We therefore performed the present study aimed at analyzing the cellular efficacy of these two compounds. By comparing the persistence of CK2 inhibition after their administration to cells, we found that the effect of TDB on CK2 activity is more long-lasting than that of CX-4945, with important consequences on cellular processes affected by CK2, such as cell survival, proliferation, and migration.

2. Materials and Methods

2.1. Inhibitors. TDB (previously called K164) was synthesized as described in [13]. CX-4945 was from AbMole Bioscience. Inhibitors solution was in made in DMSO.

2.2. Cell Culture and Treatment. All cells were cultured in an atmosphere containing 5% CO_2; CEM cells (human T lymphoblastoid) were maintained in RPMI 1640 medium (Sigma) and U2OS cells (human osteosarcoma) and HEK-293T (human embryonic kidney cells) in D-MEM medium (Sigma); both media were supplemented with 10% (v/v) fetal calf serum (FCS), 2 mM L-glutamine, 100 U/mL penicillin, and 100 mg/mL streptomycin. Cell treatments with inhibitors were performed in the culture medium. Control cells were treated with equal amounts of the inhibitor solvent, which never exceeded 0.5% (v/v).

2.3. Cell Transfection. U2OS cells were transfected with Akt1 plasmid (2 μg) [14], using TransIT (Mirus Bio, Madison, USA) as transfecting agent. After 40 h from the beginning of the transfection, cells were treated with inhibitors or vehicle for 24 h. Then the medium was removed and cells were immediately lysed or cultured for further 24 h in the absence of inhibitors.

2.4. Cell Lysis and Western Blot Experiments. For lysate preparation, cells were lysed as described in [15]. Protein concentration was determined by the Bradford method. Equal amounts of proteins were loaded on 11% SDS-PAGE, blotted on Immobilon-P membranes (Millipore), and processed in Western blot (WB) with the indicated antibody, detected by chemiluminescence. Quantitation of the signal was obtained by chemiluminescence detection on a Kodak Image Station 440MM PRO and analysis with the Kodak 1D Image software.

2.5. CK2 Activity Assay. CK2 activity in cell lysates was measured by means of radioactive assays with [γ-^{33}P]ATP towards the specific CK2 substrate peptide CK2-tide, as described in [16].

2.6. Clonogenic Survival Assays. U2OS cells were plated at 100 cells/well in 6-well plates and allowed to adhere to the plate for 16 h. Cells were then treated with variable concentrations of the inhibitors (or with equal amount of vehicle as control) in culture medium. After 24 h, cells were washed and the medium was replaced by fresh culture medium without inhibitors. After further 6 days, cells were fixed and stained with 0.5% crystal violet; images were captured using a Leica DMI4000 automated inverted microscope equipped with a Leica DFC300 FX camera.

2.7. 3D Spheroid Formation. U2OS cells were plated at 50% confluence, allowed to adhere to the plate for 16 h, and then treated with inhibitors or vehicle for 24 h. After treatment, cells were washed, detached, counted, and seeded at 1000 cells/well in 200 μL of culture medium, in a 96-well plate with round bottom wells precoated with 50 μL of 1% agar in culture medium [17]. Images were taken from each well 24 h and 96 h later, by means of a Leica DMI4000 automated inverted microscope equipped with a Leica DFC300 FX camera.

2.8. Wound-Healing Assays. Wound-healing assays were performed by creating identical wound areas into the cell monolayer using Ibidi culture-inserts (Ibidi GmbH, Cat. no. 80209, Munich, Germany). U2OS cells were seeded in complete culture medium at a density of 3×10^4 cells on each side of the Ibidi culture-insert, into a 24-well plate. After attachment, cells were treated for 24 h inhibitors (or vehicle in the controls); then the culture-insert was detached in order to form a cell-free gap into the cell monolayer. Each well was rinsed once with phosphate-buffered saline (PBS) to remove cell debris and immediately refilled with fresh medium, with new addition of the inhibitors (samples with "maintained" treatment) or without (sample with "removed" treatment). Cells were allowed to migrate for further 48 h. The wound images were captured at time zero ($t = 0$ h), $t = 24$ h, and $t = 48$ h using a Leica DMI4000 automated inverted microscope equipped with a Leica DFC300 FX camera.

3. Results

To compare the inhibitory efficacy in cells of the two compounds, CX-4945 and TDB, we analyzed their effects on two cell lines, one deriving from a blood tumor (CEM, T-cell lymphoblastoma) and the other from a solid tumor (U2OS, osteosarcoma). Their efficacy was quite similar in inhibiting cellular CK2 (Figure 1). However, based on their different in vitro IC_{50} values towards CK2 (also shown in Figure 1, box), a much stronger efficacy of CX-4945 was expectable. Moreover, the ability of TDB to induce cell death is higher than that of CX-4945 (see DC_{50} values in the box of Figure 1, calculated from [12]), suggesting that TDB has peculiar features that render it more effective than expected. We therefore decided to assess whether the permanence of CK2 inhibition in cells induced by the two compounds was different. To this purpose, we performed experiments of cell treatment for 24 h with the inhibitors, followed by cell washing and replacement of a fresh, inhibitor-free, medium; lysates from treated cells were then analyzed for CK2 activity. In this kind of experiments we observed that, in cells treated with CX-4945, CK2 activity was rapidly restored to control level, while in the case of TDB the effect was much more persistent, lasting up to 4 days after the inhibitor removal (Figure 2(a)). To address this point by a different approach allowing direct measuring of the endocellular CK2 activity, we transfected U2OS cells with Akt1, whose Ser129 works as a reporter of CK2 activity in cells [14, 18]. The results, shown in Figure 2(b), demonstrated that the phosphorylation of Akt1 Ser129 is similarly reduced by the two inhibitors immediately after treatment, while it remains significantly lower than the control only with TDB in case of inhibitor removal, thus confirming the more permanent blockage of the kinase activity by TDB than by CX-4945.

We wondered if the different duration of CK2 inhibition by CX-4945 and TDB had consequences on cellular processes controlled by CK2. To assess this point, we first performed

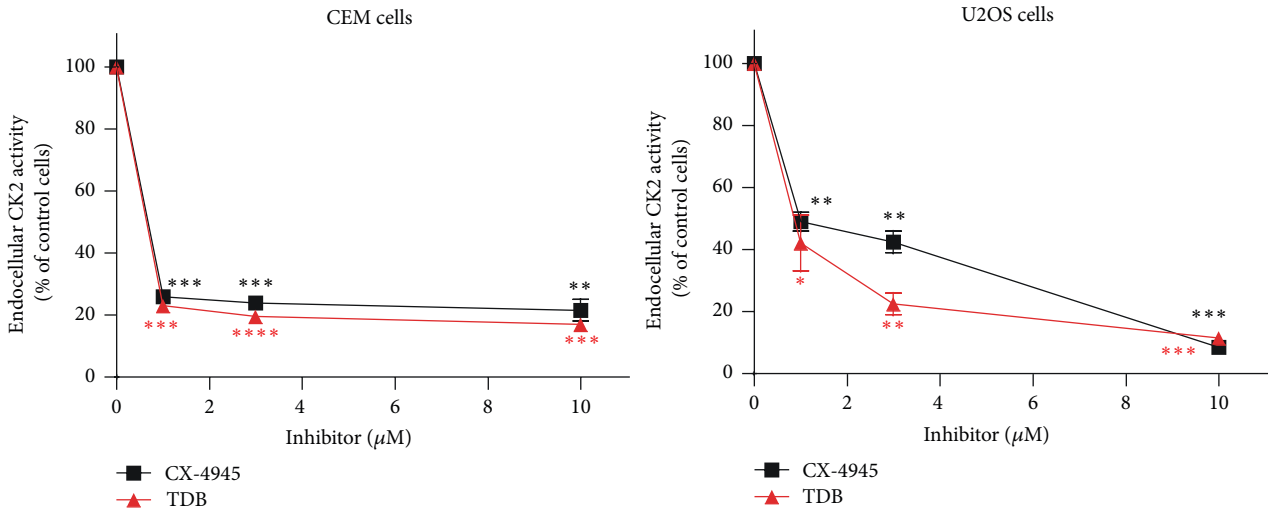

	TDB	CX-4945
IC_{50} for CK2 in CEM cells	0.65 μM	0.76 μM
IC_{50} for CK2 in U2OS cells	0.87 μM	1.00 μM
In vitro IC_{50} for CK2	32 nM[a]	1 nM[b]
DC_{50}	1.25 μM[a]	6.92 μM[a]

Figure 1: Comparison of CX-4945 and TDB efficacy on cellular CK2 activity. CEM or U2OS cells were treated for 4 h with increasing concentrations of TDB or CX-4945. Then cells were lysed and CK2 activity was assessed from 1-2 μg of lysate proteins towards a synthetic CK2-specific peptide. Activity is shown as percent of control vehicle-treated cells (mean of two independent experiments ± SEM). In the box, the IC_{50} values for CK2 inhibition in the two cell lines are reported, as extrapolated from the curves above; the in vitro IC_{50} values for CK2 are also shown for comparison, as reported in [12] ([a]) (SEM never exceeding 10%) and [7] ([b]). DC_{50} values (concentrations required to induce 50% of cell death in 24 h) are reported as in [12] ([a]) for HeLa cells, where a direct comparison between the two compounds in inducing cell death is presented. Statistical significance was calculated using unpaired t-test between control and treated cells ($^{****}p \leq 0.0001$; $^{***}p \leq 0.001$; $^{**}p \leq 0.01$; $^{*}p \leq 0.05$).

clonogenic survival assays in U2OS cells, by seeding cells in 6-wells plates, treating with increasing concentrations of CX-4945 or TDB for 24 h, then removing the medium, and allowing clones to grow for further 6 days in the absence of the inhibitors. The results, shown in Figure 3, indicate that TDB is much more effective than CX-4945 in preventing clone formation and survival. Similar results were obtained in 3D culture experiments to assess spheroid formation (Figure 4): we found that TDB-treated cells were much less prone than vehicle-treated cells to forming spheroids, while CX-4945 was similarly effective than TDB when assessed at 24 h but has much weaker effect at longer times after the inhibitor removal.

We then evaluated U2OS cells for their migration activity in wound-healing assays in the presence of the two compounds. Figure 5 shows that, as expected for CK2 inhibitors [19–21], both CX-4945 and TDB were able to inhibit cell motility in 24–48 h assays when cells were constantly exposed to them (upper part of the figure). By contrast, when the inhibitors were removed from the medium after a 24 h treatment (before starting the analysis of cell migration, $t = 0$ in Figure 5), cells migrated significantly less than the control cells only in the case of TDB (lower part of Figure 5).

All our observations unequivocally indicate that the effect of TDB persists in the cells more than that of CX-4945, suggesting more stable binding of the former to the target kinase.

4. Discussion

Theoretically, the ATP-competitive compounds work as kinase inhibitors by a reversible mechanism, relying on non-covalent interactions with the ATP pocket of the kinase. In the case of both CX-4945 and TDB, this assumption has been validated by crystallographic studies [10, 12]. Intriguingly, however, many of them are fully active at μM concentrations (or below) even in the cellular environment, where the ATP concentration, in the mM range, would be expected to vanish their efficacy. This can be explained in terms of affinity, considering that the Km values of kinases for ATP are in the μM range, while many inhibitors display Ki values in the low nM range. The possibility, however, that the occupancy of the ATP site is stabilized by additional mechanisms should be also considered. Different inhibitors may display for the same kinase similar affinity but sharply different dissociation rates, thus leading to residence times that are strikingly

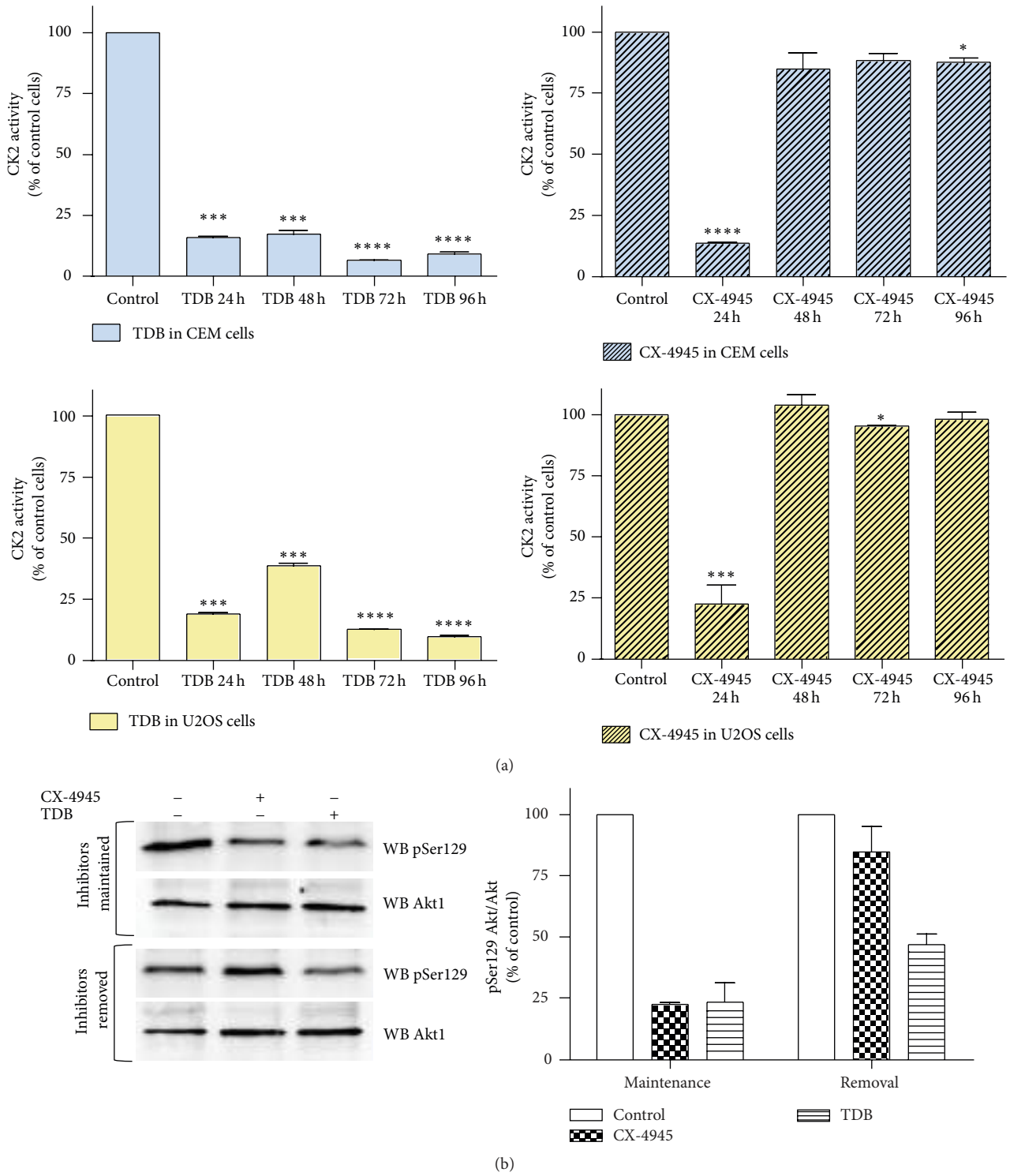

Figure 2: Duration of CK2 inhibition after TDB or CX-4945 removal from treated cells. CEM or U2OS cells were treated with TDB or CX-4945, as indicated, for 24 h. Then cells were washed and the culture medium was replaced with a fresh one devoid of inhibitors. (a) Cells were cultured for a further time, as indicated, and then lysed. CK2 activity was assessed from 1-2 μg of lysate proteins towards a synthetic CK2-specific peptide. The inhibitor concentration was 3 μM. Activity is shown as percent of control vehicle-treated cells (mean of three independent experiments ± SEM; statistical significance was calculated using unpaired t-test between control and treated cells ($^{****}p \leq 0.0001$; $^{***}p \leq 0.001$; $^{**}p \leq 0.01$; $^{*}p \leq 0.05$)). (b) Cells were lysed after the first 24 h of culture in the presence of 10 μM inhibitors (upper blots) or cultured for further 24 h after the inhibitor removal (lower blots). 10 μg of lysate proteins was analyzed by WB with the indicated antibodies. A quantification of the pSer129 (mean of three independent experiments ± SEM) normalized to Akt1 total amount is shown in the histograms on the right, where 100% values have been assigned to untreated cells of each experimental protocol.

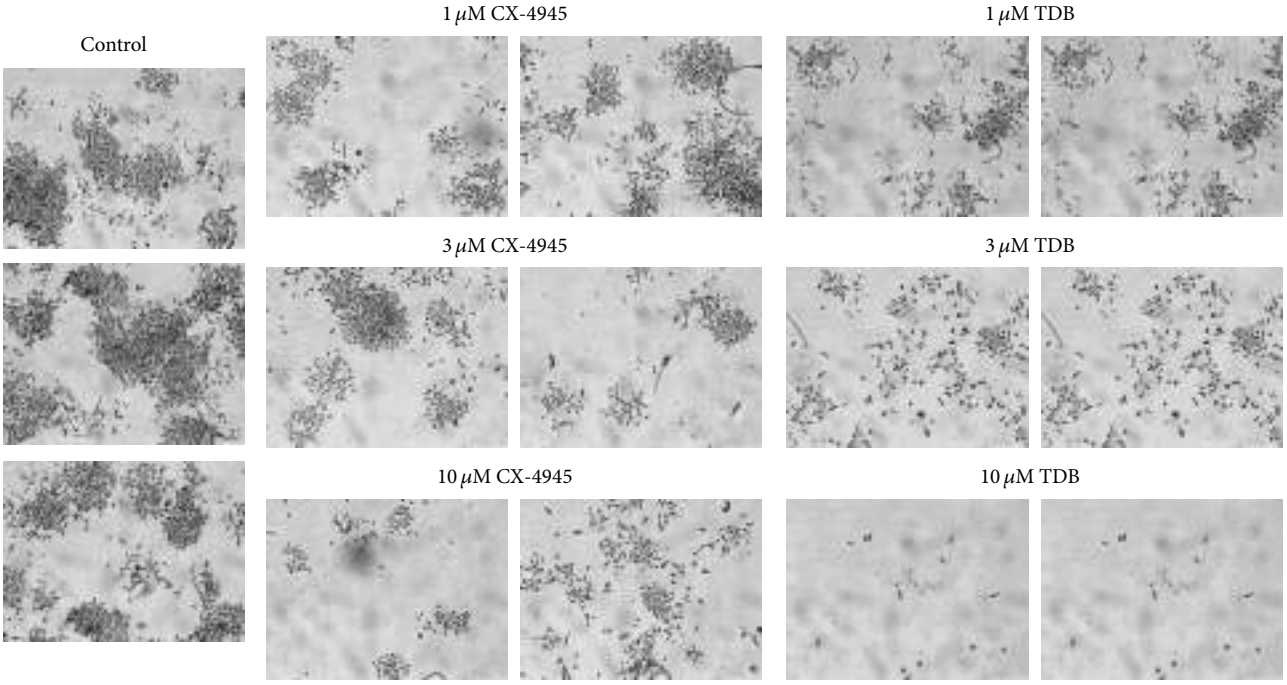

Figure 3: Effects of CX-4945 and TDB on clone formation and survival. 100 U2OS cells were plated for each well, treated for 24 h with the indicated inhibitors, and then grown for further 6 days in the absence of the inhibitors. Two representative images are shown for each condition (2.5x objective, magnification-changer 1.6); at least two separate experiments in triplicate were performed.

variable, from few minutes to several hours. This concept may also contribute to account for the observation that the ratio between DC_{50} (reflecting in cell efficacy) and IC_{50} (measured in vitro) is also very variable depending on the inhibitor considered. With this in mind we performed this study, focused on two inhibitors that induce cellular effects at concentrations that are not proportional to their inhibitory potency in vitro. One of them, CX-4945, is considered quite selective for CK2, while the other, TDB, is a dual inhibitor, targeting also PIM-1, another antiapoptotic kinase, which is often overexpressed in cancer cells [22]. However, the observation that TDB is more effective than CX-4945 in cells cannot be simply explained by the dual nature of TDB, since the combination of a CK2 and a PIM-1 inhibitor is still less effective than TDB [12]. Moreover, although CX-4945 is considered a pure CK2 inhibitor, it reduces PIM-1 activity as well: its IC_{50} for PIM-1 (216 nM [10]) is comparable to that of TDB (86 nM [12]). Consistently, the residual activity of PIM-1 in the presence of 0.5 μM CX-4945 is only 6% [10], while it is 7% in the presence of 1 μM TDB [12]. At the concentrations used in cells, therefore, it is conceivable that both inhibitors target PIM-1 besides CK2, suggesting that TDB superiority should rely on other features, and that it possess a sort of added value compared to other inhibitors. Here we show that the most relevant difference is the duration of CK2 inhibition, since in CX-4945 treated cells CK2 activity is rapidly restored to basal levels after the removal of the inhibitor, while in TDB-treated cells the inhibition lasts for several days (Figure 2). This feature was found in two different cell lines, one from hematological and one from solid tumor. We can not exclude that the cellular environment can affect the stability of the kinase/inhibitor complex in a cell-specific manner. Indeed, when we performed this kind of experiments on HEK-293T (nontumor cells), we found that the inhibition by CX-4945 was transient (13 ± 3% of residual CK2 activity after 24 h treatment with 10 μM CX-4945, 83 ± 0.5% after further 24 h in the absence of the inhibitor), similarly to what observed in tumor cells, while the effect of TDB was slightly more persistent (17.9 ± 0.9% residual activity after 24 h with 10 μM TDB, 55.5 ± 5.5% after further 24 h in the absence of the inhibitor), albeit less than in the tumor cells that we analyzed.

For the time being, what we can say is that in our cancer models this different property of the two inhibitors has important consequences on cellular processes. As expected, in fact, longer persistence of CK2 inhibition is more effective in reducing the clonogenic survival of tumor cells (Figure 3), their ability to form spheroids (Figure 4), and their migration (Figure 5).

The exact reason for the longer inhibition induced by TDB compared to CX-4945 will deserve future investigation. Here we hypothesize that a possible difference between the two compounds could be related to the stability of their complex with CK2, since the experiments have been performed in conditions of inhibitor removal. However, other possibilities should be also taken into account. In accordance with our results, Schwind and colleagues have recently published a paper [23] where the inhibition by CX-4945 and its effects on stem cell differentiation were found to decrease from 24 h to 72 h. Since in that case the inhibitor was maintained in contact with cells for all the length of the experiment,

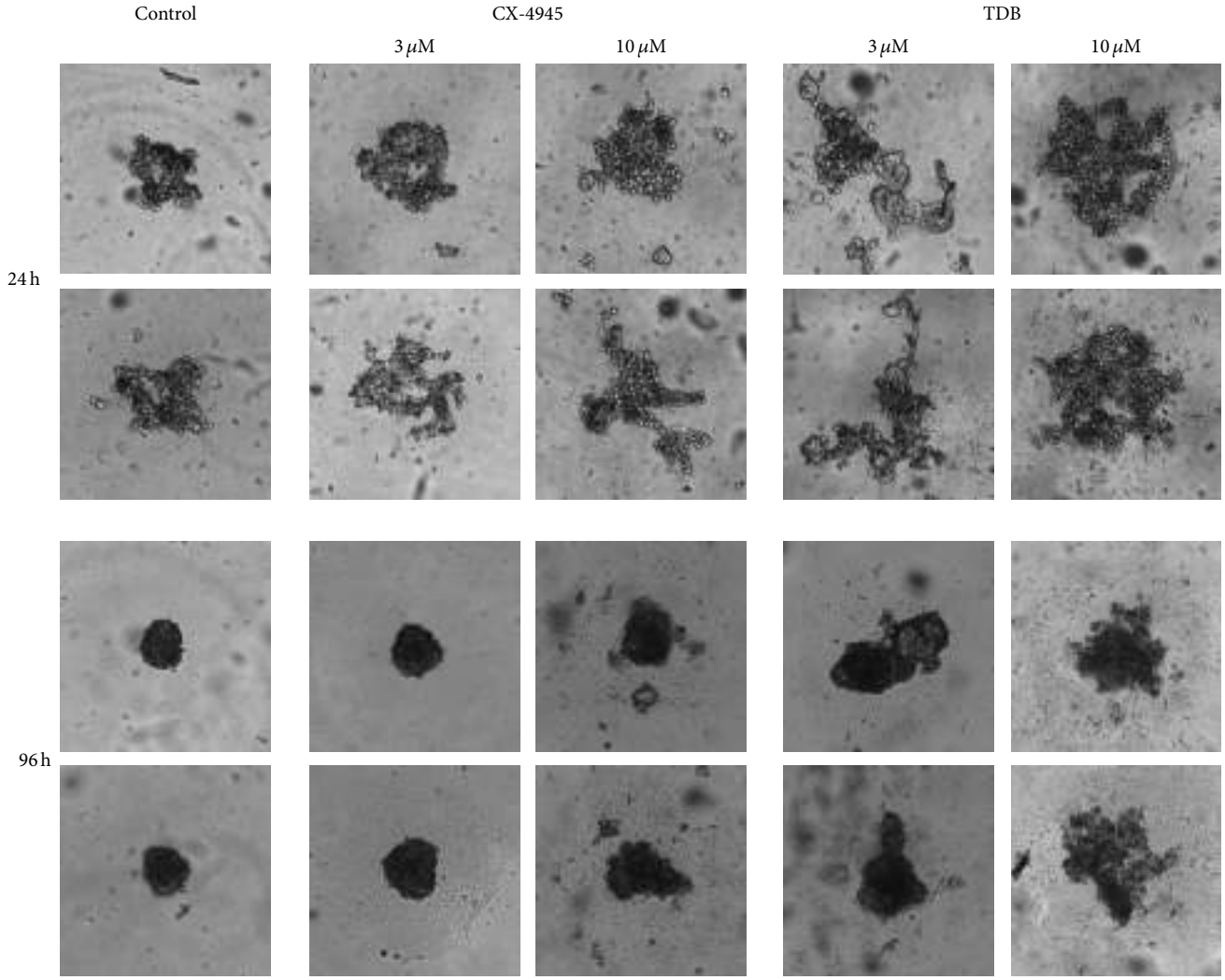

Figure 4: Effects of CX-4945 and TDB on spheroid formation. U2OS cells were pretreated for 24 h with the indicated concentrations of inhibitors and then allowed to form spheroids. Images were taken after 24 h and 96 h. Two separate experiments were performed, with triplicates of each condition (2.5x objective, magnification-changer 1.6). Two representative images for each condition are shown.

the result would indicate that its effective concentration decreased, and this could be due to several causes, such as compound extrusion, subcellular redistribution, or metabolic inactivation.

CK2 being considered a valuable therapeutic target [4, 24, 25], our results can be relevant also from a therapeutic point of view. A part from a chimeric peptide called CIGB-300 [26] which is giving promising results on cervical carcinoma [27] but whose mechanism of action is still enigmatic [28], CX-4945 is the only ATP-competitive small inhibitor of CK2 in phase II of clinical trials as anticancer agent [8]. In the comparison presented here, however, TDB is superior to CX-4945. Taking also into account that, besides CK2, it inhibits PIM-1 (a very important and innovative target in cancer therapy [29–31]), CLK2, and, with lower efficacy, also DYRK1A [12], we believe that TDB displays good features to be considered for future clinical experimentation.

In this work we focused on CK2 activity. However, we cannot exclude that the same persistence of kinase inhibition by TDB observed on CK2 can also occur on PIM-1 and the other major targets of TDB. Future studies will be required to address this point; for the time being, irrespective of the kinase affected and the molecular mechanism, we can conclude that survival, proliferation, and migration of tumor cells are more stably affected by TDB than by CX-4945.

5. Conclusions

In this paper we highlight an important difference between the two CK2 inhibitors, CX-4945 and TDB, consisting in a different duration of their effects in cells, which is longer for TDB. This feature was unpredictable from the in vitro efficacy of the two inhibitors towards protein kinase CK2, which instead indicated a superiority of CX-4945. Our findings

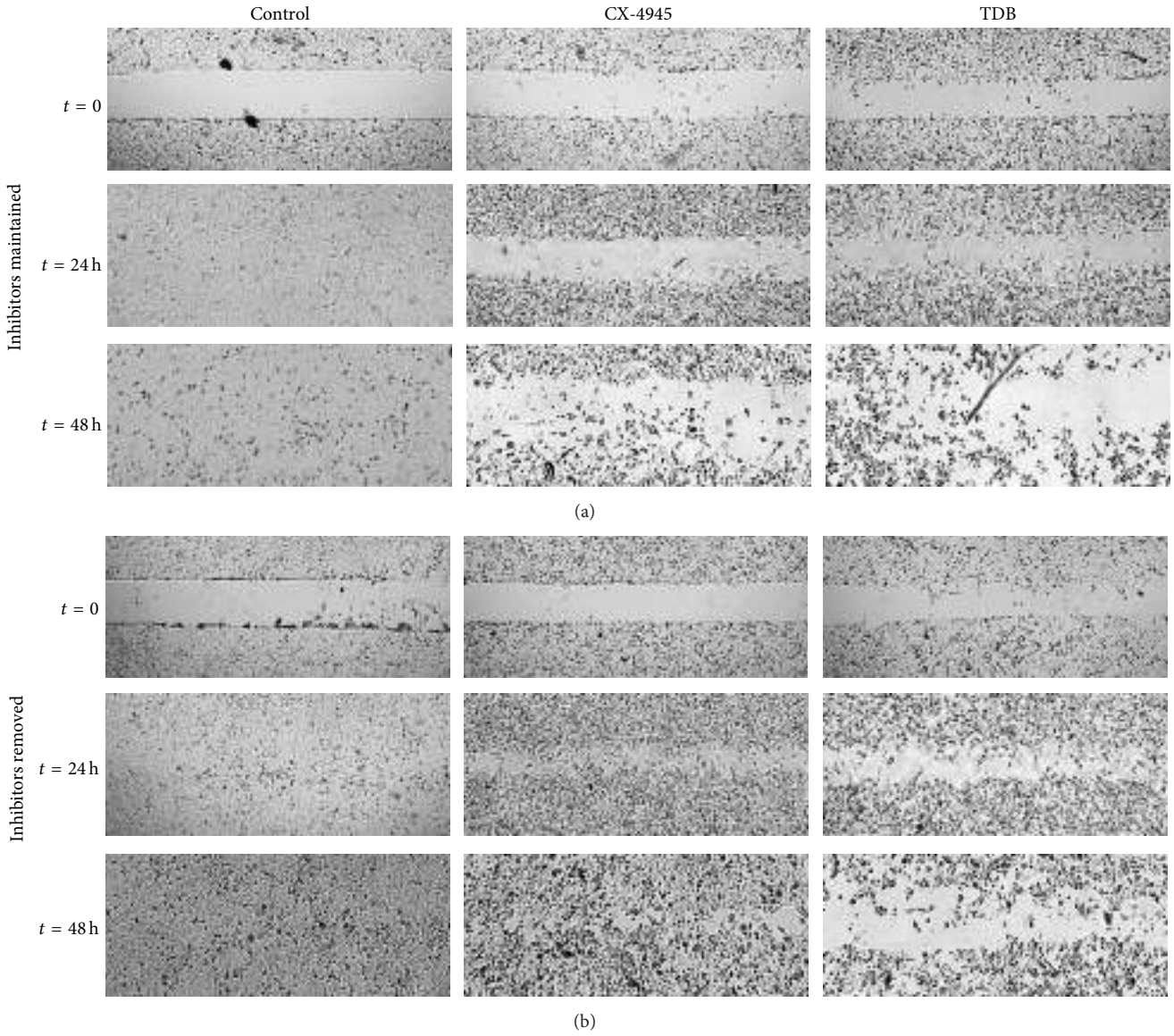

Figure 5: Effects of CX-4945 and TDB on cell migration. Cell migration was assessed by wound-healing assay, seeding U2OS cells in wells containing an insert, and incubating them for 24 h in the presence of the indicated inhibitor (10 μM) or vehicle. Then the insert was removed ($t = 0$) and cells were left to migrate for 48 h, always in the presence of the inhibitors (upper part of the figure, "inhibitors maintained") or in their absence (lower part of the figure, "inhibitors removed"). The experiment was performed three times, with each condition in duplicate. Representative images at $t = 0$, $t = 24$ h, and $t = 48$ h are shown.

suggest that the persistence of cellular effects should be therefore considered as an additional evaluation element to be taken into account in investigations on CK2 inhibitors as potential therapeutic tools.

Abbreviations

CK2: Casein kinase 2
CX-4945: 5-(3-Chlorophenylamino)benzo[c][2,6] naphthyridine-8-carboxylic acid
DC_{50}: Concentrations required to induce 50% of cell death in 24 h
DMSO: Dimethyl sulfoxide
PBS: Phosphate-buffered saline
PIM-1: Proviral integration of Moloney virus
TDB: Tetra-bromo-deoxyribofuranosyl-benzimidazole
WB: Western blot.

Conflict of Interests

The authors declare that there is no conflict of interests regarding the publication of this paper.

Acknowledgments

This work was supported by grants from Associazione Italiana per la Ricerca sul Cancro (AIRC, Grant IG 14180) to Lorenzo A. Pinna. The authors kindly acknowledge Dr. Z. Kazimierczuk for TDB synthesis.

References

[1] L. A. Pinna, "Protein kinase CK2: A challenge to canons," *Journal of Cell Science*, vol. 115, part 20, pp. 3873–3878, 2002.

[2] N. A. St-Denis and D. W. Litchfield, "From birth to death: the role of protein kinase CK2 in the regulation of cell proliferation and survival," *Cellular and Molecular Life Sciences*, vol. 66, no. 11-12, pp. 1817–1829, 2009.

[3] J. H. Trembley, G. Wang, G. Unger, J. Slaton, and K. Ahmed, "CK2: a key player in cancer biology," *Cellular and Molecular Life Sciences*, vol. 66, no. 11-12, pp. 1858–1867, 2009.

[4] M. Ruzzene and L. A. Pinna, "Addiction to protein kinase CK2: a common denominator of diverse cancer cells?" *Biochimica et Biophysica Acta*, vol. 1804, no. 3, pp. 499–504, 2010.

[5] S. Sarno, E. Papinutto, C. Franchin et al., "ATP site-directed inhibitors of protein kinase CK2: an update," *Current Topics in Medicinal Chemistry*, vol. 11, no. 11, pp. 1340–1351, 2011.

[6] G. Cozza, L. A. Pinna, and S. Moro, "Kinase CK2 inhibition: an update," *Current Medicinal Chemistry*, vol. 20, no. 5, pp. 671–693, 2013.

[7] A. Siddiqui-Jain, D. Drygin, N. Streiner et al., "CX-4945, an orally bioavailable selective inhibitor of protein kinase CK2, inhibits prosurvival and angiogenic signaling and exhibits antitumor efficacy," *Cancer Research*, vol. 70, no. 24, pp. 10288–10298, 2010.

[8] F. Pierre, P. C. Chua, S. E. Obrien et al., "Discovery and SAR of 5-(3-Chlorophenylamino)benzo[c][2,6]naphthyridine-8- carboxylic acid (CX-4945), the first clinical stage inhibitor of protein kinase CK2 for the treatment of cancer," *Journal of Medicinal Chemistry*, vol. 54, no. 2, pp. 635–654, 2011.

[9] H. J. Chon, K. J. Bae, Y. Lee, and J. Kim, "The casein kinase 2 inhibitor, CX-4945, as an anti-cancer drug in treatment of human hematological malignancies," *Frontiers in Pharmacology*, vol. 6, article 70, 2015.

[10] R. Battistutta, G. Cozza, F. Pierre et al., "Unprecedented selectivity and structural determinants of a new class of protein kinase CK2 inhibitors in clinical trials for the treatment of cancer," *Biochemistry*, vol. 50, no. 39, pp. 8478–8488, 2011.

[11] S. Zanin, C. Borgo, C. Girardi et al., "Effects of the CK2 inhibitors CX-4945 and CX-5011 on drug-resistant cells," *PLoS ONE*, vol. 7, no. 11, Article ID e49193, 2012.

[12] G. Cozza, C. Girardi, A. Ranchio et al., "Cell-permeable dual inhibitors of protein kinases CK2 and PIM-1: structural features and pharmacological potential," *Cellular and Molecular Life Sciences*, vol. 71, no. 16, pp. 3173–3185, 2014.

[13] G. Cozza, S. Sarno, M. Ruzzene et al., "Exploiting the repertoire of CK2 inhibitors to target DYRK and PIM kinases," *Biochimica et Biophysica Acta—Proteins and Proteomics*, vol. 1834, no. 7, pp. 1402–1409, 2013.

[14] C. Girardi, P. James, S. Zanin, L. A. Pinna, and M. Ruzzene, "Differential phosphorylation of Akt1 and Akt2 by protein kinase CK2 may account for isoform specific functions," *Biochimica et Biophysica Acta—Molecular Cell Research*, vol. 1843, no. 9, pp. 1865–1874, 2014.

[15] G. Di Maira, F. Brustolon, L. A. Pinna, and M. Ruzzene, "Dephosphorylation and inactivation of Akt/PKB is counteracted by protein kinase CK2 in HEK 293T cells," *Cellular and Molecular Life Sciences*, vol. 66, no. 20, pp. 3363–3373, 2009.

[16] M. Ruzzene, G. Di Maira, K. Tosoni, and L. A. Pinna, "Assessment of CK2 constitutive activity in cancer cells," *Methods in Enzymology*, vol. 484, pp. 495–514, 2010.

[17] F. Pampaloni, R. Richa, and N. Ansari, "Live spheroid formation recorded with light sheet-based fluorescence microscopy," *Methods in Molecular Biology*, vol. 1251, pp. 43–57, 2015.

[18] G. Di Maira, M. Salvi, G. Arrigoni et al., "Protein kinase CK2 phosphorylates and upregulates Akt/PKB," *Cell Death and Differentiation*, vol. 12, no. 6, pp. 668–677, 2005.

[19] J. Kim and S. H. Kim, "CK2 inhibitor CX-4945 blocks TGF-β1-induced epithelial-to-mesenchymal transition in A549 human lung adenocarcinoma cells," *PLoS ONE*, vol. 8, no. 9, Article ID e74342, 2013.

[20] Y. Zheng, B. C. McFarland, D. Drygin et al., "Targeting protein kinase CK2 suppresses prosurvival signaling pathways and growth of glioblastoma," *Clinical Cancer Research*, vol. 19, no. 23, pp. 6484–6494, 2013.

[21] M. J. Ku, J. W. Park, B. J. Ryu, Y.-J. Son, S. H. Kim, and S. Y. Lee, "CK2 inhibitor CX4945 induces sequential inactivation of proteins in the signaling pathways related with cell migration and suppresses metastasis of A549 human lung cancer cells," *Bioorganic and Medicinal Chemistry Letters*, vol. 23, no. 20, pp. 5609–5613, 2013.

[22] C. Blanco-Aparicio and A. Carnero, "Pim kinases in cancer: diagnostic, prognostic and treatment opportunities," *Biochemical Pharmacology*, vol. 85, no. 5, pp. 629–643, 2013.

[23] L. Schwind, N. Wilhelm, S. Kartarius, M. Montenarh, E. Gorjup, and C. Götz, "Protein kinase CK2 is necessary for the adipogenic differentiation of human mesenchymal stem cells," *Biochimica et Biophysica Acta*, vol. 1853, no. 10, pp. 2207–2216, 2015.

[24] J. H. Trembley, Z. Chen, G. Unger et al., "Emergence of protein kinase CK2 as a key target in cancer therapy," *BioFactors*, vol. 36, no. 3, pp. 187–195, 2010.

[25] I. Dominguez, G. E. Sonenshein, and D. C. Seldin, "Protein kinase CK2 in health and disease: CK2 and its role in Wnt and NF-kappaB signaling: linking development and cancer," *Cellular and Molecular Life Sciences*, vol. 66, no. 11-12, pp. 1850–1857, 2009.

[26] S. E. Perea, O. Reyes, I. Baladron et al., "CIGB-300, a novel proapoptotic peptide that impairs the CK2 phosphorylation and exhibits anticancer properties both in vitro and in vivo," *Molecular and Cellular Biochemistry*, vol. 316, no. 1-2, pp. 163–167, 2008.

[27] A. M. Solares, A. Santana, I. Baladrón et al., "Safety and preliminary efficacy data of a novel Casein Kinase 2 (CK2) peptide inhibitor administered intralesionally at four dose levels in patients with cervical malignancies," *BMC Cancer*, vol. 9, article 146, 2009.

[28] S. Zanin, M. Sandre, G. Cozza et al., "Chimeric peptides as modulators of CK2-dependent signaling: mechanism of action and off-target effects," *Biochimica et Biophysica Acta*, 2015.

[29] G. M. Arunesh, E. Shanthi, M. H. Krishna, J. S. Kumar, and V. N. Viswanadhan, "Small molecule inhibitors of PIM1 kinase: July 2009 to February 2013 patent update," *Expert Opinion on Therapeutic Patents*, vol. 24, no. 1, pp. 5–17, 2014.

[30] A. L. Merkel, E. Meggers, and M. Ocker, "PIM1 kinase as a target for cancer therapy," *Expert Opinion on Investigational Drugs*, vol. 21, no. 4, pp. 425–436, 2012.

[31] C. Blanco-Aparicio and A. Carnero, "Pim kinases in cancer: diagnostic, prognostic and treatment opportunities," *Biochemical Pharmacology*, vol. 85, no. 5, pp. 629–643, 2013.

.

Part VI

Bibliography

Bibliography

Ahmad, K. A., G. Wang, G. Unger, J. Slaton, and K. Ahmed (2008). Protein kinase CK2–a key suppressor of apoptosis. *Advances in Enzyme Regulation 48*, 179–187.

Anamika, n. and L. Spyracopoulos (2016, February). Molecular Basis for Phosphorylation-dependent SUMO Recognition by the DNA Repair Protein RAP80. *The Journal of Biological Chemistry 291*(9), 4417–4428.

Barata, J. T. (2011). The impact of PTEN regulation by CK2 on PI3k-dependent signaling and leukemia cell survival. *Advances in Enzyme Regulation 51*(1), 37–49.

Battistutta, R., G. Cozza, F. Pierre, E. Papinutto, G. Lolli, S. Sarno, S. E. O'Brien, A. Siddiqui-Jain, M. Haddach, K. Anderes, D. M. Ryckman, F. Meggio, and L. A. Pinna (2011, October). Unprecedented selectivity and structural determinants of a new class of protein kinase CK2 inhibitors in clinical trials for the treatment of cancer. *Biochemistry 50*(39), 8478–8488.

Benavent, F., C. S. Capobianco, J. Garona, S. M. Cirigliano, Y. Perera, A. J. Urtreger, S. E. Perea, D. F. Alonso, and H. G. Farina (2016, June). CIGB-300, an anti-CK2 peptide, inhibits angiogenesis, tumor cell invasion and metastasis in lung cancer models. *Lung Cancer (Amsterdam, Netherlands)*.

Bernatik, O., R. S. Ganji, J. P. Dijksterhuis, P. Konik, I. Cervenka, T. Polonio, P. Krejci, G. Schulte, and V. Bryja (2011, March). Sequential activation and inactivation of Dishevelled in the Wnt/beta-catenin pathway by casein kinases. *The Journal of Biological Chemistry 286*(12), 10396–10410.

Blanco-Aparicio, C. and A. Carnero (2013, March). Pim kinases in cancer: Diagnostic, prognostic and treatment opportunities. *Biochemical Pharmacology 85*(5), 629–643.

Blanquet, P. R. (2000, February). Casein kinase 2 as a potentially important enzyme in the nervous system. *Progress in Neurobiology 60*(3), 211–246.

Blumen, S. C., S. Astord, V. Robin, L. Vignaud, N. Toumi, A. Cieslik, A. Achiron, R. L. Carasso, M. Gurevich, I. Braverman, N. Blumen, A. Munich, M. Barkats, and L. Viollet (2012, April). A rare recessive distal hereditary motor neuropathy with HSJ1 chaperone mutation. *Annals of Neurology 71*(4), 509–519.

Bose, S., F. L. L. Stratford, K. I. Broadfoot, G. G. F. Mason, and A. J. Rivett (2004, February). Phosphorylation of 20s proteasome alpha subunit C8 (alpha7) stabilizes the 26s proteasome and plays a role in the regulation of proteasome complexes by gamma-interferon. *The Biochemical Journal 378*(Pt 1), 177–184.

Bulat, V., M. Rast, and J. Pielage (2014, January). Presynaptic CK2 promotes synapse organization and stability by targeting Ankyrin2. *The Journal of Cell Biology 204*(1), 77–94.

Burnett, G. and E. P. Kennedy (1954, December). The enzymatic phosphorylation of proteins. *The Journal of Biological Chemistry 211*(2), 969–980.

Cesaro, L., L. A. Pinna, and M. Salvi (2015, April). A Comparative Analysis and Review of lysyl Residues Affected by Posttranslational Modifications. *Current Genomics 16*(2), 128–138.

Chapple, J. P. and M. E. Cheetham (2003, May). The chaperone environment at the cytoplasmic face of the endoplasmic reticulum can modulate rhodopsin processing and inclusion formation. *The Journal of Biological Chemistry 278*(21), 19087–19094.

Cheetham, M. E., J. P. Brion, and B. H. Anderton (1992, June). Human homologues of the bacterial heat-shock protein DnaJ are preferentially expressed in neurons. *The Biochemical Journal 284 (Pt 2)*, 469–476.

Cheetham, M. E., A. P. Jackson, and B. H. Anderton (1994, November). Regulation of 70-kDa heat-shock-protein ATPase activity and substrate binding by human DnaJ-like proteins, HSJ1a and HSJ1b. *European journal of biochemistry / FEBS 226*(1), 99–107.

Chen, H.-J., J. C. Mitchell, S. Novoselov, J. Miller, A. L. Nishimura, E. L. Scotter, C. A. Vance, M. E. Cheetham, and C. E. Shaw (2016, May). The heat shock response plays an important role in TDP-43 clearance: evidence for dysfunction in amyotrophic lateral sclerosis. *Brain: A Journal of Neurology 139*(Pt 5), 1417–1432.

Cirigliano, S., M. I. Díaz Bessone, C. Flumian, D. Berardi, S. Perea, E. B. De Kier Joffé, H. Farina, L. Todaro, and A. Urtreger (2016, October). P2.05: The Synthetic Peptide CIGB-300 Inhibits NF-κB Translocation Affecting the Survival and Chemoresistance of NSCLC Cell Lines: Track: Biology and Pathogenesis. *Journal of Thoracic Oncology: Official Publication of the International Association for the Study of Lung Cancer 11*(10S), S218–S219.

Cohen, P. (2002, May). The origins of protein phosphorylation. *Nature Cell Biology 4*(5), E127–130.

Cozza, G., C. Girardi, A. Ranchio, G. Lolli, S. Sarno, A. Orzeszko, Z. Kazimierczuk, R. Battistutta, M. Ruzzene, and L. A. Pinna (2014, January). Cell-permeable dual inhibitors of protein kinases CK2 and PIM-1: structural features and pharmacological potential. *Cellular and Molecular Life Sciences 71*(16), 3173–3185.

Cozza, G., L. A. Pinna, and S. Moro (2012, September). Protein kinase CK2 inhibitors: a patent review. *Expert Opinion on Therapeutic Patents 22*(9), 1081–1097.

Cozza, G., L. A. Pinna, and S. Moro (2013). Kinase CK2 inhibition: an update. *Current Medicinal Chemistry 20*(5), 671–693.

Crunkhorn, S. (2016, November). Autoimmune disease: CK2 blockade ameliorates EAE. *Nature Reviews. Drug Discovery 15*(11), 750.

Cyr, D. M. and C. H. Ramos (2015). Specification of Hsp70 function by Type I and Type II Hsp40. *Sub-Cellular Biochemistry 78*, 91–102.

Di Maira, G., F. Brustolon, J. Bertacchini, K. Tosoni, S. Marmiroli, L. A. Pinna, and M. Ruzzene (2007, October). Pharmacological inhibition of protein kinase CK2 reverts the multidrug resistance phenotype of a CEM cell line characterized by high CK2 level. *Oncogene 26*(48), 6915–6926.

Di Maira, G., F. Brustolon, L. A. Pinna, and M. Ruzzene (2009, October). Dephosphorylation and inactivation of Akt/PKB is counteracted by protein kinase CK2 in HEK 293t cells. *Cellular and molecular life sciences: CMLS 66*(20), 3363–3373.

Di Maira, G., M. Salvi, G. Arrigoni, O. Marin, S. Sarno, F. Brustolon, L. A. Pinna, and M. Ruzzene (2005, June). Protein kinase CK2 phosphorylates and upregulates Akt/PKB. *Cell Death and Differentiation 12*(6), 668–677.

DiFiglia, M., E. Sapp, K. O. Chase, S. W. Davies, G. P. Bates, J. P. Vonsattel, and N. Aronin (1997, September). Aggregation of huntingtin in neuronal intranuclear inclusions and dystrophic neurites in brain. *Science (New York, N.Y.) 277*(5334), 1990–1993.

Dominguez, I., G. E. Sonenshein, and D. C. Seldin (2009, June). Protein kinase CK2 in health and disease: CK2 and its role in Wnt and NF-kappaB signaling: linking development and cancer. *Cellular and molecular life sciences: CMLS 66*(11-12), 1850–1857.

Duncan, J. S., J. P. Turowec, G. Vilk, S. S. C. Li, G. B. Gloor, and D. W. Litchfield (2010, March). Regulation of cell proliferation and survival: convergence of protein kinases and caspases. *Biochimica Et Biophysica Acta 1804*(3), 505–510.

Ebrahimi-Fakhari, D., L. Wahlster, and P. J. McLean (2012, August). Protein degradation pathways in Parkinson's disease: curse or blessing. *Acta Neuropathologica 124*(2), 153–172.

Eckhart, W., M. A. Hutchinson, and T. Hunter (1979, December). An activity

phosphorylating tyrosine in polyoma T antigen immunoprecipitates. *Cell 18*(4), 925–933.

Eddy, S. F., S. Guo, E. G. Demicco, R. Romieu-Mourez, E. Landesman-Bollag, D. C. Seldin, and G. E. Sonenshein (2005, December). Inducible IkappaB kinase/IkappaB kinase epsilon expression is induced by CK2 and promotes aberrant nuclear factor-kappaB activation in breast cancer cells. *Cancer Research 65*(24), 11375–11383.

Engert, J. C., P. Bérubé, J. Mercier, C. Doré, P. Lepage, B. Ge, J. P. Bouchard, J. Mathieu, S. B. Melançon, M. Schalling, E. S. Lander, K. Morgan, T. J. Hudson, and A. Richter (2000, February). ARSACS, a spastic ataxia common in northeastern Québec, is caused by mutations in a new gene encoding an 11.5-kb ORF. *Nature Genetics 24*(2), 120–125.

Evgrafov, O. V., I. Mersiyanova, J. Irobi, L. V. D. Bosch, I. Dierick, C. L. Leung, O. Schagina, N. Verpoorten, K. V. Impe, V. Fedotov, E. Dadali, M. Auer-Grumbach, C. Windpassinger, K. Wagner, Z. Mitrovic, D. Hilton-Jones, K. Talbot, J.-J. Martin, N. Vasserman, S. Tverskaya, A. Polyakov, R. K. H. Liem, J. Gettemans, W. Robberecht, P. D. Jonghe, and V. Timmerman (2004, June). Mutant small heat-shock protein 27 causes axonal Charcot-Marie-Tooth disease and distal hereditary motor neuropathy. *Nature Genetics 36*(6), 602–606.

Farina, H. G., F. Benavent Acero, Y. Perera, A. Rodríguez, S. E. Perea, B. A. Castro, R. Gomez, D. F. Alonso, and D. E. Gomez (2011, July). CIGB-300, a proapoptotic peptide, inhibits angiogenesis in vitro and in vivo. *Experimental Cell Research 317*(12), 1677–1688.

Filhol, O., S. Giacosa, Y. Wallez, and C. Cochet (2015, September). Protein kinase CK2 in breast cancer: the CK2β regulatory subunit takes center stage in epithelial plasticity. *Cellular and molecular life sciences: CMLS 72*(17), 3305–3322.

Franchin, C., M. Salvi, G. Arrigoni, and L. A. Pinna (2015, October). Proteomics perturbations promoted by the protein kinase CK2 inhibitor quinalizarin. *Biochimica Et Biophysica Acta 1854*(10 Pt B), 1676–1686.

Gao, X.-C., C.-J. Zhou, Z.-R. Zhou, Y.-H. Zhang, X.-M. Zheng, A.-X. Song, and H.-Y. Hu (2011). Co-chaperone HSJ1a dually regulates the proteasomal degradation of ataxin-3. *PloS One 6*(5), e19763.

Garg, A. and B. B. Aggarwal (2002, June). Nuclear transcription factor-kappaB as a target for cancer drug development. *Leukemia 16*(6), 1053–1068.

Gess, B., M. Auer-Grumbach, A. Schirmacher, T. Strom, M. Zitzelsberger, S. Rudnik-Schöneborn, D. Röhr, H. Halfter, P. Young, and J. Senderek (2014, November). HSJ1-related hereditary neuropathies: novel mutations and extended clinical spectrum. *Neurology 83*(19), 1726–1732.

Girardi, C., D. Ottaviani, L. A. Pinna, and M. Ruzzene (2015). Different Persistence of the Cellular Effects Promoted by Protein Kinase CK2 Inhibitors CX-4945 and TDB. *BioMed Research International 2015*, 185736.

González, N., J. J. Moresco, F. Cabezas, E. de la Vega, F. Bustos, J. R. Yates, and H. C. Olguín (2016). Ck2-Dependent Phosphorylation Is Required to Maintain Pax7 Protein Levels in Proliferating Muscle Progenitors. *PloS One 11*(5), e0154919.

Guerra, B. (2006, March). Protein kinase CK2 subunits are positive regulators of AKT kinase. *International Journal of Oncology 28*(3), 685–693.

Guerra, B. and O.-G. Issinger (2008). Protein kinase CK2 in human diseases. *Current Medicinal Chemistry 15*(19), 1870–1886.

Hageman, J., M. J. Vos, M. A. W. H. van Waarde, and H. H. Kampinga (2007, November). Comparison of intra-organellar chaperone capacity for dealing with stress-induced protein unfolding. *The Journal of Biological Chemistry 282*(47), 34334–34345.

Hammarsten, O. (1883). Zur Frage ob Caseïn ein einheitlicher Stoff sei. *Hoppe-Seyler's Zeitschrift fur physiologische Chemie 7*, 227–273.

Hanger, D. P., H. L. Byers, S. Wray, K.-Y. Leung, M. J. Saxton, A. Seereeram, C. H. Reynolds, M. A. Ward, and B. H. Anderton (2007, August). Novel

phosphorylation sites in tau from Alzheimer brain support a role for casein kinase 1 in disease pathogenesis. *The Journal of Biological Chemistry 282*(32), 23645–23654.

Harada, S., E. Haneda, T. Maekawa, Y. Morikawa, S. Funayama, N. Nagata, K. Ohtsuki, N. Nagata, and K. Ohtsuki (1999, October). Casein kinase II (CK-II)-mediated stimulation of HIV-1 reverse transcriptase activity and characterization of selective inhibitors in vitro. *Biological & Pharmaceutical Bulletin 22*(10), 1122–1126.

Hardy, J. A. and G. A. Higgins (1992, April). Alzheimer's disease: the amyloid cascade hypothesis. *Science (New York, N.Y.) 256*(5054), 184–185.

Hartl, F. U., A. Bracher, and M. Hayer-Hartl (2011, July). Molecular chaperones in protein folding and proteostasis. *Nature 475*(7356), 324–332.

Hecker, C.-M., M. Rabiller, K. Haglund, P. Bayer, and I. Dikic (2006, June). Specification of SUMO1- and SUMO2-interacting motifs. *The Journal of Biological Chemistry 281*(23), 16117–16127.

Hicke, L., H. L. Schubert, and C. P. Hill (2005, August). Ubiquitin-binding domains. *Nature Reviews. Molecular Cell Biology 6*(8), 610–621.

Hirano, S., M. Kawasaki, H. Ura, R. Kato, C. Raiborg, H. Stenmark, and S. Wakatsuki (2006, March). Double-sided ubiquitin binding of Hrs-UIM in endosomal protein sorting. *Nature Structural & Molecular Biology 13*(3), 272–277.

Hofmann, K. and P. Bucher (1996, May). The UBA domain: a sequence motif present in multiple enzyme classes of the ubiquitination pathway. *Trends in Biochemical Sciences 21*(5), 172–173.

Hofmann, K. and L. Falquet (2001, June). A ubiquitin-interacting motif conserved in components of the proteasomal and lysosomal protein degradation systems. *Trends in Biochemical Sciences 26*(6), 347–350.

Howarth, J. L., S. Kelly, M. P. Keasey, C. P. J. Glover, Y.-B. Lee, K. Mitrophanous, J. P. Chapple, J. M. Gallo, M. E. Cheetham, and J. B. Uney (2007, June). Hsp40

molecules that target to the ubiquitin-proteasome system decrease inclusion formation in models of polyglutamine disease. *Molecular Therapy: The Journal of the American Society of Gene Therapy 15*(6), 1100–1105.

Hunter, T. (2007, December). The age of crosstalk: phosphorylation, ubiquitination, and beyond. *Molecular Cell 28*(5), 730–738.

Hurley, J. H., S. Lee, and G. Prag (2006, November). Ubiquitin-binding domains. *The Biochemical Journal 399*(3), 361–372.

Husnjak, K. and I. Dikic (2012). Ubiquitin-binding proteins: decoders of ubiquitin-mediated cellular functions. *Annual Review of Biochemistry 81*, 291–322.

Iimoto, D. S., E. Masliah, R. DeTeresa, R. D. Terry, and T. Saitoh (1990, January). Aberrant casein kinase II in Alzheimer's disease. *Brain Research 507*(2), 273–280.

Irobi, J., K. V. Impe, P. Seeman, A. Jordanova, I. Dierick, N. Verpoorten, A. Michalik, E. D. Vriendt, A. Jacobs, V. V. Gerwen, K. Vennekens, R. Mazanec, I. Tournev, D. Hilton-Jones, K. Talbot, I. Kremensky, L. V. D. Bosch, W. Robberecht, J. Vandekerckhove, C. V. Broeckhoven, J. Gettemans, P. D. Jonghe, and V. Timmerman (2004, June). Hot-spot residue in small heat-shock protein 22 causes distal motor neuropathy. *Nature Genetics 36*(6), 597–601.

Kato, T., M. Delhase, A. Hoffmann, and M. Karin (2003, October). CK2 Is a C-Terminal IkappaB Kinase Responsible for NF-kappaB Activation during the UV Response. *Molecular Cell 12*(4), 829–839.

Kelliher, M. A., D. C. Seldin, and P. Leder (1996, October). Tal-1 induces T cell acute lymphoblastic leukemia accelerated by casein kinase IIalpha. *The EMBO journal 15*(19), 5160–5166.

Kohlstedt, K., F. Shoghi, W. Müller-Esterl, R. Busse, and I. Fleming (2002, October). CK2 phosphorylates the angiotensin-converting enzyme and regulates its retention in the endothelial cell plasma membrane. *Circulation Research 91*(8), 749–756.

Kosmaoglou, M., N. Schwarz, J. S. Bett, and M. E. Cheetham (2008, July). Molecular chaperones and photoreceptor function. *Progress in Retinal and Eye Research 27*(4), 434–449.

Kramerov, A. A., M. Saghizadeh, H. Pan, A. Kabosova, M. Montenarh, K. Ahmed, J. S. Penn, C. K. Chan, D. R. Hinton, M. B. Grant, and A. V. Ljubimov (2006, May). Expression of protein kinase CK2 in astroglial cells of normal and neovascularized retina. *The American Journal of Pathology 168*(5), 1722–1736.

Labbadia, J., S. S. Novoselov, J. S. Bett, A. Weiss, P. Paganetti, G. P. Bates, and M. E. Cheetham (2012, April). Suppression of protein aggregation by chaperone modification of high molecular weight complexes. *Brain: A Journal of Neurology 135*(Pt 4), 1180–1196.

Leliveld, S. R. and C. Korth (2007, August). The use of conformation-specific ligands and assays to dissect the molecular mechanisms of neurodegenerative diseases. *Journal of Neuroscience Research 85*(11), 2285–2297.

Ljubimov, A. V., S. Caballero, A. M. Aoki, L. A. Pinna, M. B. Grant, and R. Castellon (2004, December). Involvement of protein kinase CK2 in angiogenesis and retinal neovascularization. *Investigative Ophthalmology & Visual Science 45*(12), 4583–4591.

Long, J., T. R. A. Gallagher, J. R. Cavey, P. W. Sheppard, S. H. Ralston, R. Layfield, and M. S. Searle (2008, February). Ubiquitin recognition by the ubiquitin-associated domain of p62 involves a novel conformational switch. *The Journal of Biological Chemistry 283*(9), 5427–5440.

Luan, B., Z. Zhang, Y. Wu, J. Kang, and G. Pei (2005, December). Beta-arrestin2 functions as a phosphorylation-regulated suppressor of UV-induced NF-kappaB activation. *The EMBO journal 24*(24), 4237–4246.

Manning, G., D. B. Whyte, R. Martinez, T. Hunter, and S. Sudarsanam (2002, December). The Protein Kinase Complement of the Human Genome. *Science 298*(5600), 1912–1934.

Martins, L. R., Y. Perera, P. Lúcio, M. G. Silva, S. E. Perea, and J. T. Barata (2014, January). Targeting chronic lymphocytic leukemia using CIGB-300, a clinical-stage CK2-specifc cell-permeable peptide inhibitor. *Oncotarget 5*(1), 258.

Matsumoto, G., K. Wada, M. Okuno, M. Kurosawa, and N. Nukina (2011, October). Serine 403 phosphorylation of p62/SQSTM1 regulates selective autophagic clearance of ubiquitinated proteins. *Molecular Cell 44*(2), 279–289.

McElhinny, J. A., S. A. Trushin, G. D. Bren, N. Chester, and C. V. Paya (1996, March). Casein kinase II phosphorylates I kappa B alpha at S-283, S-289, S-293, and T-291 and is required for its degradation. *Molecular and Cellular Biology 16*(3), 899–906.

Meggio, F., A. Donella Deana, M. Ruzzene, A. M. Brunati, L. Cesaro, B. Guerra, T. Meyer, H. Mett, D. Fabbro, and P. Furet (1995, November). Different susceptibility of protein kinases to staurosporine inhibition. Kinetic studies and molecular bases for the resistance of protein kinase CK2. *European journal of biochemistry / FEBS 234*(1), 317–322.

Meggio, F., O. Marin, and L. A. Pinna (1994). Substrate specificity of protein kinase CK2. *Cellular & Molecular Biology Research 40*(5-6), 401–409.

Meggio, F. and L. A. Pinna (2003, March). One-thousand-and-one substrates of protein kinase CK2? *FASEB journal: official publication of the Federation of American Societies for Experimental Biology 17*(3), 349–368.

Miller, S. L. H., E. Malotky, and J. P. O'Bryan (2004, August). Analysis of the role of ubiquitin-interacting motifs in ubiquitin binding and ubiquitylation. *The Journal of Biological Chemistry 279*(32), 33528–33537.

Mueller, T., P. Breuer, I. Schmitt, J. Walter, B. O. Evert, and U. Wüllner (2009, September). CK2-dependent phosphorylation determines cellular localization and stability of ataxin-3. *Human Molecular Genetics 18*(17), 3334–3343.

Niefind, K., B. Guerra, I. Ermakowa, and O. G. Issinger (2001, October). Crystal structure of human protein kinase CK2: insights into basic properties of the CK2 holoenzyme. *The EMBO journal 20*(19), 5320–5331.

Niefind, K., B. Guerra, L. A. Pinna, O.-G. Issinger, and D. Schomburg (1998, May). Crystal structure of the catalytic subunit of protein kinase CK2 from Zea mays at 2.1 å resolution. *The EMBO Journal 17*(9), 2451–2462.

Novoselov, S. S., W. J. Mustill, A. L. Gray, J. R. Dick, N. Kanuga, B. Kalmar, L. Greensmith, and M. E. Cheetham (2013). Molecular chaperone mediated late-stage neuroprotection in the SOD1(G93a) mouse model of amyotrophic lateral sclerosis. *PloS One 8*(8), e73944.

Okochi, M., J. Walter, A. Koyama, S. Nakajo, M. Baba, T. Iwatsubo, L. Meijer, P. J. Kahle, and C. Haass (2000, January). Constitutive phosphorylation of the Parkinson's disease associated alpha-synuclein. *The Journal of Biological Chemistry 275*(1), 390–397.

Okur, V., M. T. Cho, L. Henderson, K. Retterer, M. Schneider, S. Sattler, D. Niyazov, M. Azage, S. Smith, J. Picker, S. Lincoln, M. Tarnopolsky, L. Brady, H. T. Bjornsson, C. Applegate, A. Dameron, R. Willaert, B. Baskin, J. Juusola, and W. K. Chung (2016, July). De novo mutations in CSNK2a1 are associated with neurodevelopmental abnormalities and dysmorphic features. *Human Genetics 135*(7), 699–705.

Pagano, M. A., L. Cesaro, F. Meggio, and L. A. Pinna (2006, December). Protein kinase CK2: a newcomer in the 'druggable kinome'. *Biochemical Society Transactions 34*(Pt 6), 1303–1306.

Pagano, M. A., S. Sarno, G. Poletto, G. Cozza, L. A. Pinna, and F. Meggio (2005, June). Autophosphorylation at the regulatory beta subunit reflects the supramolecular organization of protein kinase CK2. *Molecular and Cellular Biochemistry 274*(1-2), 23–29.

Perea, S. E., O. Reyes, I. Baladron, Y. Perera, H. Farina, J. Gil, A. Rodriguez, D. Bacardi, J. L. Marcelo, K. Cosme, M. Cruz, C. Valenzuela, P. A. López-Saura, Y. Puchades, J. M. Serrano, O. Mendoza, L. Castellanos, A. Sanchez, L. Betancourt, V. Besada, R. Silva, E. López, V. Falcón, I. Hernández, M. Solares, A. Santana, A. Díaz, T. Ramos, C. López, J. Ariosa, L. J. González, H. Garay, D. Gómez, R. Gómez, D. F. Alonso, H. Sigman, L. Herrera, and B. Acevedo

(2008, June). CIGB-300, a novel proapoptotic peptide that impairs the CK2 phosphorylation and exhibits anticancer properties both in vitro and in vivo. *Molecular and Cellular Biochemistry 316*(1-2), 163–167.

Perera, Y., H. G. Farina, I. Hernández, O. Mendoza, J. M. Serrano, O. Reyes, D. E. Gómez, R. E. Gómez, B. E. Acevedo, D. F. Alonso, and S. E. Perea (2008, January). Systemic administration of a peptide that impairs the protein kinase (CK2) phosphorylation reduces solid tumor growth in mice. *International Journal of Cancer 122*(1), 57–62.

Perera, Y., N. D. Toro, L. Gorovaya, J. Fernandez-DE-Cossio, H. G. Farina, and S. E. Perea (2014, November). Synergistic interactions of the anti-casein kinase 2 CIGB-300 peptide and chemotherapeutic agents in lung and cervical preclinical cancer models. *Molecular and Clinical Oncology 2*(6), 935–944.

Peter, J.-C., J.-P. Briand, and J. Hoebeke (2003, March). How biotinylation can interfere with recognition: a surface plasmon resonance study of peptide-antibody interactions. *Journal of Immunological Methods 274*(1-2), 149–158.

Piazza, F., S. Manni, M. Ruzzene, L. A. Pinna, C. Gurrieri, and G. Semenzato (2012, June). Protein kinase CK2 in hematologic malignancies: reliance on a pivotal cell survival regulator by oncogenic signaling pathways. *Leukemia 26*(6), 1174–1179.

Pinna, L. A. (2002, October). Protein kinase CK2: a challenge to canons. *Journal of Cell Science 115*(Pt 20), 3873–3878.

Rabellino, A., B. Carter, G. Konstantinidou, S.-Y. Wu, A. Rimessi, L. A. Byers, J. V. Heymach, L. Girard, C.-M. Chiang, J. Teruya-Feldstein, and P. P. Scaglioni (2012, May). The SUMO E3-ligase PIAS1 regulates the tumor suppressor PML and its oncogenic counterpart PML-RARA. *Cancer Research 72*(9), 2275–2284.

Reyes-Turcu, F. E., J. R. Horton, J. E. Mullally, A. Heroux, X. Cheng, and K. D. Wilkinson (2006, March). The ubiquitin binding domain ZnF UBP recognizes the C-terminal diglycine motif of unanchored ubiquitin. *Cell 124*(6), 1197–1208.

Rose, J. M., S. S. Novoselov, P. A. Robinson, and M. E. Cheetham (2011, January). Molecular chaperone-mediated rescue of mitophagy by a Parkin RING1 domain mutant. *Human Molecular Genetics 20*(1), 16–27.

Rosen, D. R., T. Siddique, D. Patterson, D. A. Figlewicz, P. Sapp, A. Hentati, D. Donaldson, J. Goto, J. P. O'Regan, and H. X. Deng (1993, March). Mutations in Cu/Zn superoxide dismutase gene are associated with familial amyotrophic lateral sclerosis. *Nature 362*(6415), 59–62.

Ruzzene, M. and L. A. Pinna (2010, March). Addiction to protein kinase CK2: a common denominator of diverse cancer cells? *Biochimica Et Biophysica Acta 1804*(3), 499–504.

Ruzzene, M., K. Tosoni, S. Zanin, L. Cesaro, and L. A. Pinna (2011, October). Protein kinase CK2 accumulation in "oncophilic" cells: causes and effects. *Molecular and Cellular Biochemistry 356*(1-2), 5–10.

Salvi, M., S. Sarno, L. Cesaro, H. Nakamura, and L. A. Pinna (2009, May). Extraordinary pleiotropy of protein kinase CK2 revealed by weblogo phosphoproteome analysis. *Biochimica Et Biophysica Acta 1793*(5), 847–859.

Salvi, M., E. Trashi, G. Cozza, C. Franchin, G. Arrigoni, and L. A. Pinna (2012, December). Investigation on PLK2 and PLK3 substrate recognition. *Biochimica Et Biophysica Acta 1824*(12), 1366–1373.

Sanchez, E., H. Darvish, R. Mesias, S. Taghavi, S. G. Firouzabadi, R. H. Walker, A. Tafakhori, and C. Paisán-Ruiz (2016, July). Identification of a Large DNAJB2 Deletion in a Family with Spinal Muscular Atrophy and Parkinsonism. *Human Mutation*.

Sarno, S., H. Reddy, F. Meggio, M. Ruzzene, S. P. Davies, A. Donella-Deana, D. Shugar, and L. A. Pinna (2001, May). Selectivity of 4,5,6,7-tetrabromobenzotriazole, an ATP site-directed inhibitor of protein kinase CK2 ('casein kinase-2'). *FEBS letters 496*(1), 44–48.

Sarno, S., P. Vaglio, F. Meggio, O. G. Issinger, and L. A. Pinna (1996, May). Protein

kinase CK2 mutants defective in substrate recognition. Purification and kinetic analysis. *The Journal of Biological Chemistry 271*(18), 10595–10601.

Scaglioni, P. P., T. M. Yung, L. F. Cai, H. Erdjument-Bromage, A. J. Kaufman, B. Singh, J. Teruya-Feldstein, P. Tempst, and P. P. Pandolfi (2006, July). A CK2-dependent mechanism for degradation of the PML tumor suppressor. *Cell 126*(2), 269–283.

Sharma, K., R. C. J. D'Souza, S. Tyanova, C. Schaab, J. R. Wiśniewski, J. Cox, and M. Mann (2014, September). Ultradeep human phosphoproteome reveals a distinct regulatory nature of Tyr and Ser/Thr-based signaling. *Cell Reports 8*(5), 1583–1594.

Shekhtman, A. and D. Cowburn (2002, September). A ubiquitin-interacting motif from Hrs binds to and occludes the ubiquitin surface necessary for polyubiquitination in monoubiquitinated proteins. *Biochemical and Biophysical Research Communications 296*(5), 1222–1227.

Siddiqui-Jain, A., D. Drygin, N. Streiner, P. Chua, F. Pierre, S. E. O'Brien, J. Bliesath, M. Omori, N. Huser, C. Ho, C. Proffitt, M. K. Schwaebe, D. M. Ryckman, W. G. Rice, and K. Anderes (2010, December). CX-4945, an orally bioavailable selective inhibitor of protein kinase CK2, inhibits prosurvival and angiogenic signaling and exhibits antitumor efficacy. *Cancer Research 70*(24), 10288–10298.

Siepmann, M., S. Kumar, G. Mayer, and J. Walter (2010). Casein kinase 2 dependent phosphorylation of neprilysin regulates receptor tyrosine kinase signaling to Akt. *PloS One 5*(10).

Smith, H. L., W. Li, and M. E. Cheetham (2015, April). Molecular chaperones and neuronal proteostasis. *Seminars in Cell & Developmental Biology 40*, 142–152.

Sokratous, K., A. Hadjisavvas, E. P. Diamandis, and K. Kyriacou (2014, October). The role of ubiquitin-binding domains in human pathophysiology. *Critical Reviews in Clinical Laboratory Sciences 51*(5), 280–290.

Solares, A. M., A. Santana, I. Baladrón, C. Valenzuela, C. A. González, A. Díaz, D. Castillo, T. Ramos, R. Gómez, D. F. Alonso, L. Herrera, H. Sigman, S. E. Perea, B. E. Acevedo, and P. López-Saura (2009, May). Safety and preliminary efficacy data of a novel casein kinase 2 (CK2) peptide inhibitor administered intralesionally at four dose levels in patients with cervical malignancies. *BMC cancer 9*, 146.

Solimini, N. L., J. Luo, and S. J. Elledge (2007, September). Non-oncogene addiction and the stress phenotype of cancer cells. *Cell 130*(6), 986–988.

Song, D. H., I. Dominguez, J. Mizuno, M. Kaut, S. C. Mohr, and D. C. Seldin (2003, June). CK2 phosphorylation of the armadillo repeat region of beta-catenin potentiates Wnt signaling. *The Journal of Biological Chemistry 278*(26), 24018–24025.

Soto, C. and L. D. Estrada (2008, February). Protein misfolding and neurodegeneration. *Archives of Neurology 65*(2), 184–189.

Spillantini, M. G., R. A. Crowther, R. Jakes, M. Hasegawa, and M. Goedert (1998, May). alpha-Synuclein in filamentous inclusions of Lewy bodies from Parkinson's disease and dementia with lewy bodies. *Proceedings of the National Academy of Sciences of the United States of America 95*(11), 6469–6473.

Stehmeier, P. and S. Muller (2009, February). Phospho-regulated SUMO interaction modules connect the SUMO system to CK2 signaling. *Molecular Cell 33*(3), 400–409.

Tagliabracci, V. S., J. L. Engel, J. Wen, S. E. Wiley, C. A. Worby, L. N. Kinch, J. Xiao, N. V. Grishin, and J. E. Dixon (2012, June). Secreted kinase phosphorylates extracellular proteins that regulate biomineralization. *Science (New York, N.Y.) 336*(6085), 1150–1153.

Taus, T., T. Köcher, P. Pichler, C. Paschke, A. Schmidt, C. Henrich, and K. Mechtler (2011, December). Universal and confident phosphorylation site localization using phosphoRS. *Journal of Proteome Research 10*(12), 5354–5362.

Taylor, S. S., E. Radzio-Andzelm, D. R. Knighton, L. F. Ten Eyck, J. M. Sowadski, F. W. Herberg, W. Yonemoto, and J. Zheng (1993). Crystal structures of the catalytic subunit of cAMP-dependent protein kinase reveal general features of the protein kinase family. *Receptor 3*(3), 165–172.

Torres, J. and R. Pulido (2001, January). The tumor suppressor PTEN is phosphorylated by the protein kinase CK2 at its C terminus. Implications for PTEN stability to proteasome-mediated degradation. *The Journal of Biological Chemistry 276*(2), 993–998.

Tsuchiya, Y., H. Taniguchi, Y. Ito, T. Morita, M. R. Karim, N. Ohtake, K. Fukagai, T. Ito, S. Okamuro, S.-I. Iemura, T. Natsume, E. Nishida, and A. Kobayashi (2013, September). The casein kinase 2-nrf1 axis controls the clearance of ubiquitinated proteins by regulating proteasome gene expression. *Molecular and Cellular Biology 33*(17), 3461–3472.

Venerando, A., C. Franchin, N. Cant, G. Cozza, M. A. Pagano, K. Tosoni, A. Al-Zahrani, G. Arrigoni, R. C. Ford, A. Mehta, and L. A. Pinna (2013). Detection of phospho-sites generated by protein kinase CK2 in CFTR: mechanistic aspects of Thr1471 phosphorylation. *PloS One 8*(9), e74232.

Venerando, A., M. Ruzzene, and L. A. Pinna (2014, June). Casein kinase: the triple meaning of a misnomer. *The Biochemical Journal 460*(2), 141–156.

Walsh, C. T., S. Garneau-Tsodikova, and G. J. Gatto (2005, December). Protein posttranslational modifications: the chemistry of proteome diversifications. *Angewandte Chemie (International Ed. in English) 44*(45), 7342–7372.

Wang, D., S. D. Westerheide, J. L. Hanson, and A. S. Baldwin (2000, October). Tumor necrosis factor alpha-induced phosphorylation of RelA/p65 on Ser529 is controlled by casein kinase II. *The Journal of Biological Chemistry 275*(42), 32592–32597.

Wang, L. G., X. M. Liu, H. Wikiel, and A. Bloch (1995, February). Activation of casein kinase II in ML-1 human myeloblastic leukemia cells requires IGF-1 and transferrin. *Journal of Leukocyte Biology 57*(2), 332–334.

Watabe, M. and T. Nakaki (2011, May). Protein kinase CK2 regulates the formation and clearance of aggresomes in response to stress. *Journal of Cell Science 124*(Pt 9), 1519–1532.

Westhoff, B., J. P. Chapple, J. van der Spuy, J. Höhfeld, and M. E. Cheetham (2005, June). HSJ1 is a neuronal shuttling factor for the sorting of chaperone clients to the proteasome. *Current biology: CB 15*(11), 1058–1064.

Wirkner, U. and W. Pyerin (1999, January). CK2alpha loci in the human genome: structure and transcriptional activity. *Molecular and Cellular Biochemistry 191*(1-2), 59–64.

Young, P., Q. Deveraux, R. E. Beal, C. M. Pickart, and M. Rechsteiner (1998, June). Characterization of Two Polyubiquitin Binding Sites in the 26 S Protease Subunit 5a. *Journal of Biological Chemistry 273*(10), 5461–5467.

Zandomeni, R., M. C. Zandomeni, D. Shugar, and R. Weinmann (1986, March). Casein kinase type II is involved in the inhibition by 5,6-dichloro-1-beta-D-ribofuranosylbenzimidazole of specific RNA polymerase II transcription. *The Journal of Biological Chemistry 261*(7), 3414–3419.

Zhang, C., G. Vilk, D. A. Canton, and D. W. Litchfield (2002, May). Phosphorylation regulates the stability of the regulatory CK2beta subunit. *Oncogene 21*(23), 3754–3764.

List of Figures

7.14 **HSJ1 phosphorylation in response to the removal of the CK2 inhibition**

HSJ1a expression was induced in CHO cells by 3 μg/ml tetracycline. Where indicated (+) cells were treated for 3 h with CX-4945; +/- refers to cells that where incubated with CX-4945 for 3 h, then the inhibitor was removed and cells incubated for further 3 h before lysis. 20 μg of total lysate proteins were analysed by WB as indicated. 67

7.15 **Kinetics of the phospho-HSJ1 antibody (pHSJ1) interactions by means of SPR signal**

A. The first batch (pHSJ1) of antibodies was purified by affinity against mono- and bis-phospho peptides while the second batch (ppHSJ1) **(B)** was purified by affinity against bis-phospho peptides only.

Increasing concentration of the pHSJ1 antibody (M values indicated) were injected over a sensor chip where pSer250 peptide (left panel) or pSer247/pSer250 peptide (right panel) were immobilized in a Biacore T100 instrument (see the Methods for details). Surface plasmon resonance (SPR) signal is shown as sensorgram (time course of the response) reported in resonance units (RU). Each sensorgram has been subtracted from the corresponding signal produced on a control surface and normalized to baseline. 0 concentrations corresponded to dilution buffer.

C. 0.002 M phospho-HSJ1 antibody was injected over the pSer250 peptide immobilized on the chip, in the presence of increasing concentrations of pSer250 peptide or pSer247/pSer250 peptide. The RU signals at the end of the binding time (relative response subtracted of the control signal) for each condition were plotted and the calculation of the IC_{50} was performed by GraphPad software. 69

List of Tables

Part VII

Acknowledgements

Acknowledgements

I am profoundly grateful to my P.I. Prof. Maria Ruzzene for the support, suggestions and trust during these years.

I thank Distinguished Prof. Lorenzo Alberto Pinna, Prof. Arianna Donella-Deana, Prof. Mauro Salvi, Prof. Stefania Sarno, Prof. Oriano Marin, Prof. Giorgio Arrigoni, and all the colleagues; thanks to Cristina, Valentina, Sofia, Cinzia, Francesca, Christian, Luca, Jordi, Michele for their encouragements and support throughout these years. A special mention for Nicoletta, Giorgio and Andrea for their kindness and faith in me.

I am deeply grateful to Prof. Mike Cheetham for his support, suggestions and encouragements. I also thank all the Cheetham lab for the kindness, moral support, help in setting up experiments and for being such an amazing Group that truly made me feel at home during my visit.

I also thank all my closest friends.

My personal love goes to to my Darling Elena and my Family for their unconditioned love, support and sense of freedom.